DEVELOPMENT OF BIOCOMPOSITE SCAFFOLDS AND INJECTABLE BIOCEMENT FOR BONE REGENERATION

Fan Wu

A thesis submitted for the degree of

Doctor of Philosophy

School of Chemical Engineering

The University of Adelaide

Australia

February 2013

Table of Contents

Abstract

To repair massive bone defects caused by disease and trauma, a bone grafting procedure is required. The limitations associated with the use of autografts (tissue grafts from one point to another of the same individual's body) and allografts (tissue grafts between genetically nonidentical individuals) have boosted the research and development of bone graft substitutes.

Calcium phosphate cement (CPC) is a promising bone graft substitute because of its bioactivity, osteoconductivity and bone replacement capability. However, difficulties with injectability and slow resorption rate have limited the wider applications of CPC. To overcome these limitations, premixed and injectable calcium deficient apatite biocement (cd-AB) were prepared in the initial phase of this study. Using a non-aqueous solution as the liquid phase, the resulting premixed cd-AB had the advantage of remaining stable in the syringe and only hardened following delivery to the defect site. As well, when injected into an aqueous environment, this premixed cd-AB exhibited improved washout resistance when compared to the conventional cd-AB using water as the liquid phase. However, the premixed cd-AB required a longer setting time and developed a reduced compressive strength compared to the conventional cd-AB. The hydration products of premixed cd-AB were a mixture of calcium deficient hydroxyapatite (cd-HA) and PLA. *In vitro* Tris-HCl immersion tests demonstrated that the premixed cd-AB was degradable. The results revealed

that the premixed cd-AB was cytocompatible and no adverse effects were observed after attachment and proliferation of MG-63 osteoblast-like cells *in vitro*. The most distinct advantages of premixed and injectable PLA-modified cd-AB were its excellent washout resistance and *in vitro* degradability, suggesting that it may be a promising candidate for future bone reconstruction.

In recent years, bone tissue engineering has emerged as a promising approach for the repair of bone damage and defects. In this approach, a scaffold is normally used alone or in combination with growth factors and/or cells to guide bone regeneration. Among the synthetic polymers used as scaffold materials, poly(ε-caprolactone) (PCL) has been widely used given its excellent biocompatibility and ease of processing. However, the use of PCL scaffolds is limited as a consequence of potential drawbacks including a slow degradation rate and their hydrophobic surface. These disadvantages may be overcome by incorporating additional natural polymer or inorganic fillers into the PCL matrix.

In the second section of this study, porous scaffolds of zein/PCL biocomposite were fabricated and characterized. These scaffolds were prepared using the particulate leaching method with sodium chloride particles as porogen. Porous biocomposite scaffolds with porosity around 70% and well-interconnected network were obtained. The incorporation of zein into PCL led to an improvement of the surface hydrophilicity as confirmed by the results of water contact angle measurement.

Following immersion in a phosphate buffered saline solution (PBS) *in vitro* for 28 days, it was observed that the zein/PCL scaffolds degraded more rapidly than the PCL scaffolds and the degradation rate could be controlled by adjusting the amount of zein in the composite. These results demonstrated the potential of the zein/PCL biocomposite scaffolds to be exploited in tissue engineering strategies for the repair of bone defects.

In the final section of this study, porous scaffolds using a magnesium phosphate (MP)/PCL biocomposite were developed for bone tissue engineering applications. The composite scaffolds were fabricated by the particulate leaching method again using sodium chloride particles as porogen. The resulting scaffolds had interconnected macroporous structure with porosity around 73%. The surface hydrophilicity of the scaffolds was enhanced by the incorporation of MP component and confirmed by water contact angle measurement. The results from subsequent *in vitro* degradation experiments showed that the MP/PCL composite scaffolds degraded faster than PCL scaffolds in a PBS solution. An additional benefit was that the degradation rate of the scaffolds could be tuned by adjusting the content of MP component in the composite. These results indicated that the MP/PCL composite scaffolds have potential application in bone tissue engineering.

Declaration

I certify that this work contains no material which has been accepted for the award of any other degree or diploma in any university or other tertiary institution and, to the best of my knowledge and belief, contains no material previously published or written by another person, except where due reference has been made in the text. In addition, I certify that no part of this work will, in the future, be used in a submission for any other degree or diploma in any university or other tertiary institution without the prior approval of the University of Adelaide and where applicable, any partner institution responsible for the joint-award of this degree.

I give consent to this copy of my thesis when deposited in the University Library, being made available for loan and photocopying, subject to the provisions of the Copyright Act 1968.

The author acknowledges that copyright of published works contained within this thesis resides with the copyright holder(s) of those works.

I also give permission for the digital version of my thesis to be made available on the web, via the University's digital research repository, the Library catalogue and also through web search engines, unless permission has been granted by the University to restrict access for a period of time.

SIGNED: DATE:

Acknowledgement

I owe many thanks to my principal supervisor Dr. Yung Ngothai who has provided guidance and encouragement throughout my PhD studies. I am particularly grateful to my external supervisor Prof. Changsheng Liu for providing the opportunity of studying in his research group in East China University of Science and Technology. I would like to thank A/Prof. Jie Wei for his advice, guidance and encouragement. I would also like to thank A/Prof. Brian O'Neill for his support.

I want to thank all members from Prof. Liu's research group for their support. I would like to thank Mr. Yuequn Wu, Ms. Wei Tang, Mr. Xiangde Li and Ms. Yingmei Zhao for their help with the experiments.

I would like to thank Dr. Joan Thomas for her advice. I would also like to thank Ms. Aoife McFadden for her help with the scanning electron microscopy and micro-CT.

Finally, I would like to express my deepest gratitude to my parents and my husband Milan for their love, encouragement and ongoing support.

爸爸妈妈，谢谢你们!

List of Publications

Journal papers

F. Wu, Y. Ngothai, J. Wei, C. Liu, B. O'Neill, Y. Wu. Premixed, injectable PLA–modified calcium deficient apatite biocement (cd-AB) with washout resistance. Colloids and Surfaces B: Biointerfaces, 2012, 92, 113–120.

F. Wu, J. Wei, C. Liu, B. O'Neill, Y. Ngothai. Fabrication and properties of porous scaffold of zein/PCL biocomposite for bone tissue engineering. Composites: Part B, 2012, 43, 2192–2197.

F. Wu, C. Liu, B. O'Neill, J. Wei, Y. Ngothai. Fabrication and properties of porous scaffold of magnesium phosphate/polycaprolactone biocomposite for bone tissue engineering. Applied Surface Science, 2012, 258, 7589–7595.

Conference paper

F. Wu, Y. Ngothai, C. Liu, J. Wei, B. O'Neill, R. Musgrove. Preparation and characterization of macroporous magnesium phosphate scaffold for bone regeneration. CHEMECA 2011, Sydney, Australia, September 2011.

Conference abstract

F. Wu, Y. Ngothai, C. Liu, J. Wei, B. O'Neill, R. Musgrove. PLA–modified magnesium phosphate bone cement with anti-washout property and degradability. CHEMECA 2011, Sydney, Australia, September 2011.

List of Figures

List of Tables

List of Abbreviations

ANOVA	analysis of variance
cd-AB	calcium deficient apatite biocement
CPC	calcium phosphate cement
DMSO	dimethyl sulfoxide
ECM	extracellular matrix
FBS	fetal bovine serum
FDA	Food and Drug Administration
FTIR	Fourier transform infrared
HA	hydroxyapatite
HCA	hydroxycarbonate apatite
HPMC	hydroxypropyl methylcellulose
hMSCs	human mesenchymal stem cells
LPR	liquid-to-powder ratio
micro-CT	micro-computed tomography
MgO	magnesium oxide
MP	magnesium phosphate
MPC	magnesium phosphate cement
MTT	methyl thiazolyl tetrazolium
NMP	N-methyl-2-pyrrolidone
OD	optical density
PDLA	poly(D-lactide)
PDLLA	poly(DL-lactide)
PLLA	poly(L-lactide)
P/L	powder-to-liquid
PBS	phosphate buffer saline
PEG	polyethylene glycol

PHA	precipitated hydroxyapatite
PLA	polylactide
PCL	polycaprolactone
PTFE	polytetrafluoroethylene
RH	relative humidity
rpm	revolutions per minute
SBF	simulated body fluid
SD	standard deviation
SEM	scanning electron microscopy
TCP	tissue culture polystyrene
TCP	tricalcium phosphate
Tris	tris(hydroxymethyl)aminomethane
WCA	water contact angle
XRD	X-ray diffraction

Chapter 1 Introduction

1.1 Background

Bone is a physiologically dynamic tissue with considerable self-regeneration capability. However, for the treatment of critical size defects (defects that would not fully heal spontaneously), bone grafting procedures are often necessary [1]. It is estimated that more than 500,000 bone grafting procedures per annum are performed in the United States [2].

For many years, autologous bone (bone harvested in a second surgery from a skeletal site remote from the defective site in the same patient) has been considered as the gold standard for bone graft material [3, 4]. Autografts incorporate the three essential elements for bone regeneration, namely osteogenicity, osteoconductivity and osteoinductivity [5]. However, there are some drawbacks associated with the use of autografts such as donor site morbidity, limited availability and contouring difficulty [6, 7]. The use of allografts is also limited due to the concerns of immune rejection and disease transmission [6, 8]. As a result, a variety of biomaterials have been developed as bone graft substitutes.

Calcium phosphate cement (CPC) is a promising biomaterial as a bone graft substitute. It consists of a powder phase and a liquid phase. The powder is mixed with the liquid to form a paste that can be easily shaped and fitted to the defect area. Subsequently, the paste can harden *in situ*. Due to its excellent biocompatibility, osteoconductivity and

bone replacement capability, CPC has been applied in a wide range of clinical applications. However, wider use of CPC is limited by some drawbacks, such as the poor injectability and low *in vivo* resorption rate.

Over the past few years, bone tissue engineering has been proposed as a promising approach to the repair of bone defects. Tissue engineering was defined by Langer and Vacanti [9] as "*an interdisciplinary field that applies the principles of engineering and life sciences toward the development of biological substitutes that restore, maintain, or improve tissue or organ function*". In this approach, scaffolds alone or in combination with growth factors and/or cells are used to guide bone regeneration and repair defects [10]. Thus, the design and fabrication of scaffolds with optimal characteristics are of great importance. Poly(ε-caprolactone) (PCL) has been widely used as the scaffold material due to its superior biocompatibility and ease of processing. However, some disadvantages associated with the use of PCL in particular its slow degradation rate and surface hydrophobicity.

1.2 Thesis aims

The work presented in this thesis addresses two main research aims.

The first aim was to develop a premixed, injectable calcium-deficient apatite biocement (cd-AB) for use in the reconstruction of bone defects. PLA was dissolved in NMP to form PLA-NMP solutions which were then used as the liquid phase for premixed cd-AB. The influences of PLA concentration on physicochemical properties

of the premixed cd-AB were investigated. The *in vitro* degradability of the premixed cd-AB was studied by immersion in a Tris-HCl solution. The *in vitro* cytocompatibility of the premixed cd-AB to MG-63 osteoblast-like cells was also evaluated.

The second aim was to fabricate biodegradable composite scaffolds for bone tissue engineering applications. One group of scaffolds was prepared using a blend of PCL and zein (a corn protein). The other group of scaffolds was made using a blend of PCL and magnesium phosphate (MP) powder. The composite scaffolds were prepared by the particulate leaching method. The microstructure of the scaffolds was determined using micro-computed tomography (micro-CT) and scanning electron microscopy (SEM). The mechanical properties were examined by compression tests. The hydrophilicity and *in vitro* degradability were also investigated.

1.3 Scope of the thesis

Chapter 2 provides an overview of bone biology, bone graft substitutes, CPC and its recent development, bone tissue engineering, materials and the methods used to fabricate bone tissue engineering scaffolds. Chapter 3 reports the development of premixed, injectable PLA-modified calcium deficient apatite biocement (cd-AB) with washout resistance. Chapter 4 presents the fabrication and properties of porous scaffold of zein/PCL biocomposite for bone tissue engineering. Chapter 5 contains the preparation and characterization of MP/PCL biocomposite scaffold for bone tissue

engineering. Chapter 6 presents a summary of the current findings, together with future directions.

Chapter 2 Literature review

2.1 Bone

Bone is a highly complex tissue that provides many important functions in the body: (1) it protects vital organs; (2) it provides mechanical support for soft tissues; (3) it serves as a reservoir of calcium, phosphate, magnesium and other important ions; and (4) it is the major site of hematopoiesis (the production of blood cells) in the body [11, 12] .

Bone is composed of hydroxyapatite (HA) crystals and an organic matrix (~ 95% is type I collagen) [13]. In an adult human skeleton, there are two types of bone tissue: cortical (compact) bone and trabecular (cancellous) bone. Cortical bone, which represents approximately 80% of the skeletal mass, has a dense and compact structure [14]. Cortical bone is located in the outer part of the skeleton and its major function is to provide mechanical support and protection [11]. Trabecular bone comprises 20% of the skeletal mass [14]. Compared to cortical bone, trabecular bone is more elastic and has a higher turn-over rate [11].

Bone is a dynamic tissue that constantly undergoes remodeling [15]. Bone remodeling involves the resorption and synthesis of bone [16]. According to their function in bone remodeling, cells present in bone may be divided into two principal groups: osteoblasts and osteoclasts [17]. Osteoblasts are responsible for the formation of new bone [17]. Osteoclasts play an important role in the resorption of

bone [18].

As a tissue with considerable self-regenerative potential, bone can heal some small defects by itself without surgical intervention [19]. However, in the case of extensive bone defects, such as critical size defect and bone fracture, this self-regeneration capability is insufficient for bone reconstruction [19, 20]. Therefore, a bone grafting procedure is required to repair massive bone defects caused by disease and trauma.

2.2 Bone graft substitutes

A majority of current bone grafting procedures were involved with the use of autografts or allografts. However, the limitations related to the use of autografts include donor site morbidity, limited availability and contouring difficulty [6, 7]. The applications of allografts are limited due to the concerns about immunorejection and disease transmission [6, 8].

To overcome the disadvantages of autograft and allograft, a wide range of materials have been developed as bone graft substitutes: including metals such as titanium, iron, and magnesium; polymers such as polylactide (PLA), polyglycolide (PGA), and polycaprolactone (PCL); and ceramics such as bioactive glasses, sintered hydroxyapatite, calcium carbonate, calcium sulphate hemihydrate (CSH), calcium sulphate dihydrate (CSD), and calcium phosphates [21].

In the early days, bone graft substitutes in the form of granules [22] or porous blocks

[23] were principally used. Later on, bone graft substitutes were developed in the form of self-hardening pastes, which offered the advantages of easy shaping and good adaptation to the defect site.

2.3 Calcium phosphate cement (CPC)

In late 1980s, Brown and Chow [24, 25] developed the first self-hardening calcium phosphate cement (CPC). It is made from the combination of a powder phase and a liquid phase. The powder phase is mixed with the aqueous solution to form a paste which can be easily shaped and fitted to the damaged area. Subsequently, the paste hardened *in situ* to provide a solid restoration [6, 25].

2.3.1 Formulations of CPC

The CPC powder was composed of one or several calcium phosphate compounds [26]. Table 2.1 lists the main calcium phosphate compounds [26, 27]. The first CPC, developed by Brown and Chow [24, 25], contained TTCP and DCPA or DCPD. Since then, many other combinations of different calcium phosphate compounds have been proposed and investigated as the CPC powder.

A wide range of aqueous solutions have been used as the liquid phase of CPC in the literature. For instance, distilled water, phosphate buffer saline (PBS), sodium phosphate aqueous solution with 1% sodium alginate [28], hydroxypropyl methylcellulose (HPMC) aqueous solution [29], aqueous solution of sodium or calcium salts of the oligocarboxylic acids (malic, tartaric, and citric acids) [30], citric

Table 2.1 Principal calcium phosphate compounds [26, 27].

Ca/P molar ratio	Compound	Chemical formula
0.5	Monocalcium phosphate monohydrate (MCPM)	$Ca(H_2PO_4)_2 \cdot H_2O$
0.5	Monocalcium phosphate anhydrous (MCPA)	$Ca(H_2PO_4)_2$
1.0	Dicalcium phosphate dihydrate (DCPD)	$CaHPO_4 \cdot 2H_2O$
1.0	Dicalcium phosphate anhydrous (DCPA)	$CaHPO_4$
1.33	Octacalcium phosphate (OCP)	$Ca_8(HPO_4)_2(PO_4)_4 \cdot 5H_2O$
1.5	α-Tricalcium phosphate (α-TCP)	$\alpha\text{-}Ca_3(PO_4)_2$
1.5	β-Tricalcium phosphate (β-TCP)	$\beta\text{-}Ca_3(PO_4)_2$
1.2–2.2	Amorphous calcium phosphate (ACP)	$Ca_xH_y(PO_4)_z \cdot nH_2O$, n=3–4.5; 15–20% H_2O
1.5–1.67	Calcium-deficient hydroxyapatite (CDHA)	$Ca_{10-x}(HPO_4)_x(PO_4)_{6-x}(OH)_{2-x}$ $(0 < x < 1)$
1.67	Hydroxyapatite (HA)	$Ca_{10}(PO_4)_6(OH)_2$
2.0	Tetracalcium phosphate (TTCP)	$Ca_4(PO_4)_2O$

acid solution [31] and aqueous solution of Na_2HPO_4 [32].

Powder-to-liquid (P/L) ratio is an important parameter in the formulation of CPC. P/L ratio has been found to influence the handling and mechanical properties of CPC. Previous studies have demonstrated that a decrease of P/L ratio contributed to a better injectability, but had an adverse effect on the mechanical properties of hardened cement body because of the high porosity [32-34]. An increase in P/L ratio shortened the setting time of cement paste and decreased the porosity of hardened cement [35, 36]. However, the injectability of cement paste may decrease due to its high viscosity [35, 36].

2.3.2 The setting reaction of CPC

CPC undergoes two major setting reaction. The first type occurs as an acid-base reaction. For instance, a relatively acidic calcium phosphate compound reacts with a relatively basic calcium phosphate compound to produce a relatively neutral compound [26]. The CPC proposed by Brown and Chow [24, 25] provides a typical example:

$$2Ca_4(PO_4)_2O + 2CaHPO_4 \rightarrow Ca_{10}(PO_4)_6(OH)_2 \quad (2.1)$$

TTCP which is basic reacts with DCPA which is neutral in an aqueous solution to form a precipitated HA which is slightly basic [26]. The cement proposed by Lemaitre et al. [37] is another example, where β-TCP (slightly basic) reacts with MCPM (acidic) to form DCPD (neutral) [26].

$$\beta\text{-}Ca_3(PO_4)_2 + Ca(H_2PO_4)_2{\cdot}H_2O + 7H_2O \rightarrow 4CaHPO_4{\cdot}2H_2O \quad (2.2)$$

The second type of setting reaction occurs when the initial and final calcium phosphate compounds have the same Ca/P molar ratio [26]. Typical examples are cements composed of α-TCP and an aqueous solution [38], β-TCP and an aqueous solution [39].

$$3\ \alpha\text{-}Ca_3(PO_4)_2 + H_2O \rightarrow Ca_9(HPO_4)(PO_4)_5(OH) \quad (2.3)$$

$$3\ \beta\text{-}Ca_3(PO_4)_2 + H_2O \rightarrow Ca_9(HPO_4)(PO_4)_5(OH) \quad (2.4)$$

According to the end products of setting reaction, all CPC formulations could be divided into two groups: apatite CPC and brushite CPC [26, 27]. Apatite cements usually form precipitated HA or CDHA as the main end product [26]. Brushite cements form DCPD as the end product of setting reaction [26].

2.3.3 Biological properties of CPC

Several *in vivo* studies have demonstrated the excellent biocompatibility and osteoconductivity of CPC [40-43]. CPC is also resorbable. The resorption of CPC is influenced by its physicochemical properties, such as chemical composition, crystal structure, density and porosity [27]. Experimental conditions, for instance, implantation sites, experimental models and animal species, also influence the resorption of CPC [44]. Brushite CPC undergoes faster resorption than apatite CPC since DCPD has higher solubility than HA under normal physiological conditions [45]. During resorption, CPC is gradually replaced by new bone [43, 46]. To achieve

optimum clinical results, the rate of cement resorption should be adjusted to match that of new bone formation [27].

2.3.4 Clinical and medical applications of CPC

Due to its excellent biocompatibility, osteoconductivity and bone replacement capability, CPC has been used in a wide range of clinical applications. Examples include the treatment of maxillofacial defects and deformities, unstable fractures, and osteoporosis related fractures [47-50]. CPC is also promising for dental applications, including root canal filling [51], ridge augmentation [52] and periodontal defects healing [40].

2.4 New developments in CPC

In recent years, several CPCs with improved properties have been developed to meet the clinical requirements.

2.4.1 Injectable CPC

Over the last few years, the application of CPC in minimally invasive surgery aimed for the reconstruction of bone defects has attracted much attention [6, 53, 54]. The cement paste can be extruded into the defective area through a thin long needle attached with a syringe. Unfortunately, the injectability of most CPCs is not satisfactory for their potential clinical use [55].

Bohner and Baroud [56] investigated the injectability of calcium phosphate pastes using a theoretical approach. They related the poor injectability to the concept of

“filter pressing”, in which the pressure applied to the cement paste leads to the separation of the solid and liquid phases [56]. Habib et al. [57] further studied the mechanisms underlying the poor injectability. These investigators observed that a continuous solid–liquid separation process occurred during the course of the injection of a poorly injectable paste [57]. The extruded paste contained excess liquid whilst the water content in the paste remaining in the syringe was reduced [57]. These results suggest that the poor injectability of the paste is consequence of migration of the liquid phase [57]. The solid particles plugged the tip of the syringe while the liquid phase passed through.

Factors that influence the injectability of CPC have been extensively investigated [32, 36, 56-59]. Key factors relating to the cement composition included the powder to liquid ratio, the particle shape, the particle size distribution and the liquid viscosity [32, 56, 60, 61]. Important process parameters included the post-mixing time interval, the injection force, the delivery rate and the geometry of the injection system [36, 54, 56, 58, 59, 62].

In the literature, several approaches have been proposed to improve the injectability of calcium phosphate pastes [58, 63, 64]. One approach involved the modification of liquid phase with additives. Gbureck et al. [58] used a trisodium citrate solution as the liquid phase. Adsorption of citrate ions onto the particle’s surface led to a high surface charge for the calcium phosphate particles [58]. The viscosity of the cement paste

decreased and its injectability improved [58]. Baroud et al. [63] found that the addition of xanthan into the liquid phase increased the viscosity of the cement paste and improved the injectability. Leroux et al. [64] experimented with lactic acid, glycerol and sodium glycerophosphate to improve the injectability of a CPC.

As well, physical changes have also been used to improve the injectability. Ishikawa et al. [55] noted that the cement injectability could be improved by utilizing spherical TTCP particles. However, this strategy led to a limited apatite formation and reduced mechanical strength. Baroud et al. [63] improved the cement's injectability through optimizing the particle size distribution by milling. Habib et al. [65] confirmed that ultrasonication provides an effective method to improve the injectability of an aqueous calcium phosphate paste.

2.4.2 Premixed CPC

A drawback of CPC relates to its handling properties. Most of the currently available CPCs consist of a powder and a liquid [60]. The cement paste must be prepared just before use because the setting reaction commences when the powder comes in contact with water [50]. This raises concerns about insufficient mixing and resulting product inhomogenity which may compromise the performance of the implant [66-68]. Chow [60] noted that "*the ability of the surgeon to properly mix the cement and then place the cement paste in the defect within the prescribed time is a crucial factor in achieving optimum results*." It has been reported that the clinically induced

variability has an influence on the mechanical strength of zinc phosphate dental cement [69]. A further concern relates to the increase of the surgery time required for preparation of cement paste in the operation theatre [50]. In total knee replacement surgery, the duration of the surgical procedure has been found to increase the risk of postoperative infection [70].

Consequently, it is desirable to develop a premixed CPC that can be prepared in advance which is also stable in the package until use. The key point is to use a non-aqueous but water-miscible liquid to prepare the cement paste. The water-free cement paste is stable in the package and hardens only upon being delivered to the damaged area. The exchange of non-aqueous liquid with the surrounding physiological liquid leads to the hardening of CPC [71]. The principal advantages of premixed CPCs include: (1) as the cement paste is prepared in advance under well-controlled conditions, the risk of operator-induced error is reduced [72]; (2) the premixed cement paste can be directly applied by the surgeon, resulting in a reduced surgery time; (3) the cement paste won’t harden until get contact with physiological liquid, thereby providing the surgeon with sufficient operating time as needed.

In 1990, Sugawara et al. [73] developed a premixed CPC formulation containing glycerol as the liquid phase. The glycerol containing cement paste was stable in the syringe and hardened only after delivery to the root canal [73]. Subsequently, Sugawara et al. [74] proposed the use of polyethylene glycol (PEG) as the liquid

phase for premixed CPC. These premixed CPCs, designed as endodontic materials for root canal sealing, exhibited strong biocompatibility to periapical bone tissue [74]. However, the glycerol containing CPC paste did not provide good washout resistance when used in an open wet field [71]. To improve the washout resistance, different gelling agents such as hydroxypropyl methylcellulose (HPMC) [71] and chitosan malate [66] were added to the premixed CPC formulations. Xu et al. [67] developed fast-setting premixed CPC formulations by incorporating hardening accelerators including tartaric acid, malic acid, malonic acid, citric acid and glycolic acid. Xu et al. [68] fabricated premixed macroporous CPC scaffold by the addition of mannitol as porogen.

Table 2.2 summarizes the formulations of some premixed CPCs. Most of the premixed CPCs are apatite cements which form HA as the major product. Recently, several premixed brushite cements have been developed [75, 76].

2.5 Bone tissue engineering scaffolds

2.5.1 Bone tissue engineering

During the last few years, bone tissue engineering has emerged as a promising approach to the repair of bone defects. A common tissue engineering approach is to seed specific cells on a scaffold under controlled culture conditions [77]. Subsequently, the resulting tissue engineering construct is implanted into the defective bone area of the patient in order to generate new tissue formation [77]. In

Table 2.2 Formulations of some premixed CPCs.

Cement powder	Non-aqueous, water-miscible liquid	Gelling agent	Hardening accelerator	Ref
(TTCP + DCPA) or (TTCP + DCPD) + 2.8 wt% HA + 0.2 wt% NaF	Glycerol			[73]
TTCP + DCPA + 15 wt% ZrO_2	PEG			[74]
TTCP + DCPA, α-TCP + $CaCO_3$, DCPA + $Ca(OH)_2$	Glycerol	HPMC	Na_2HPO_4	[71]
TTCP + DCPA	Glycerol (a,c), Polypropylene glycol (b)	HPMC(a,b), chitosan malate (c)	MCPM (a), D-tartaric acid (b), $Ca(OH)_2$ (c)	[66]
TTCP + DCPA	PEG	HPMC	Tartaric acid, malic acid, malonic acid, citric acid, glycolic acid	[67]
TTCP + DCPA	Glycerol	HPMC	MCPM	[68]
β-TCP + MCPM	Glycerol, PEG			[75]
β-TCP + MCPM	Glycerol	HPMC		[76]

this approach, the scaffold serves as an adhesive substrate for the seeded cells and to support cell proliferation, differentiation and the formation of new tissues [10, 78]. In parallel with tissue formation, the scaffold gradually degrades and is eventually eliminated [78].

2.5.2 Characteristics of an ideal tissue engineering scaffold

Hutmacher [79] has summarized the characteristics of an ideal scaffold for tissue engineering applications:

(1) The scaffold should have a three-dimensional and highly porous structure with an interconnected pore network for cell growth and flow transport of nutrients and metabolic waste [79].

(2) The scaffold should be biocompatible [79].

(3) The scaffold should be bioresorbable with a controllable degradation and resorption rate to match the ingrowth rate of cell/tissue *in vitro* and/or *in vivo* [79].

(4) The scaffold should provide suitable surface chemistry for cell attachment, proliferation and differentiation [79].

(5) The mechanical properties of the scaffolds should match as closely as possible those of the tissues at the implantation site [79].

In addition, Rezwan et al. [77] noted some other highly desirable features concerning the scaffold processing, such as “near-net-shape fabrication” and

“scalability for cost-effective industrial production”.

2.5.3 Scaffold materials

The key properties of a scaffold depend primarily on the nature of material and the fabrication process [13]. In the following section, several scaffold materials are reviewed.

A wide variety of materials, both natural and synthetic, have been studied for the design and fabrication of bone tissue engineering scaffolds [10]. These include ceramics, natural and synthetic polymers.

2.5.3.1 Ceramics

Bioceramics, such as HA, β-TCP and bioactive glasses, have been intensively investigated as scaffold materials for bone tissue engineering scaffolds.

HA ceramic has a chemical composition similar to the mineral component of bone [80]. Previous studies have demonstrated that HA ceramic is biocompatible and osteoconductive [81-83]. HA ceramics have been used in dental, craniofacial and orthopaedic surgery in the form of granules or blocks [84, 85]. However, the major limitations to the use of HA ceramic as scaffold material are its brittleness and difficulty to processing [86].

β-TCP is a calcium phosphate ceramic with a Ca/P ratio of 1.5. It has a stoichiometry similar to amorphous bone precursors [3]. Both *in vitro* and *in vivo*

assessments have demonstrated that β-TCP provides excellent biocompatibility and osteoconductivity [87, 88]. β-TCP has been used in orthopaedic and dental applications [89, 90]. However, the use of β-TCP is limited by its rapid and uncontrolled rate of degradation, coupled with poor mechanical properties [91, 92].

An important biological property of bioactive glasses is their bioactivity, which means they can bond to hard and soft tissues [93]. The bone bonding ability of the glasses has been attributed to their ability to form a surface layer of hydroxycarbonate apatite (HCA) [94]. Hench LL and his colleagues [95] first observed this bioactive behavior in a group of glasses belonging to the SiO_2–Na_2O–CaO–P_2O_5 system. The biocompatibility and osteoconductivity of bioactive glasses were confirmed [96, 97]. Bioactive glasses have been exploited in dental, orthopaedic, maxillofacial and otolaryngological applications [98].

2.5.3.2 Natural polymers

A number of natural polymers have been studied and proposed for biomedical applications, namely polysaccharides (alginate, agarose, chitin/chitosan, starch, hyaluronic acid derivatives) or proteins (collagen, fibrin gels, silk, soy) and, as reinforcement, various biofibres such as lignocellulosic natural fibres [77, 99].

Starch is a polysaccharide present as granules in the roots, stems and seeds of a variety of plants, such as rice, wheat, barley, corn and potatoes [100]. Starch consists of two major components: amylose and amylopectin. Amylose is a linear polymer

consisting of α-(1→4)-glucan while amylopectin is a highly branched polymer [99]. Starch-based blends have been widely used in a range of biomedical applications, such as tissue engineering scaffolds [101, 102], bone cements [103, 104], drug delivery devices [103, 105, 106], and bone replacement applications [107].

Chitosan is a basic linear polysaccharide. It is a partially deacetylated derivative of chitin, which is the second most abundant natural polysaccharide on the earth's surface [108]. Chitosan is soluble in weak acids (pH < 6.3) and can be easily processed and purified [108]. Chitosan has several advantages including biocompatibility, biodegradability, low toxicity, high anti-microbial activity and low production cost [109, 110]. Chitosan has been studied for use in various biomedical applications, including wound dressings [109], drug delivery systems [110, 111] and tissue engineering scaffolds [112].

Collagen is the most abundant protein in the human body [113]. It is a key constituent of the extracellular matrix (ECM), and it provides structural integrity and tensile strength to tissues [113]. To date, 28 collagen types have been identified [114]. I, II, III, and V are the main types which make up the essential part of collagen in bone, tendon, cartilage, muscle and skin [114]. Collagen has been used in a variety of tissue engineering applications since it has low antigenicity, high water affinity, very good cell compatibility and ability to promote tissue regeneration [115]. It is naturally degraded by metalloproteases, in particular,

collagenase and serine proteases [116]. Thus, its degradation can be locally controlled by cells present in the engineered tissue [116].

2.5.3.3 Synthetic polymers

Compared with natural polymers, synthetic polymers are postulated to be more promising. Since the synthesis process can be strictly controlled, synthetic polymers have in general predictable and reproducible physical and mechanical properties [77].

The most extensively used synthetic biodegradable polymers in tissue engineering applications are saturated poly(α-hydroxy esters), including PLA, PGA, PCL, as well as poly(lactic-*co*-glycolide) (PLGA) copolymers [77]. The chemical structures of PLA, PGA, PLGA and PCL are listed in Table 2.3. These polymers have been shown to degrade primarily as a consequence of hydrolysis of ester bonds into acidic monomers, which then may be removed from the body by normal metabolic pathways [117, 118]. Furthermore, the degradation rates can be adjusted by using various molecular weights and copolymers [77]. PLA, PGA and PLGA are biocompatible and have been approved by the United Sates Food and Drug Administration (FDA) for specific human clinical applications such as surgical sutures [78].

PGA is the simplest linear aliphatic polyester [119]. It has a high melting point

Table 2.3 Synthetic biodegradable polymers.

Synthetic biodegradable polymers	Chemical structure
PLA	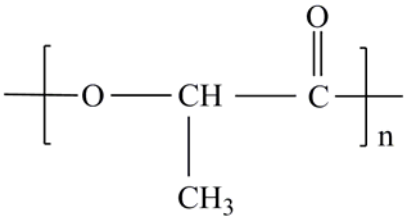
PGA	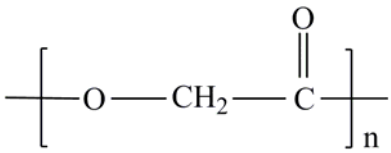
PLGA	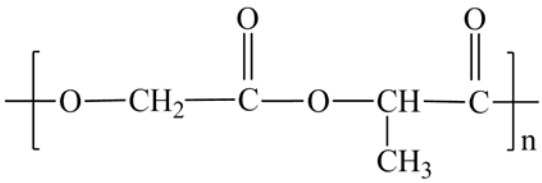
PCL	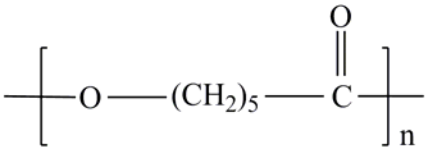

(220–225 °C) and a high glass transition temperature (35–40 °C) [120]. PGA is insoluble in most organic solvents as a consequence of its high crystallinity [119].

PLA has three forms: poly(L-lactide) (PLLA), poly(D-lactide) (PDLA), and racemic mixture of poly(DL-lactide) (PDLLA) [77]. Because of the hydrophobic methyl group in the backbone, PLA has a slower degradation rate than PGA [121].

PLGA is a copolymer of lactide and glycolide. There is no linear relationship between the composition of copolymer and the mechanical and degradation properties [119]. For example, a copolymer of 50% glycolide and 50% DL-lactide degraded faster than either homopolymer [122].

Some disadvantages of PLA and PLGA are their hydrophobicity, which hinders even seeding of sufficient cell mass in three dimensions, and the release of acidic degradation products, which may adversely affect biocompatibility [78, 123].

PCL is biodegradable and biocompatible aliphatic polyester. Its glass transition temperature is around –60 °C, thereby producing in the compound a rubbery state at room temperature [124]. PCL has a relatively low melting point around 60 °C, thus can be easily processed by conventional procedures [99]. The degradation of PCL involves random hydrolytic chain scission of the ester linkages [99]. PCL has been approved as safe by the United Sates FDA for clinical use [124].

However, drawbacks have limited the use of PCL as scaffold material. Owing to its

semicrystalline nature and hydrophobicity, the degradation of PCL is rather slow and may require 3–4 years for total degradation in some conditions [125, 126]. The hydrophobicity of PCL has also led to limited cell-scaffold interactions [127].

2.5.4 Composite scaffolds of PCL/natural polymer

As previously mentioned, the necessary requirements for successful scaffold materials are numerous. In order to satisfy as many requirements as possible, scaffolds that are made of composites and contain at least two or more materials appear to be a promising choice. This review focuses on the development of PCL-based composite scaffolds for tissue engineering applications.

Blending PCL with natural polymer offers an attractive approach to develop composite scaffold materials.

2.5.4.1 PCL/starch composite scaffolds

Blends of PCL with starch have been proposed as potential biodegradable materials for fabricating tissue engineering scaffolds. Ciardelli et al. [100] found that blending PCL with hydrophilic natural polymer such as starch was a promising way to improve the biocompatibility of PCL. The results of cell adhesion tests confirmed that the inclusion of starch greatly increased fibroblast adhesion when compared to PCL alone [100]. Gomes et al. [128] prepared starch-PCL fibre-mesh scaffolds by a fibre-bonding process. The results of *in vitro* degradation tests indicated that the obtained scaffolds are susceptible to enzymatic degradation [128]. Moreover, Duarte

et al. [129] systematically investigated the enzymatic degradation of starch-PCL scaffolds prepared by supercritical fluid technology and found that the scaffolds underwent bulk degradation.

2.5.4.2 PCL/chitosan composite scaffolds

The use of PCL-chitosan blends for tissue engineering applications has also been studied [130, 131]. Sarasam et al. [130] reported the production of porous scaffolds by freeze drying using 25% acetic acid solution as the solvent. Wan et al. [131] used particulate leaching method to fabricate the scaffolds. The authors investigated the degradation behavior of the scaffolds in PBS or enzymatic solutions [131]. The results showed that degradation of the PCL component can be accelerated depending on the scaffold composition and the media [131]. In addition, the acidic degradation products of the PCL component were effectively buffered by chitosan [131]. Recently, processing of PCL-chitosan blend in the form of fibers has been reported. Malheiro et al. [132] produced PCL–chitosan blend fibers by wet spinning using a common solvent mixture. Moreover, Neves et al. [133] developed PCL–chitosan blend fiber-mesh scaffolds and examined their suitability as support structures for articular cartilage tissue repair.

2.5.4.3 PCL/collagen composite scaffolds

Collagen in the native ECM serves as an adhesive protein that enhances attachment and subsequent proliferation of cell [114]. Clearly, the incorporation of collagen into

PCL scaffolds may help improve the biocompatibility of the scaffolds. Lee et al. [134] developed composite vascular scaffolds by electrospinning PCL and type I collagen. The composite scaffolds exhibited excellent biomechanical properties and provided a favorable environment that supports adhesion and proliferation of vascular cells [134]. Venugopal et al. [135] fabricated PCL-collagen biocomposite nanofibre scaffolds by electrospinning. Human coronary artery smooth muscle cells were seeded onto the scaffolds and their proliferation was quantified. Compared to PCL nanofibre scaffolds, cell proliferation on PCL-collagen nanofibre scaffolds increased up to 63%, 73% and 82% after 2, 4 and 6 days [135].

2.5.5 Composite scaffolds of PCL/ceramic

Incorporating an inorganic ceramic phase into PCL is another attractive approach to develop successful composite scaffold materials. Combining a ceramic phase with PCL may provide a promising combination of bioactivity, mechanical strength and biodegradability [136, 137].

2.5.5.1 PCL/HA composite scaffolds

HA has been used in clinic applications for bone regeneration due to its excellent biocompatibility and osteoconductivity [81, 82]. However, a significant limitation of HA is its intrinsic brittleness [86]. As well, a drawback of PCL is a lack of bioactivity [137]. However, the inclusion of HA into PCL matrix presents a potential way to combine the mechanical reliability of the polymer phase with the excellent

osteoconductivity of the HA phase.

Lebourg et al. [138] investigated *in vitro* mineralization of the PCL-HA scaffolds in SBF after or without a nucleation treatment. The composite scaffolds demonstrated enhanced bioactivity caused by the incorporation of HA and the nucleation treatment. Moreover, Heo et al. [137] examined the effect of HA particle size on the mechanical properties, wettability and *in vitro* biocompatibility of the PCL-HA composite scaffolds. The results showed that the scaffolds containing nano-sized HA particles had higher compressive modulus and hydrophilicity than the scaffolds containing micro-sized HA. The cell attachment and proliferation were better on the scaffolds with nano-sized HA.

2.5.5.2 PCL/TCP composite scaffolds

As a bioactive and biocompatible ceramic, TCP has been incorporated into PCL to fabricate composite scaffolds with both bioactive and biodegradable properties.

Lei et al. [139] investigated the bioactivity of PCL-TCP composite scaffolds composed of 80% PCL and 20% TCP. These scaffolds exhibited a bioactive nature by nucleating the formation of HA on their surface upon immersion in SBF (simulated body fluid). Yeo et al. [140] studied the *in vitro* and *in vivo* degradation behavior of PCL-TCP composite scaffolds. Their results revealed that the degradation *in vivo* was more rapid than that *in vitro*. After implantation in the rats' abdomen for 6 months, a decrease of 88.7% by molecular weight average was

reported. Lam et al. [141] investigated the degradation of PCL-TCP and PCL scaffolds in alkaline medium. The results indicated that the incorporation of β-TCP reduced the hydrophobicity of the polymer and significantly increased the degradation rate.

2.5.5.3 PCL/bioactive glasses composite scaffolds

In recent studies [142-144], bioactive glasses have been incorporated into PCL matrix to enhance the bioactivity.

Li et al. [143] produced PCL–mesoporous bioactive glass composite scaffolds and demonstrated that the incorporation of bioglass can improve the hydrophilicity and the bioactivity of the resulting composites. Fabbri et al. [142] developed highly porous PCL–Bioglass®45S5 scaffolds and evaluated the ability of the composites to induce HA precipitation by *in vitro* immersion tests. After 4 weeks of immersion in SBF, only the samples containing 50 wt% of bioglass developed a stable layer of apatite [142]. The results indicated that high contents of bioglass and long immersion time in SBF favored the precipitation of HA.

2.5.6 Zein

Zein is a corn protein which represents about 80% of the total proteins in corn grains [145]. It has been used in a wide range of applications, such as adhesives, biodegradable plastics, coating for food products and fibers [146]. Owing to its nontoxicity, good biodegradability and biocompatibility, zein has a great potential for

use in biomedical applications. Zein has been used for preparing microspheres as drug delivery systems [147, 148]. Both zein and its degradation products exhibited good cell compatibility [147, 149, 150]. Recently, three-dimensional porous zein scaffolds have been developed for tissue engineering applications [151-153]. *In vitro* tests showed that porous zein scaffolds could support the adhesion, proliferation and osteoblastic differentiation of human mesenchymal stem cells (hMSCs) [153]. The results of an *in vivo* study using a rabbit subcutaneous implantation model demonstrated the good tissue compatibility and degradability of the zein scaffolds [152]. In addition, the porous zein scaffolds degraded completely within 8 months [152].

2.5.7 Magnesium phosphate cement

Given its fast setting and high early strength properties, magnesium phosphate cement (MPC) has been used in civil engineering for rapid repair of concrete [154]. The principal components of MPC include magnesium oxide (MgO) and ammonium dihydrogen phosphate ($NH_4H_2PO_4$) [155]. MPC powder reacts with water to form $NH_4MgPO_4 \cdot 6H_2O$ (struvite) as the major hydration product [156]. In recent years, clinic applications of MPC as bone substitution materials have attracted much attention [157]. Liu [158] first applied MPC as inorganic bone adhesive in screw fixation, artificial joints fixation and comminuted fracture fixation. Wu et al. [159, 160] investigated the use of MPC in the treatment of tibial plateau fractures of rabbits. The results indicated that MPC degraded gradually and the ingrowth of new

bone was detected after implantation for 3 weeks. At 9 weeks after implantation, the fracture was healed without displacement and MPC was completely resorbed. Yu et al. [161] evaluated the *in vivo* biocompatibility of MPC by implantation into the cavities of rabbits' femur condyles for 6 months. No foreign body reaction, inflammation and necrosis were observed throughout the observation period [161]. It was observed that MPC formed direct bonding with host bone [161]. The results of histological studies and macroscopic evaluation suggested that MPC has good *in vivo* biocompatibility and degradability.

2.5.8 Processing techniques for composite scaffolds

There are numerous techniques to fabricate composite scaffolds, including solvent casting and particulate leaching [143, 144], thermally induced phase separation [136, 162], microsphere sintering [163], scaffold coating [164, 165], solid freeform fabrication [166], precision extrusion deposition [167], selective laser sintering [100, 168] and electrospinning [134].

In the present research, the PCL-based composite scaffolds were fabricated using particulate leaching technique. This technique was chosen because of its ease of processing. The pores are created by washing out the particles. Moreover, the particulate leaching is a low-temperature processing method which helps preserve the properties of polymer [144]. Blaker et al. [169] produced composites of PDLLA and Bioglass® using high-temperature extrusion and compression moulding. They

demonstrated that, in the presence of Bioglass®, the high-temperature processing method led to the degradation of PDLLA [169].

The ideal particulates could be NaCl and/or $NaHCO_3$, as suggested by Cannillo et al. [144]. The chloride and bicarbonate salts can be easily removed from the matrix due to their high solubility in water. Furthermore, if trapped in the scaffold, these salts do not release any dangerous ions for human body [144]. Na^+, Cl^- and HCO_3^- ions are abundant in the human plasma [170].

The suitability of the particulate leaching technique for producing PCL-based composite scaffolds has been proven by several studies reported in literature. For instance, Li et al. [143] produced composite scaffolds of PCL and mesoporous bioactive glass by the solvent casting–particulate leaching method. Moreover, via the particulate leaching technique, Cannillo et al. [144] fabricated Bioglass®45S5-PCL composite scaffolds with interconnected pore structure suitable for bone regeneration and vascularization. Guarino et al. [171] produced PCL-HA porous scaffolds by the phase inversion and particulate leaching method.

2.6 The research gap

Owing to its bioactivity, osteoconductivity and bone replacement capability, CPC is a promising candidate as bone graft substitute. However, the injectability of most CPCs cannot meet the stringent requirement of clinical use [55]. The cement's injectability has been found to relate to the post-mixing time interval [32, 62]. The

injectability worsened with the extension of time after mixing [32, 62]. Based on this observation, premixed CPC should be advantageous since the injectability would "remain essentially constant with time", as noted by Chow [60]. Most CPCs reported in the literature hardened to form apatite as the final product [172]. A significant disadvantage of CPC is its slow resorption rate *in vivo* due to the low solubility of stoichiometric HA with Ca/P ratio of 1.67 [173]. Liu et al. [174] suggested that the resorption rate of CPC *in vivo* could be controlled to certain extent by adjusting its Ca/P ratio. A CPC with Ca/P ratio of 1.5 was reported to degrade faster than the CPC with Ca/P ratio of 1.67 after implantation *in vivo* [175]. There are few previous reports about the preparation of premixed CPC forming calcium deficient apatite as the final product [66, 67, 71].

Bone tissue engineering is a promising approach to the repair of bone defects. In this approach, scaffolds alone or in combination with growth factors and/or cells are used to guide bone regeneration and repair defects [10]. One of the key challenges associated with bone tissue engineering is the design and fabrication of scaffolds with optimal characteristics. Among the synthetic polymers used for fabrication of scaffolds, PCL has been commonly used because of its high biocompatibility and ease of processing property. However, some drawbacks have limited the use of PCL as scaffold material, such as its slow degradation rate and hydrophobic surface property.

Chapter 3

Premixed, injectable PLA-modified calcium deficient apatite biocement (cd-AB) with washout resistance

F. Wu [a], Y. Ngothai [a], J. Wei [b], C. Liu [b], B. O'Neill [a], Y. Wu [b]

[a] School of Chemical Engineering, The University of Adelaide, Adelaide, SA 5005, Australia
[b] The State Key Laboratory of Bioreactor Engineering, and Engineering Research Center for Biomedical Materials of Ministry of Education, East China University of Science and Technology, Shanghai 200237, China

This is a revised and corrected version of the paper which appears in:

Colloids and Surfaces B: Biointerfaces, 2012, 92, 113–120.

STATEMENT OF AUTHORSHIP

Premixed, injectable PLA-modified calcium deficient apatite biocement (cd-AB) with washout resistance

Colloids and Surfaces B: Biointerfaces, 2012, 92, 113–120.

Fan Wu (Candidate)

Designed and performed experiments, interpreted and processed data, wrote manuscript and acted as corresponding author

I hereby certify that the statement of contribution is accurate

Signed ……..Date.……..

Yung Ngothai

Manuscript evaluation

I hereby certify that the statement of contribution is accurate and I give permission for the inclusion of the paper in the thesis

Signed.……..Date.……...

Jie Wei

Helped with the design of experiments and manuscript evaluation, acted as corresponding author

I hereby certify that the statement of contribution is accurate and I give permission for the inclusion of the paper in the thesis

Signed ……Date.……...

Changsheng Liu

Manuscript evaluation

I hereby certify that the statement of contribution is accurate and I give permission for the inclusion of the paper in the thesis

Signed ……..Date.……..…

Brian O’Neill

Manuscript evaluation

I hereby certify that the statement of contribution is accurate and I give permission for the inclusion of the paper in the thesis

Signed ……..*Date*.……..

Yuequn Wu

Assisted with experiments

I hereby certify that the statement of contribution is accurate and I give permission for the inclusion of the paper in the thesis

Signed ……..*Date*.……..

Chapter 3 Premixed, injectable PLA-modified calcium deficient apatite biocement (cd-AB) with washout resistance

3.1 Introduction

The use of CPC as a biomaterial for bone reconstruction has been well studied [71, 174]. CPC consists of an equimolar mixture of TTCP and DCPA. Upon mixing with water, the cement paste hardens within 30 min and forms HA as the final product [25]. With characteristics of easy manipulation, good moldability, excellent biocompatibility and osteoconductivity, CPC is a promising material for bone regeneration [27]. One disadvantage of CPC is the need to mix the cement powder uniformly with the liquid and place the paste into the defect in a prescribed time before the paste hardens [66-68, 71]. This increases the surgical operating time and raises concerns about insufficient mixing which may compromise the implant performance [66-68]. Thus, premixed CPC was developed to overcome such problems. The CPC powder was mixed with a non-aqueous but water-miscible liquid in advance under well-controlled conditions [71]. This water-free cement paste was stable in the package and hardened only upon contact with an aqueous environment. Once the paste was placed into a physiological solution, the exchange of non-aqueous liquid with aqueous liquid occurred, resulting in the hardening of CPC [71]. Most of the CPCs reported in the literature hardened to form apatite as the final product [172]. There were few previous reports about the preparation of premixed CPC forming calcium deficient apatite as the final product [66, 67, 71].

A major shortcoming of CPC is its slow resorption rate *in vivo* due to the low solubility of stoichiometric HA with a Ca/P ratio of 1.67 [173]. For some clinical applications, it would be desirable to obtain a more rapid resorption and replacement by new bone. The resorption properties of bioceramics are generally believed to relate to their solubility [27] and porosity [176]. Driessens [177] found that CDHA had a higher solubility than stoichiometric HA due to calcium deficiency in the crystal. A CPC with Ca/P ratio of 1.5 was reported to degrade faster than the CPC with Ca/P ratio of 1.67 after implantation *in vivo* [175]. Liu et al. [174] suggested that the resorption rate of CPC *in vivo* could be controlled to certain extent by adjusting its Ca/P ratio. Previous studies demonstrated that HA with Ca/P ratios ranging from 1.67 to 1.5 can be formed from cement-type reaction between TTCP and DCPA in physiological environment [174]. Brown and Fulmer [178] reported a calcium deficient apatite with a Ca/P of 1.5 formed from the hardening of a mixture of TTCP and DCPA with molar ratio of 0.5.

With the increasing demand of minimally invasive techniques in surgical procedures, much effort has been invested in the development of injectable CPC [6, 54]. The factors affecting the injectability of CPC have been investigated extensively [32, 36, 56-59]. Some factors relate to the cement composition, such as: powder to liquid ratio, particle size and shape, particle size distribution, liquid viscosity [32, 56, 60, 61]. Other factors relate to process parameters, such as: the injection force, the delivery rate and geometry of the injection system [36, 54, 56, 58, 59]. Several researchers have

found the injectability of CPC had a strong dependence on the post-mixing time interval [32, 62]. The injectability worsened with the increase of time after mixing [32, 62]. Considering this, premixed CPC might be advantageous since the injectability would “remain essentially constant with time”, as noted by Chow [60].

The aim of this work was to develop a premixed, injectable calcium deficient apatite biocement (cd-AB) with a Ca/P ratio of 1.5. The cement paste could be produced under well-controlled conditions in advance, avoiding the need for on-site powder-liquid mixing during surgery [67]. It was assumed that the low Ca/P ratio would be beneficial to the rapid resorption of the apatite precipitate. PLA was dissolved in N-methyl-2-pyrrolidone (NMP) to form PLA-NMP solutions which were used as the liquid phase of the premixed cd-AB. NMP was selected since it is water-miscible and has been used in a few commercially available injectable formulations [179-181]. PLA is a biocompatible polymer widely used in biomedical applications [182]. The influences of PLA content on the physicochemical properties of the premixed cd-AB were investigated. The *in vitro* degradability of premixed cd-AB was studied by immersion in Tris-HCl solution, and the cytocompatibility of premixed cd-AB to MG-63 osteoblast-like cells was assessed.

3.2 Materials and methods

3.2.1 Cement powder and cement liquids

The calcium phosphates used in this experiment were prepared in our laboratory, and

the preparation methods can be obtained from the relevant literature [49]. The cd-AB powder was composed of TTCP and DCPA in a molar ratio of 1:2 [174]. TTCP was synthesized by a solid-to-solid reaction between calcium phosphate and calcium carbonate at a temperature of 1500 °C for 8 h [49]. DCPD was prepared from $(NH_4)_2HPO_4$ and $Ca(NO_3)_2$ in an acidic environment [49]. DCPA was obtained by removing the crystallization water in DCPD by heating at 120 °C [49].

Deionized water was used as the liquid phase for conventional cd-AB. The liquid phases for premixed cd-AB were PLA-NMP solutions prepared by dissolving PLA pellets in NMP (Sinopham Chemical Reagent Co., Ltd.) at 60 °C for 6 h. The PLA concentrations of 10%, 15% and 20% were selected based on achieving good washout resistance in preliminary results.

3.2.2 Evaluation of washout resistance

The powder-to-liquid (P/L) ratio of 3 g/g was used for preparing premixed cd-AB and conventional cd-AB pastes. The cement powder and liquid were mixed properly to form a homogeneous paste, which was then placed into a 2.5 mL disposable syringe with a nozzle diameter of 2.0 mm. The paste was extruded through the syringe into the water and shaken at 100 rpm for 5 min at 37 °C. The material was considered to pass the washout resistance test if the paste did not visibly disintegrate in the water [66, 71]. Quantitative measurements of, e.g. washout mass loss ratio, were not done considering the exchange of the solutions [75].

3.2.3 Setting time

The premixed cd-AB and conventional cd-AB pastes were prepared with P/L ratios ranging from 2 to 3.5 g/g. The cement powder and liquid were mixed using a spatula to form a homogeneous paste which was then placed into plastic tubes (diameter: 6 mm, height: 3 mm). The tubes containing premixed cd-AB were immersed in deionized water kept in a 100% relative humidity environment at 37 °C. The tubes containing conventional cd-AB were stored in the 100% relative humidity environment at 37 °C.

The setting time was measured according to the method described in ASTM Test Method C 187–98 using a Vicat apparatus which consists of a frame bearing a movable rod, weighing 300 g, with a 1 mm stainless steel needle at the end [183, 184]. At different time point, the cement samples were removed from the 100% relative humidity environment and centered under the 1 mm end of the needle. The rod was lowered vertically onto the cement surface. The cement is considered to have set when the needle penetrates less than 1 mm into the sample. The time measured from the paste being immersed in the water to this point was taken as the setting time. Each experiment was performed in triplicates.

3.2.4 Compressive strength

The premixed cd-AB and conventional cd-AB pastes were prepared with P/L ratios ranging from 2 to 3.5 g/g. The premixed cd-AB paste was loaded into a polytetrafluoroethylene (PTFE) mold (diameter: 6 mm, height: 10 mm), which was

immersed in deionized water kept in a 100% relative humidity (RH) environment at 37 °C. After 6 h, samples were removed from the mold and immersed in deionized water for 66 h. The conventional cd-AB paste was placed into a glass tube (diameter: 6 mm, height: 10 mm), which was then stored in a 100% relative humidity environment at 37 °C for 3 days.

Before testing, both sides of the hardened samples were uniformly polished. The compressive strength of the sample was measured at a loading rate of 1 mm/min using a universal testing machine (AG-2000A, Shimadzu Autograph, Shimadzu Co., Ltd., Japan). Three replicates were performed for each group.

3.2.5 Analysis by XRD, FTIR and SEM

The premixed cd-AB and conventional cd-AB samples (diameter: 6 mm, height: 10 mm) were prepared as the method described in Section 3.2.4 with P/L ratio of 3 g/g. After hardening for 3 days, the cement samples were dried and ground into powder by mortar and pestle. The composition of the hardened samples was characterized by X-ray diffraction (XRD; D/MAX 2550, Rigaku) with Cu K_α radiation and Ni filter (λ =1.5406 A, 100 mA, 40 kV) in a continuous scan mode. The 2θ range was from 10° to 80° at a scanning speed of 10 °/min. The cement samples and PLA pellets were also analysed by Fourier transform infrared (FTIR) spectroscopy (Magna-IR 550, Nicolet). Scanning electron microscopy (SEM; JSM6360, JEOL) was used to examine the fracture surface morphology of the cement samples.

3.2.6 Injectability of the cement

The premixed cd-AB and conventional cd-AB pastes were prepared with P/L ratios ranging from 2 to 3.5 g/g. The injectability of the cement paste was measured according to the method described by Khairoun et al. [32] with some modifications. The 2.5 mL disposable syringes with a nozzle diameter of 2.0 mm were used for injectability measurement. The effect of P/L ratio on the injectability of cement pastes was studied when prepared with 10%, 15% and 20% PLA-NMP solutions. First, the cement powder and liquid were manually mixed properly using a spatula to form a homogeneous paste. The paste was placed into a syringe 2 min after the start of mixing. Then the paste was extruded through the syringe by a force of 10 N. The "injectability" was calculated by the weight of the paste extruded through the syringe divided by the original weight of paste in the syringe [6, 32, 58, 62]. Three replicates were carried out for each group.

3.2.7 *In vitro* degradation

The degradation rates of the samples were characterized by their weight loss ratios in 0.05 M Tris-HCl solution (pH 7.4) at different time periods. The premixed cd-AB and conventional cd-AB samples (diameter: 10 mm, height: 3 mm) were prepared as the method described in Section 3.2.4 with P/L ratio of 3 g/g.

Prior to immersion, cement samples were dried at 60 °C for 6 h. The sample, with initial weight W_0, was immersed in Tris-HCl solution at 37 °C with a volume-to-weight ratio of 200 mL/g. The solution was continuously shaken at a rate

of 100 rpm at 37 °C and refreshed every 3 days. After the preselected immersing time, the samples were removed from the solution, rinsed with deionized water and dried at 60 °C for 2 h. Its new weight W_t was recorded. The weight loss ratio of each sample was calculated according to the equation (3.1):

$$\text{weight loss (\%)} = \frac{(W_0 - W_t)}{W_0} \times 100\% \quad (3.1)$$

Three samples of each kind of cement were tested and the results presented as mean ± SD. The surface morphology of the samples after immersion in Tris-HCl solution for 1 and 28 days was characterized by SEM (JSM6360, JEOL; XL30 FEGSEM, Philips). The pH change of the Tris-HCl solution during the immersion of samples was measured using a pH meter (FE20, Mettler Toledo).

3.2.8 *In vitro* cytocompatibility

In vitro cell culture was performed to evaluate the cytocompatibility of the cements. MG-63 osteoblast-like cells were cultured in DMEM medium supplemented with 10% volume fraction of fetal bovine serum (FBS) at 37 °C in a humid atmosphere of 5% CO_2 in air. The medium was replaced every 2 days.

3.2.8.1 Cell proliferation

Three materials were tested: premixed cd-AB, conventional cd-AB, and tissue culture polystyrene (TCP) as a control. The proliferation of MG-63 cells cultured on the samples was assessed quantitatively using a methyl thiazoly tetrazolium (MTT)

assay. The disc-shaped (diameter: 5 mm, height: 2 mm) samples were prepared as the method described in Section 3.2.4 with P/L ratio of 3 g/g. The set samples were sterilized by autoclaving at 121 °C for 20 min and then put in a 96-well plate. Cells were added to each well at a density of 5×10^4 cells/well. The cell-seeded samples were incubated in DMEM–FBS medium at 37 °C in a humid atmosphere of 5% CO_2 in air. The medium was replaced every 2 days. After culturing for 3 and 5 days, 100 μL MTT solution was added into each well. The plate was incubated for further 4 h. The supernatant of each well was then removed and 200 μL dimethyl sulfoxide (DMSO) solution added. After shaking for 10 min, the optical density (OD) at 490 nm was measured with an enzyme-linked immunoadsorbent assay plate reader. Three samples of each kind of cement were tested for each culture time and each test was performed in triplicate.

3.2.8.2 Cell attachment

Three disc-shaped (diameter: 10 mm, height: 2 mm) samples of each cement group were used for cell attachment study. The sterilized samples were put in a 24-well plate. MG-63 cells were seeded onto the cement samples at a density of 1×10^5 cells/well, followed by incubation at 37 °C and 100% humidity with 5% CO_2 in a DMEM–FBS medium. The medium was replaced every 2 days. After culturing for 3 days, the sample-cell constructs were rinsed twice with PBS, fixed with 1% volume fraction of glutaraldehyde and subjected to graded ethanol dehydrations. The samples were air-dried in a desiccator overnight and sputter-coated with gold palladium prior to

SEM observation. The morphology of the cells was observed using SEM (JSM6360, JEOL).

3.2.9 Statistical analysis

All quantitative data are expressed as mean ± standard deviation (SD). Comparisons between the groups were made by using the analysis of variance (ANOVA) test. The level of statistical significance was defined as $p < 0.05$.

3.3 Results

3.3.1 Washout resistance

In Figure 3.1 A, slight disintegration was observed for conventional cd-AB paste. As shown in Figure 3.1 B, no noticeable disintegration occurred for the premixed cd-AB paste prepared with 20% PLA-NMP solution. The premixed cd-AB paste remained stable and began to harden into a solid, exhibiting excellent washout resistance. The preliminary results indicated that the premixed cd-AB paste prepared with higher content of PLA in the liquid phase showed better washout resistance. Thus, 20% PLA-NMP solution was chosen as the liquid phase for premixed cd-AB.

3.3.2 Setting time and compressive strength

Figure 3.2 presents the effect of P/L ratio on the setting time and compressive strength of the different cements. The setting time of premixed cd-AB significantly decreased with increasing P/L ratio ($p < 0.05$). For the lower P/L ratio of 2 g/g, the setting time was over 60 min, whereas for higher P/L ratio of 3.5 g/g, the setting time

A

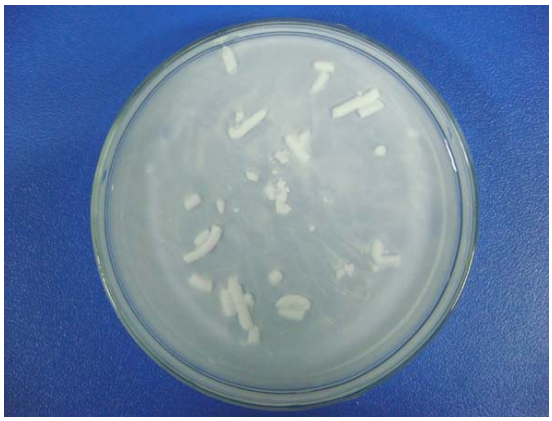

B

Figure 3.1 Behaviour of cement pastes after 5-min immersion in deionized water at 37 °C: (A) conventional cd-AB and (B) premixed cd-AB (prepared with 20% PLA-NMP solution).

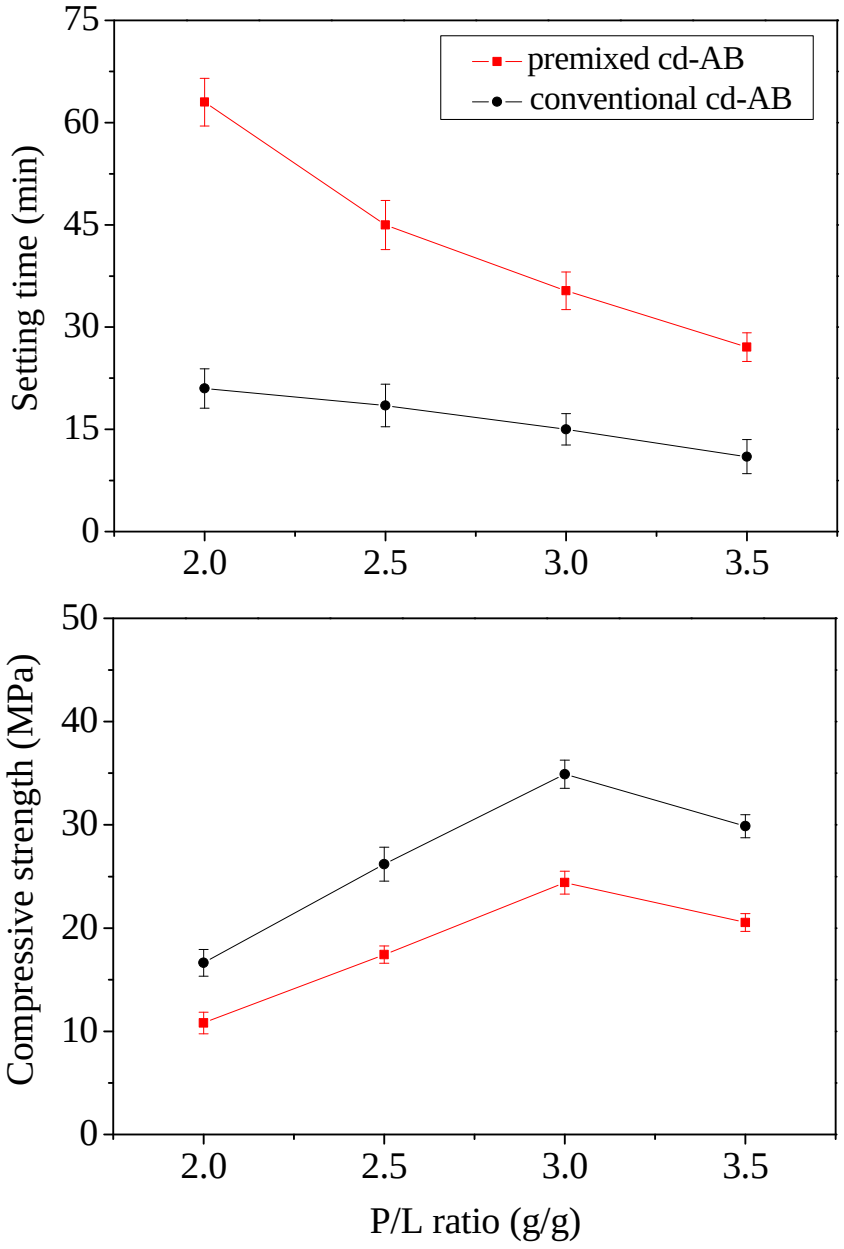

Figure 3.2 The effect of P/L ratio on the setting time and compressive strength of the different cements

was less than 30 min. For conventional cd-AB, the setting time shortened from 21 min to 11 min as the P/L ratio increased. For both conventional cd-AB and premixed cd-AB, the compressive strength significantly increased as the P/L ratio increased from 2 g/g to 3 g/g ($p < 0.05$). However, a decrease of compressive strength was observed when the P/L ratio increased from 3 g/g to 3.5 g/g ($p < 0.05$). Considering the effects of P/L ratio on setting time and compressive strength, the P/L ratio of 3 g/g was chosen to prepare premixed cd-AB samples for other experiments.

3.3.3 Chemical compositions

Figure 3.3 shows the XRD patterns of the different cements. In Figure 3.3 A, the hydration product of the premixed cd-AB was cd-HA as shown by the typical peaks at 2θ = 25.9°, 31.8°, 32.2°, 32.9°, 34.0°, 39.8°, 46.7°, 49.5°, 52.2°. It was found that unreacted TTCP appeared in the premixed cd-AB sample. As illustrated in Figure 3.3 B, the hydration product of the conventional cd-AB was cd-HA. Remains of unreacted TTCP were also detected (Figure 3.3 B).

Figure 3.4 presents the FTIR spectra of PLA, conventional cd-AB and premixed cd-AB samples after hardening for 3 days. In Figure 3.4 C, the υ_2 peak (469 cm^{-1}), υ_3 peak (1032 cm^{-1}) and υ_4 peaks (603 cm^{-1} and 564 cm^{-1}) of PO_4^{3-} group in cd-HA [182] were observed. The band at 3570 cm^{-1} is related to the stretching vibration of –OH in cd-HA [185]. The band at 872 cm^{-1} arises from the υ_5 P–O(H) deformation of HPO_4^{2-} groups, confirming the calcium deficiency of HA [186]. A strong absorption

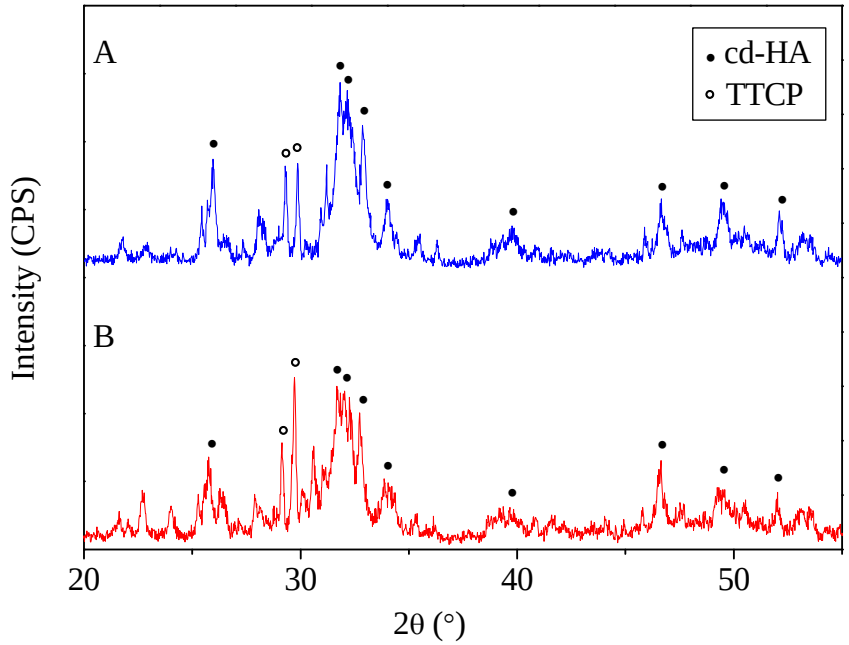

Figure 3.3 XRD patterns of the cements after hardening for 3 days: (A) premixed cd-AB and (B) conventional cd-AB.

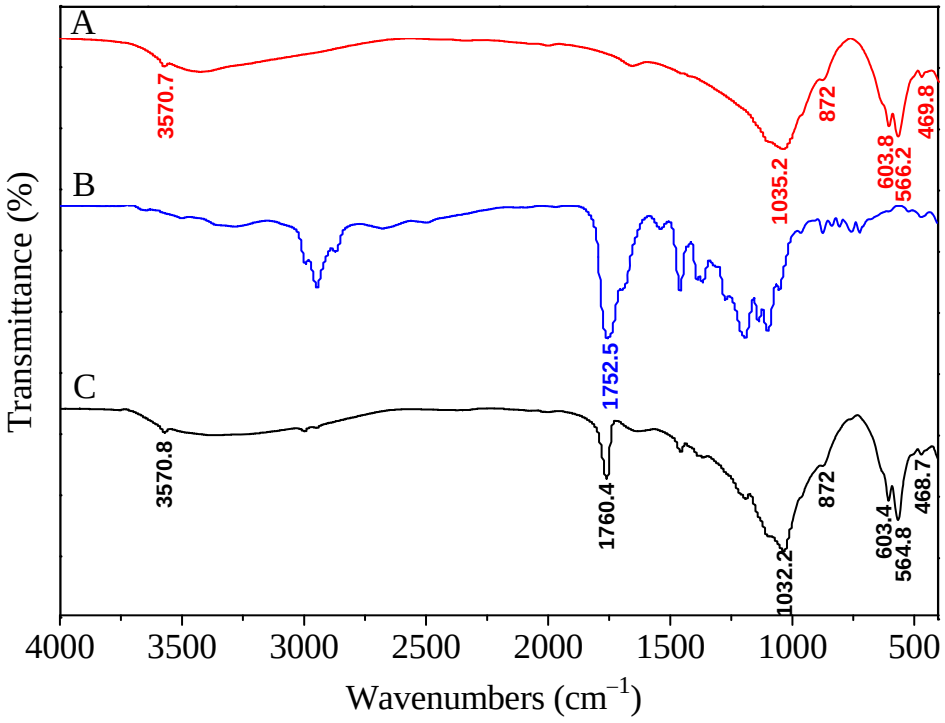

Figure 3.4 FTIR spectra of (A) conventional cd-AB after hardening for 3 days, (B) PLA and (C) premixed cd-AB after hardening for 3 days.

band at 1760 cm^{-1}, corresponding to the carbonyl group (C=O) of PLA [182], was shown in Figure 3.4 B. The FTIR analysis results suggested that the hydration products of premixed cd-AB were a mixture of cd-HA and PLA.

3.3.4 Microstructural morphology

The fracture surface morphology of the hardened cements is shown in Figure 3.5. In Figure 3.5 A, a mixture of needle-like and plate-like apatite crystals appeared on the fracture surface of premixed cd-AB. The needle-like crystal's length varied from 500 nm to 1 μm and a diameter of approximately 100 nm. Some plate-like crystals were observed with a thickness of about 100–200 nm and a width of 1 μm. As shown in Figure 3.5 B, the fracture surface of conventional cd-AB mainly consisted of needle-like crystals with a length from 500 nm to 1 μm.

3.3.5 Injectability

Table 3.1 presents the percent injectability of premixed cd-AB pastes prepared at different P/L ratios as a function of PLA content in the liquid phase 2 min after the start of mixing. For pastes made with the same PLA-NMP solution, the injectability increased with decreasing P/L ratio. Pastes made with the P/L ratio of 2 g/g had adequate injectability. Pastes made at the P/L ratio of 3.5 g/g were relatively difficult to extrude from the syringe. The PLA content in the liquid phase had an obvious influence on the paste injectability. When prepared with the same P/L ratio, the paste injectability decreased with increasing PLA content in the liquid phase.

A

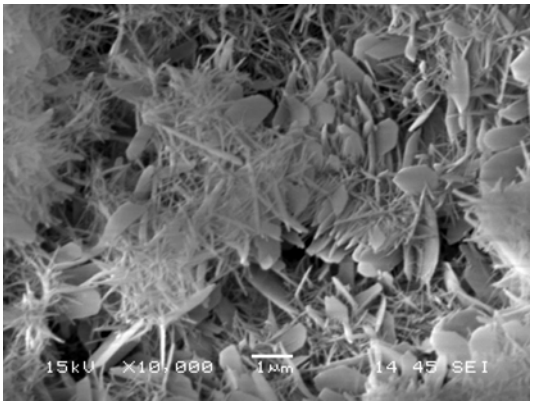

B

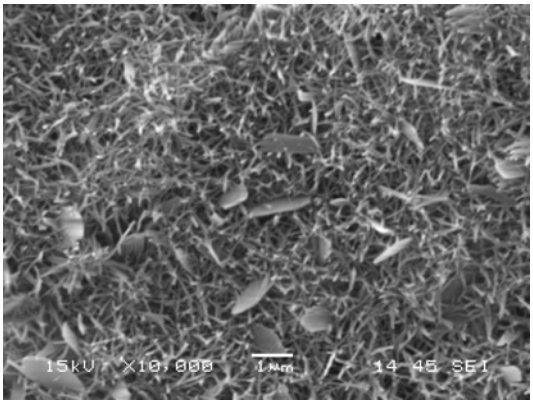

Figure 3.5 SEM micrographs of the fracture surface of cements after hardening for 3 days: (A) premixed cd-AB and (B) conventional cd-AB.

Table 3.1 Injectability of premixed cd-AB pastes made with different liquids and P/L ratios.

Liquid phase	Injectability (%)			
	P/L = 2 g/g	P/L = 2.5 g/g	P/L = 3 g/g	P/L = 3.5 g/g
PLA-NMP (10%)	98 ± 2	98 ± 2	63 ± 3	15 ± 3
PLA-NMP (15%)	97 ± 2	69 ± 3	38 ± 2	not injectable
PLA-NMP (20%)	97 ± 2	56 ± 2	27 ± 3	not injectable

3.3.6 *In vitro* degradability

Figure 3.6 shows the weight loss ratios of the different cements after immersion in Tris-HCl solution for 28 days. With the addition of PLA in the liquid phase, the degradation rate of premixed cd-AB was higher than conventional cd-AB. Conventional cd-AB showed a weight loss ratio of approximately 5.6 wt% after immersion for 28 days. For the premixed cd-AB prepared with 20 wt% PLA-NMP solution, the weight loss ratio reached 15.6 wt% after 28-day immersion. Moreover, the degradation rate of premixed cd-AB increased with the increasing content of PLA in the liquid phase.

Figure 3.7 shows the pH variations of Tris-HCl solution after the immersion of different cements. In the early stage of immersion, both premixed cd-AB and conventional cd-AB caused an increase of pH value of the solution. The initial increase in pH value could be attributed to the dissolution of cd-HA that released OH^- into the solution. After 10 days, the pH value of the solution containing premixed cd-AB reached its maximum and then decreased with the extension of immersion time. The decrease in pH value could be explained by the release of acidic degradation products of PLA. As for the conventional cd-AB, the pH value of the solution decreased slightly after about 13 days of immersion. This might be attributed to the buffer-mediating effect of tris(hydroxymethyl)aminomethane (Tris) [187, 188].

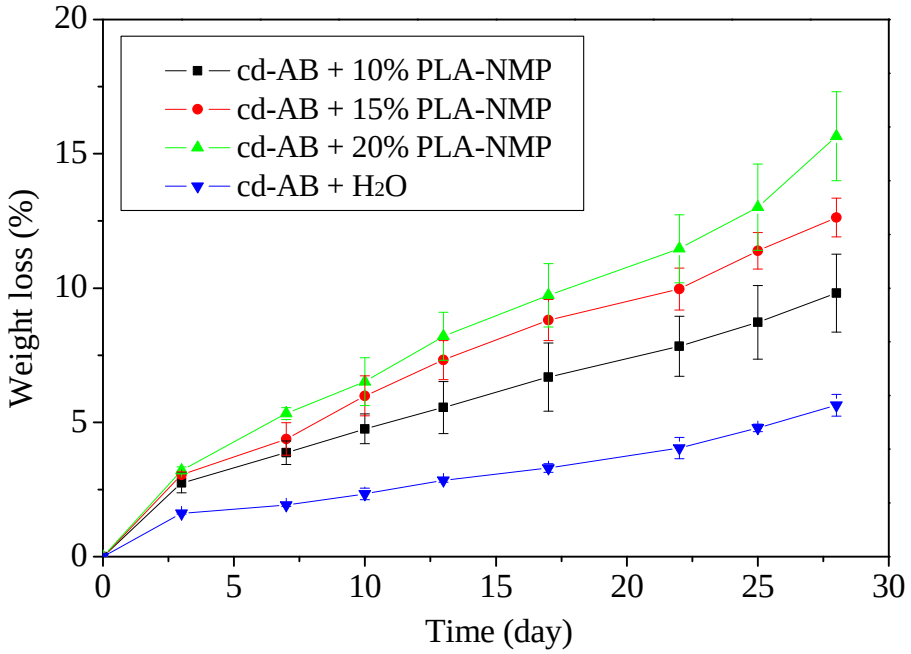

Figure 3.6 Weight loss ratios of the different cements after immersion in Tris-HCl solution for different time.

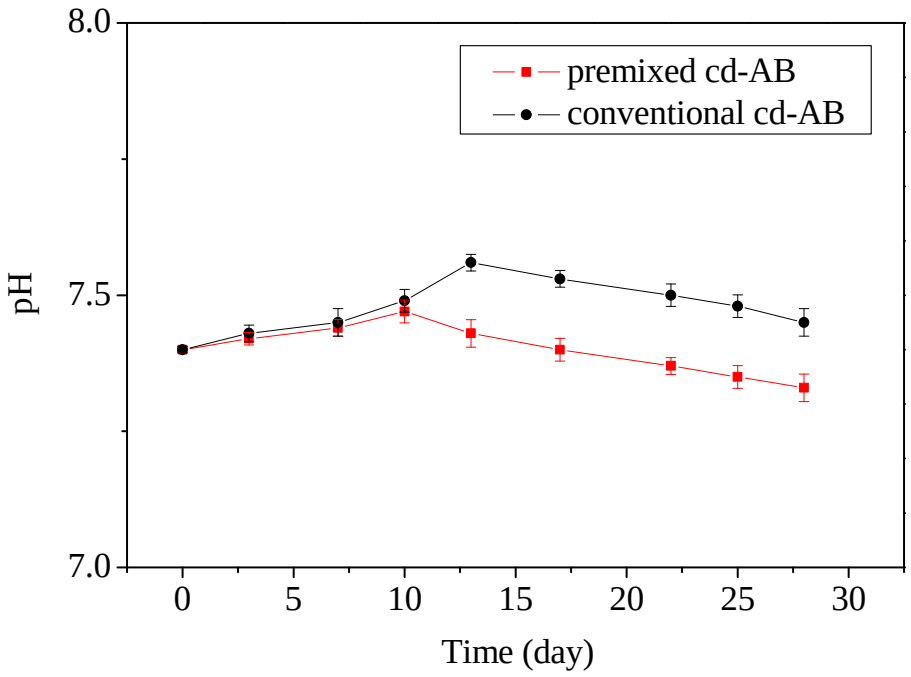

Figure 3.7 Variations in the pH value of Tris-HCl solution after the immersion of different cements.

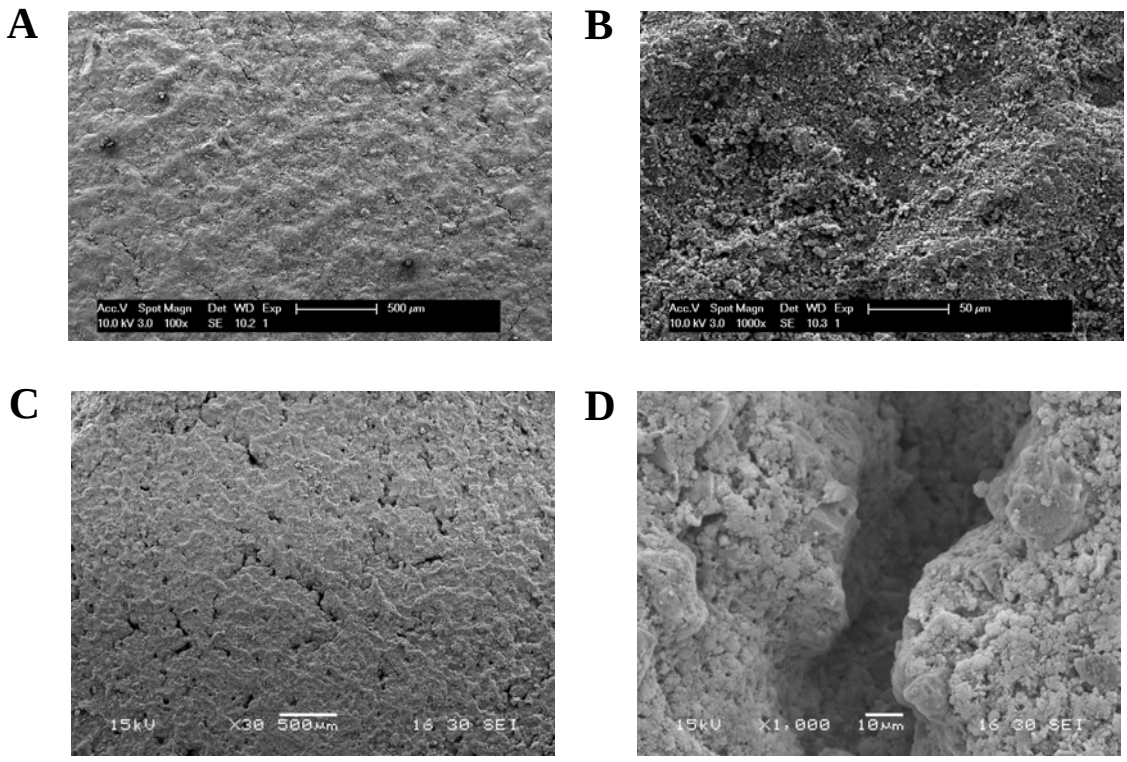

Figure 3.8 SEM micrographs of premixed cd-AB samples after immersion in Tris-HCl solution for (A and B) 1 day and (C and D) 28 days.

Figure 3.8 exhibits the surface morphology of premixed cd-AB after immersion in Tris-HCl solution for different time. As shown in Figure 3.8 A and B, some tiny cracks were observed on the cement surface after 1-day immersion. After 28 days of immersion, a more marked degradation of the cement was noted (Figure 3.8 C and D). Larger pits and deeper cracks appeared on the cement surface.

3.3.7 Cytocompatibility

The results of MTT assay for MG-63 cell proliferation are shown in Figure 3.9. The OD value for both cements increased with the extension of incubation time. Moreover, the OD value for premixed cd-AB was not significantly different from conventional cd-AB or for the TCP control at 3 and 5 days ($p > 0.05$). This demonstrated that the number of viable cells on the premixed cd-AB was not significantly different from the conventional cd-AB, indicating that premixed cd-AB was as non-cytotoxic as conventional cd-AB.

The SEM micrographs of MG-63 cells cultured on conventional cd-AB and premixed cd-AB samples for 3 days are shown in Figure 3.10. The cells were attached to and spread well on both cements. The cells exhibited similar spindle-like morphology and had developed cytoplasmic extensions with lengths up to 50 μm. The cytoplasmic extensions were firmly anchored on the apatite crystals and the connection between neighbouring cells had been established. Both MTT assay results and SEM images suggested that premixed cd-AB was as cytocompatible as conventional cd-AB.

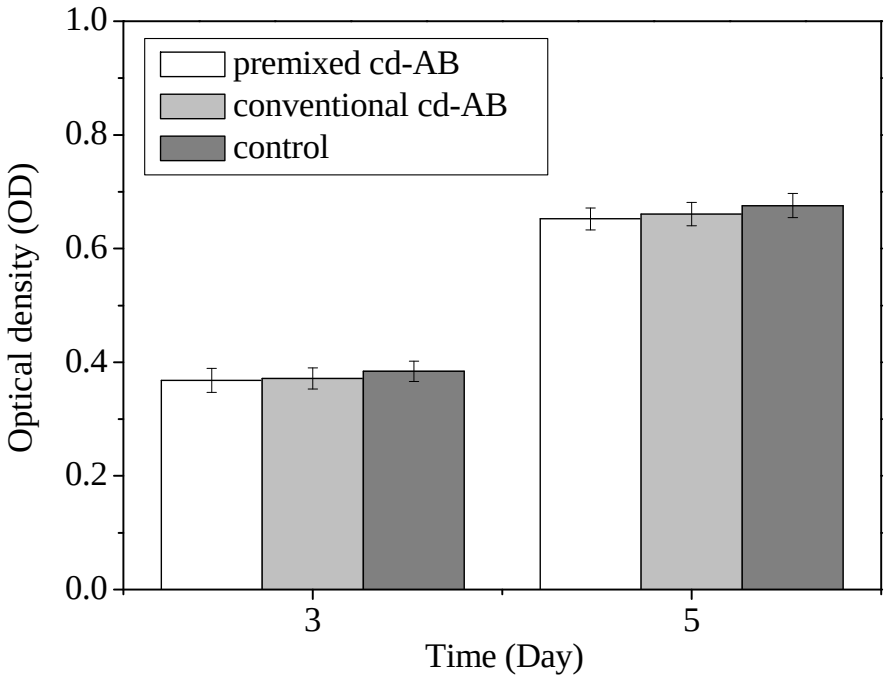

Figure 3.9 MTT assay for proliferation of MG-63 cells cultured on different cements at 3 and 5 days of incubation.

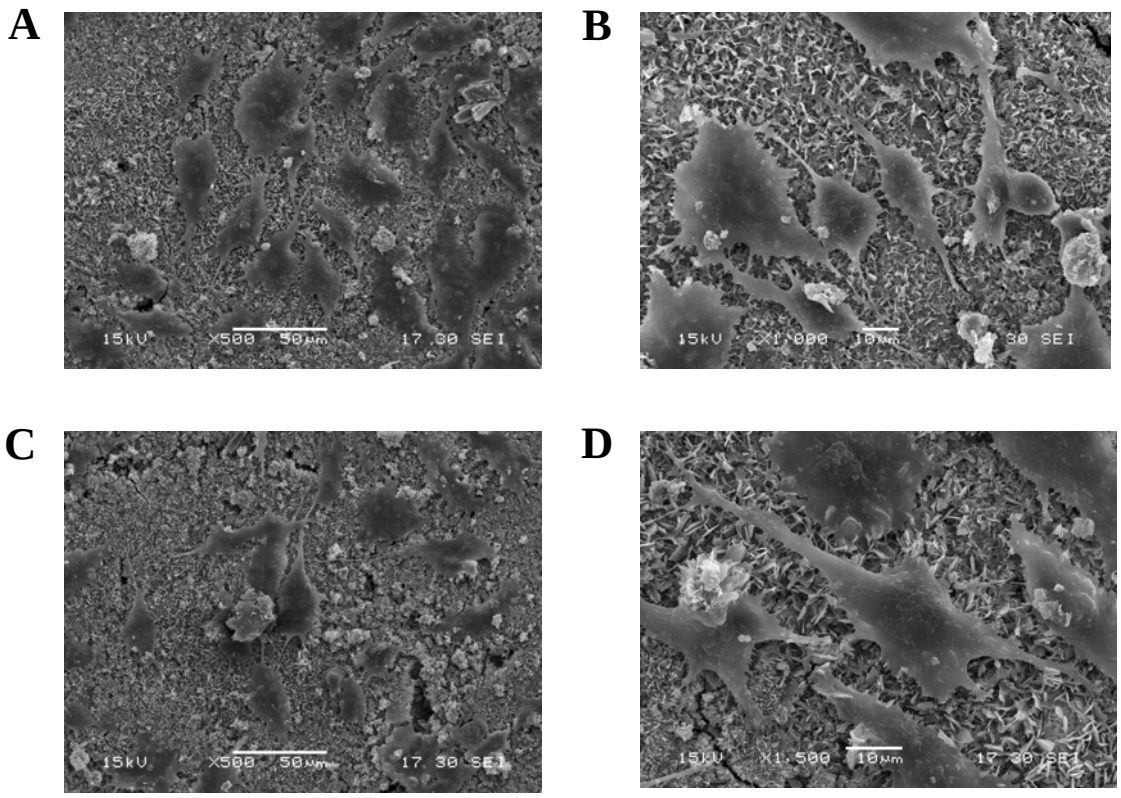

Figure 3.10 SEM micrographs of MG-63 cells attached to: (A and B) conventional cd-AB; (C and D) premixed cd-AB.

3.4 Discussion

In this study, the applicability of using PLA-NMP solution as the liquid phase to prepare premixed and injectable cd-AB for bone reconstruction was investigated. When premixed cd-AB paste came in contact with water, the exchange of NMP for water occurred. Since PLA is hydrophobic, the removal of NMP resulted in the deposition of PLA. Meanwhile, the reach of water into the bulk of the cement paste initiated the hydration of calcium phosphates. Since both TTCP and DCPA are more soluble than cd-HA, the dissolution of TTCP and DCPA resulted in a solution that is supersaturated with respect to cd-HA [60, 189]. Subsequently, cd-HA precipitated. The hydration products of premixed cd-AB were a mixture of cd-HA and PLA. A schematic representation of the hardening process of premixed cd-AB paste is shown in Figure 3.11.

Zhou et al. [182] observed a blue-shift of the C=O vibration peak (1755 cm^{-1}) of PLA from the IR spectrum of PDLLA/HA nanocomposites. The blue-shift phenomena could be attributed to the interaction between PLA and HA [182]. However, no blue-shift of C=O vibration peak was observed in present work, implying that the carbonyl group (C=O) of PLA was free and not bonded with cd-HA particles. It is assumed that the molecular chains of PLA were dispersed in the calcium phosphate matrix.

The premixed cd-AB paste exhibited much better washout resistance than

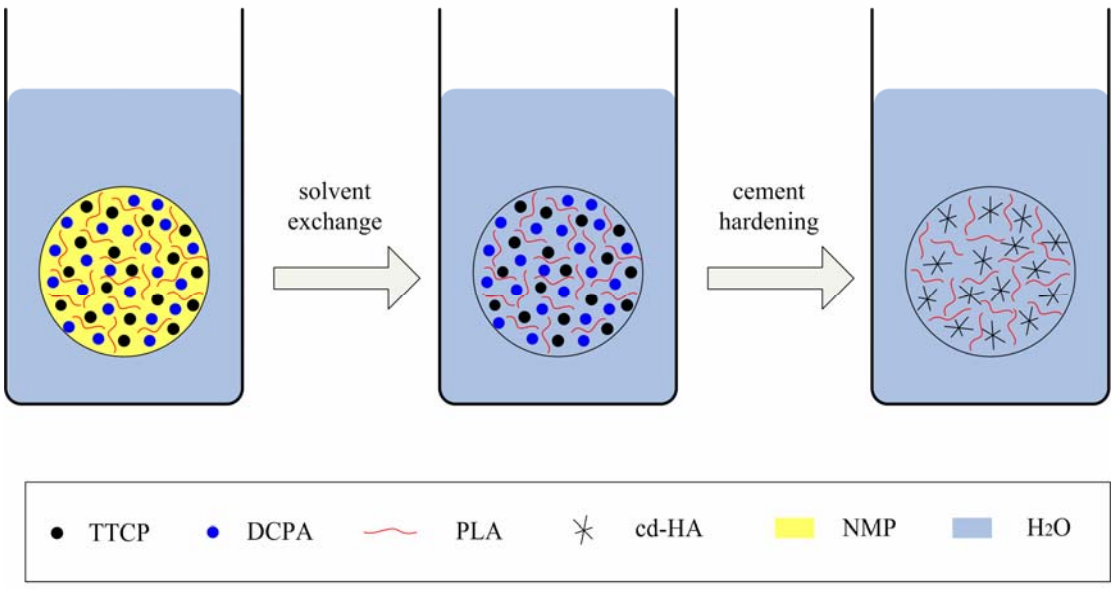

Figure 3.11 Schematic representation of the hardening process of premixed cd-AB

conventional cd-AB paste. With the incorporation of viscous PLA-NMP solution, the viscosity of premixed CPC paste increased, reducing the risk of paste disintegration when got in contact with fluids [59, 190]. When the premixed cd-AB paste came in contact with water, NMP diffused into water thus causing the precipitation of PLA. The precipitation of PLA could help trap calcium phosphate particles and avoid potentially deleterious migration of those particles, contributing to the excellent washout resistance of premixed cd-AB. Le Renard et al. [191] investigated the use of organogels based on precipitating polymers as carriers for magnetic microparticles. They thought that the solvent diffusion through exchange with circulating water could trigger precipitation of polymers, leading to “an entangled network trapping magnetic microparticles” [191].

Premixed cd-AB had longer setting time than conventional cd-AB. The hardening of premixed cd-AB strongly depends on the solvent exchange. NMP must be exchanged by water to trigger the hydration of calcium phosphates. Similar extension of setting time was previously observed by Takagi et al. [71] for premixed CPC using glycerol as the non-aqueous liquid. Compared with conventional cd-AB, premixed cd-AB exhibited lower compressive strength. This might be attributed to a higher porosity produced by the solvent exchange. The influence of P/L ratio on the mechanical properties of the cements was investigated. A higher P/L ratio was beneficial to the improvement of mechanical properties, implying that less mixing liquid results in a more compact cement bulk after hardening. However, it should be noted that if the P/L

ratio is too high, it may result in inhomogeneous mixing of the cement paste, compromising the cement performance [59]. Too low P/L ratio would cause high porosity in the hardened cement body, which is adverse to the enhancement of mechanical strength.

A decrease of P/L ratio led to an improvement of the cement injectability. Previous studies indicated that decreasing P/L ratio is a common method to increase the injectability [32]. In addition, a higher PLA content in the liquid phase decreased the cement injectability. This effect might be attributed to the increase of the paste viscosity. The viscosity of PLA-NMP solution increased with the addition of PLA, leading to an increase of the paste viscosity. Although the increase of PLA content reduced the paste injectability, it might be effective in preventing “filter pressing” during injection. The “filter pressing” was termed by Bohner and Baroud [56, 57] as the phase separation phenomenon during injection where “the liquid comes out without the particles”. The increase of the viscosity of PLA-NMP solution could reduce the possibility of the mixing liquid to pass through the calcium phosphate particles, thus lowering the risk of “filter pressing”.

Proper degradability is an important characteristic for bone grafting material. The results demonstrated that the premixed cd-AB could be degradable during the incubation in Tris-HCl solution. The premixed cd-AB prepared with 20% PLA-NMP solution lost 15.6 wt% of its initial weight after immersion for 28 days. In contrast,

conventional cd-AB did not show significant weight loss and lost only 5.6% of its initial weight by the end of immersion. The results showed that the degradation of premixed cd-AB was faster than conventional cd-AB in Tris-HCl solution. Comparison of the premixed cd-AB prepared with different PLA contents in the liquid phases indicated that the cement made with 20% PLA-NMP solution showed the highest degradation rate.

According to the results of XRD and FTIR analysis, the hydration products of the premixed cd-AB were a mixture of cd-HA and PLA. When immersed in Tris-HCl solution, the hardened premixed cd-AB underwent two degradation processes: that of PLA and that of cd-HA [192]. The degradation of PLA was generally considered to be a hydrolytic process [193]. The release of the acidic hydrolytic products of PLA could result in a slight increase of the acidity of the surrounding medium. This explained the faster decrease of pH value of solution containing premixed cd-AB, as shown in Figure 3.7. Wang et al. [194] noted that *in vitro* degradation of HA was relatively more rapid in the environment with lower pH value. Thus, the hydrolysis of PLA might help accelerate the degradation of cd-HA. As shown in Figure 3.8 C and D, a more marked degradation of premixed cd-AB was observed after 28-day immersion. The presence of large pits and deep cracks could facilitate the penetration of fluids and the leakage of degradation products, furthermore accelerating the cement degradation [195].

The cytocompatibility of premixed cd-AB was evaluated by monitoring the

attachment and proliferation of MG-63 osteoblast-like cells cultured on the cement. The cell proliferation of premixed cd-AB was not significantly different from conventional cd-AB. MG-63 cells attained normal spindle-like morphology on both premixed and conventional cd-AB with cytoplasmic extensions adhering to the cd-HA crystals. The results suggested that premixed cd-AB was as cytocompatible as conventional cd-AB. The conventional cd-AB was cytocompatible since the individual components (TTCP and DCPA) and the hydration product (cd-HA) were non-cytotoxic, as demonstrated in previous work [66, 196]. Among the constituents of premixed cd-AB, NMP is known to be non-cytotoxic and has been approved by FDA to be used in fabrication of *in situ* forming drug delivery system [179]. PLA is semicrystalline aliphatic polyester and has good biocompatibility [182]. Thus, from the view of cement composition, it is not surprised that premixed cd-AB was compatible to MG-63 cells in present study.

3.5 Conclusion

The work presented within this chapter describes a premixed and injectable cd-AB. The cement pastes could be prepared in advance under well-controlled environment thus eliminating the on-site mixing in surgery. The premixed cd-AB paste remained stable in the syringe and hardened only after being injected into the defect site. When contacted with an aqueous environment, the premixed cd-AB paste exhibited excellent washout resistance. Due to the exchange of solvent with water, premixed cd-AB had longer setting time than conventional cd-AB. The hydration products of

premixed cd-AB were a mixture of nanocrystalline cd-HA and PLA. The degradation of premixed cd-AB was faster than that of conventional cd-AB in Tris-HCl solution. The premixed cd-AB supported the attachment and proliferation of MG-63 osteoblast-like cells, indicating good cytocompatibility. Premixed and injectable PLA-modified cd-AB may be useful in dental, craniofacial and periodontal repairs.

Chapter 4

Fabrication and properties of porous scaffold of zein/PCL biocomposite for bone tissue engineering

F. Wu [a], J. Wei [b], C. Liu [b], B. O'Neill [a], Y. Ngothai [a]

[a] School of Chemical Engineering, The University of Adelaide, Adelaide, SA 5005, Australia
[b] The State Key Laboratory of Bioreactor Engineering, and Engineering Research Center for Biomedical Materials of Ministry of Education, East China University of Science and Technology, Shanghai 200237, China

This is a revised and corrected version of the paper which appears in:

Composites: Part B, 2012, 43, 2192–2197.

STATEMENT OF AUTHORSHIP

Fabrication and properties of porous scaffold of zein/PCL biocomposite for bone tissue engineering

Composites: Part B, 2012, 43, 2192–2197.

Fan Wu (Candidate)

Designed and performed experiments, interpreted and processed data, wrote manuscript

I hereby certify that the statement of contribution is accurate

Signed ……*Date*……....

Jie Wei

Helped with the design of experiments and manuscript evaluation

I hereby certify that the statement of contribution is accurate and I give permission for the inclusion of the paper in the thesis

Signed ……*Date*……....

Changsheng Liu

Manuscript evaluation

I hereby certify that the statement of contribution is accurate and I give permission for the inclusion of the paper in the thesis

Signed ……*Date*……....

Brian O'Neill

Manuscript evaluation

I hereby certify that the statement of contribution is accurate and I give permission for the inclusion of the paper in the thesis

Signed ……*Date*……....

Yung Ngothai

Manuscript evaluation and acted as corresponding author

I hereby certify that the statement of contribution is accurate and I give permission for the inclusion of the paper in the thesis

Signed ……*Date*……

Chapter 4 Fabrication and properties of porous scaffold of zein/PCL biocomposite for bone tissue engineering

4.1 Introduction

Reconstruction or regeneration of hard tissue (such as bone and cartilage) using tissue engineering techniques requires the use of temporary porous scaffolds within which the cells are seeded and cultured *in vitro* before implantation. The scaffolds should provide an appropriate environment for cell attachment, proliferation and differentiation, as well as the formation of new tissue [13]. Scaffolds for bone tissue engineering should satisfy some requirements [197]. Appropriate porosity, pore size and pore structure are necessary to facilitate the ingrowth of cells and new tissue. The scaffolds should possess good biodegradability and suitable degradation rate to match the new tissue formation rate. Good biocompatibility and suitable mechanical property are also required.

Among the polymeric materials used for fabrication of bone tissue engineering scaffolds, PCL has been widely used due to its (a) good biocompatibility, (b) easy-processing ability, and (c) non-toxic degradation products [124]. The degradation of PCL is considered to occur by the hydrolysis of ester bonds into acidic monomers, which can be removed from the body by physiological metabolic pathways [117, 198]. However, some drawbacks have limited the wider applications of PCL scaffolds: (1) slow degradation rate, which might be related with the highly crystalline character of

PCL; (2) hydrophobicity, which is adverse for the cell attachment and penetration into the porous structure; and (3) acidic degradation products, which might lead to side effects [133].

Blending PCL with natural polymer is an approach to overcoming those limitations. For example, the degradation of PCL was accelerated by blending with chitosan [131]. In addition, the acidic degradation products of PCL were effectively buffered by chitosan [131]. Ciardelli et al. [100] found that blending PCL with hydrophilic natural polymer such as starch is a promising way to improve the biocompatibility of PCL.

In this study, we used a blend of zein, a natural polymer, and PCL to prepare scaffolds. It is expected that blending PCL with zein could have a synergic effect on the control of hydrophilicity and degradation behavior of the scaffolds.

Zein is a corn protein which represents about 80% of the total proteins in corn grains [145]. It has been used in a wide range of applications, such as adhesives, biodegradable plastics, coating for food products and fibers [146]. Due to its nontoxicity, good biodegradability and biocompatibility, zein has a great potential for use in biomedical applications. Zein has been used for preparing microspheres as drug delivery systems [147, 148]. Both zein and its degradation products exhibited good cell compatibility [147, 149, 150]. Recently, three-dimensional porous zein scaffolds have been developed for tissue engineering applications [151-153]. *In vitro* tests showed that porous zein scaffolds could support the adhesion, proliferation and

osteoblastic differentiation of human mesenchymal stem cells (hMSCs) [153]. The results of an *in vivo* study using a rabbit subcutaneous implantation model demonstrated the good tissue compatibility and degradability of the zein scaffolds [152]. In addition, the porous zein scaffolds degraded completely within 8 months [152].

This work reported the fabrication of porous scaffolds of zein/PCL biocomposite for bone tissue engineering. The scaffolds were fabricated using particulate leaching technique. The pore structure, hydrophilicity and mechanical properties of the scaffolds were determined. *In vitro* degradation behavior of the scaffolds in PBS was monitored.

4.2 Materials and methods

4.2.1 Materials

PCL (M_n = 80,000, T_m = 60 °C and ρ = 1.145 g/cm^3) was purchased from Sigma–Aldrich. Zein (Z3625-250 g) was purchased from Shanghai CpG Biotech Co., Ltd. NaCl particulates with diameter ranging from 300 to 500 μm were used as porogen.

4.2.2 Preparation of composite scaffolds

Porous zein/PCL scaffolds were prepared by the particulate leaching method [144, 199]. PCL pellets were weighed and dissolved in selected volumes of dichloromethane. A selected amount of zein was added into the solution,

followed by continuous stirring to disperse uniformly. NaCl particulates were added into the zein/PCL solution and stirred for 10 min. The mixture was then cast into the molds. The samples were air-dried by natural evaporation for 24 h and subsequently vacuum-dried at 40 °C for 48 h to completely remove the solvent. The salt particulates were leached out by immersing the samples in deionized water for 72 h at 37 °C. The water was refreshed three times a day to favor the complete dissolution of the salt. After leaching, the scaffolds were air-dried for 24 h and then vacuum-dried for 12 h. The zein/PCL biocomposite scaffolds with the incorporation of 20 wt% and 40 wt% zein were prepared, respectively. Pure PCL scaffolds were prepared as the control. Table 4.1 lists the compositions of the scaffolds prepared.

4.2.3 Scaffold characterization

4.2.3.1 Micro-CT analysis

The scaffolds (4 × 4 × 20 mm^3) were analyzed using a high-resolution micro-computed tomography (micro-CT) scanner (Skyscan 1072, Kontich, Belgium). The samples (n = 3 for each group) were scanned at 11.01 μm resolution. The X-ray source was set at 50 kV of energy and 120 μA of current. No filter was applied. The obtained isotropic slice data were reconstructed into 2D images. These 2D images were compiled to build 3D models in CTan (Skyscan). The 3D models were visualized using CTvol (Skyscan). The 3D analysis was performed in CTan (Skyscan) for porosity calculation.

4.2.3.2 Analysis by FTIR and SEM

The FTIR spectra of the different scaffolds were recorded on a FTIR spectroscopy (Magna-IR 550, Nicolet) from 4000 to 400 cm^{-1}. SEM (XL30 FEGSEM, Philips) was used to examine the cross-sectional morphology of the scaffolds (4 × 4 × 10 mm^3). The scaffolds were cut by a blade and coated with gold.

4.2.3.3 Mechanical properties

The mechanical properties of the scaffolds were tested by compression experiments using a universal testing machine (AG-2000A, Shimadzu Autograph, Shimadzu Co., Ltd.). Compression tests were carried out at a loading rate of 1 mm/min, until obtaining a maximum reduction in samples' height of 80%. Three samples (diameter: 6 mm, height: 12 mm) of each group were tested.

4.2.3.4 Hydrophilicity

Water contact angle measurements were conducted using a contact angle system (JC2000D3, Shanghai Zhongchen Digital Technology Apparatus Co., Ltd.). A water droplet (1 μL) was poured on the material surface and the water contact angle was measured after 30 s. The results are presented as mean ± SD of five measurements per sample.

4.2.4 *In vitro* degradation

To assess the *in vitro* degradation behavior of the scaffolds, the samples (10 × 10 × 3 mm^3) were weighed (W_i), immersed in PBS (0.01 M, pH 7.4) and incubated at 37 °C

with constant shaking at 100 rpm for 28 days. Three samples of each group were tested. The PBS solutions were changed twice a week. At preselected time point, the samples were removed from the solution, rinsed gently with deionized water, dried at 37 °C until exhaustion and weighed (W_f). The weight loss was calculated according to the following equation [128]:

$$\text{weight loss (\%)} = \frac{(W_i - W_f)}{W_i} \times 100\% \quad (4.1)$$

The surface morphology of the scaffolds before and after degradation was characterized by SEM (JSM6360, JEOL). The FTIR spectra of the scaffolds after immersion in PBS for different time were assessed by a FTIR spectroscopy (Magna-IR 550, Nicolet). The pH variation of PBS during the whole immersion period was monitored using a pH meter (FE20, Mettler Toledo).

4.3 Results

Porous scaffolds of zein/PCL biocomposite were successfully fabricated using the solvent casting–particulate leaching method. The as-prepared zein/PCL-40 scaffold presented a sponge-like structure (Figure 4.1).

4.3.1 SEM analysis

Figure 4.2 presents the cross-sectional morphology of the scaffolds examined by SEM. Macropores with sizes ranging from a few microns to hundreds of microns were observed for PCL scaffold (Figure 4.2 A and B). As shown in Figure 4.2 C,

Figure 4.1 Macroscopic image of the zein/PCL-40 scaffold

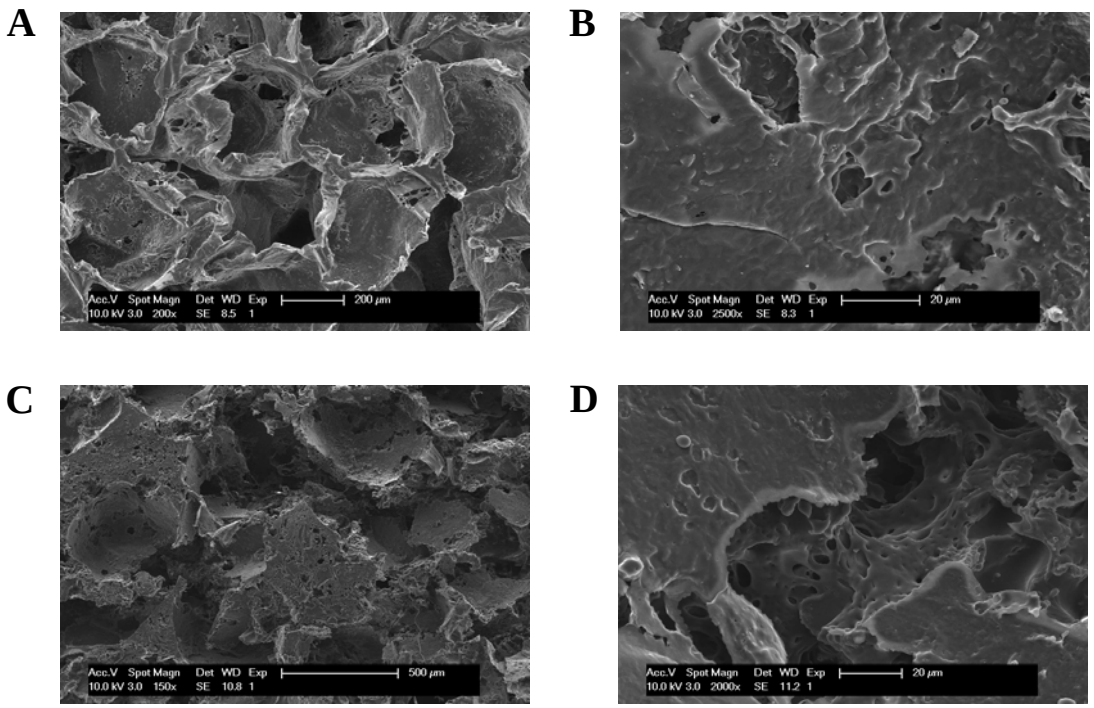

Figure 4.2 SEM images of the cross-sectional morphology of (A and B) PCL scaffold and (C and D) zein/PCL-40 scaffold.

for zein/PCL-40 scaffold, the majority of the macropores are larger than 300 μm. Several macropores varying from 5 to 20 μm were observed on the walls of the scaffold (Figure 4.2 D).

4.3.2 Micro-CT analysis

Representative 3D images of the zein/PCL-40 scaffold reconstructed by micro-CT are presented in Figure 4.3. The 3D model reveals a highly porous structure (Figure 4.3 A). To show clearly the pores and interconnections between pores, a semi-transparent overlay was put over a cross-section of the 3D model. A well-interconnected pore structure was observed from the micro-CT image shown in Figure 4.3 B.

The porosities of the scaffolds determined from micro-CT data is shown in Table 4.1. The introduction of 20 wt% and 40 wt% zein into the PCL matrix did not noticeably change the porosity of the PCL scaffold.

4.3.3 FTIR analysis

The FTIR spectra of zein powder, PCL scaffold and zein/PCL-40 scaffold are illustrated in Figure 4.4 A–C. The characteristic band of PCL appears at 1730 cm^{-1}, corresponding to the C=O stretching of the ester carbonyl group. In Figure 4.4 B, the peaks at 1500–1550 cm^{-1}, 1600–1700 cm^{-1} and 3100–3500 cm^{-1} correspond to the characteristic absorptions of amide II, amide I and amide A, which are typical protein absorption bands [200]. As can be seen in Figure 4.4 C, the spectrum of the zein/PCL-40 scaffold exhibits the characteristic bands from both PCL and zein.

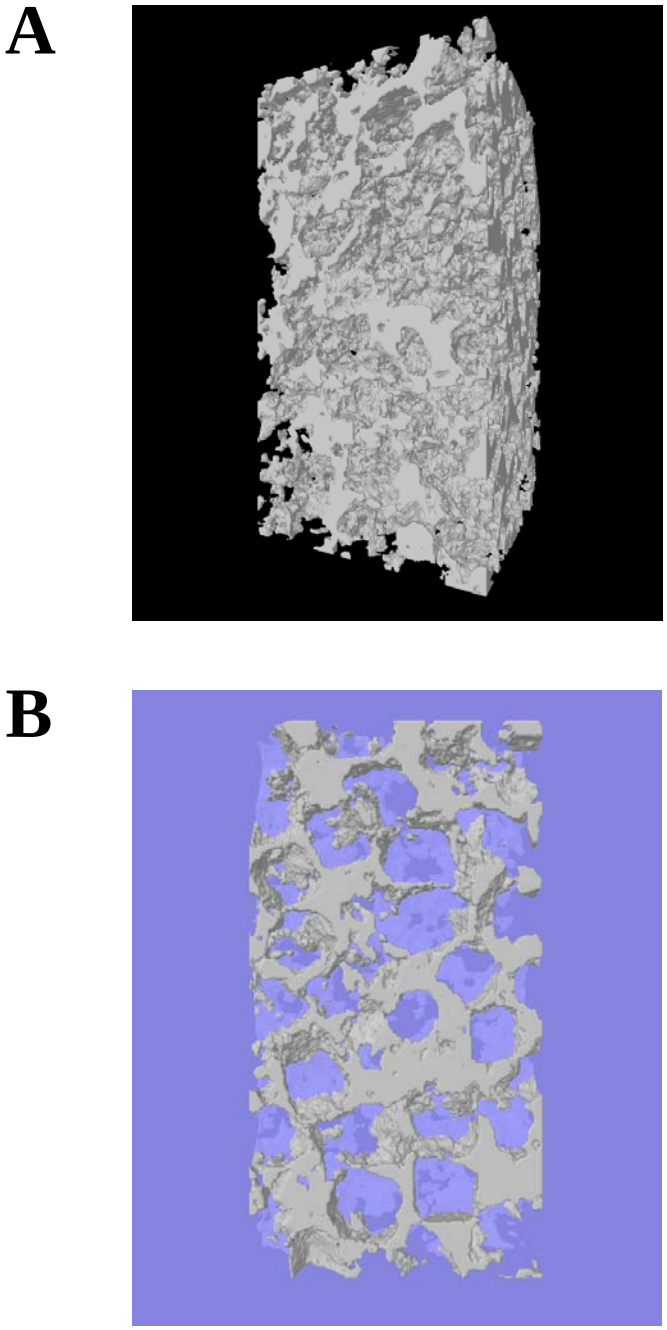

Figure 4.3 Micro-CT visualizations of the zein/PCL-40 scaffold: (A) 3D model and (B) semi-transparent overlay of a cross-section of the 3D model (the overlapping area is shown in light blue).

Table 4.1 Compositions and porosities of the PCL/zein composite scaffolds.

Scaffold	Matrix materials		NaCl/matrix (wt/wt)	Porosity (%)
	zein (wt%)	PCL (wt%)		
PCL	0	100	8:1	76.32 ± 1.93
zein/PCL-20	20	80	8:1	74.01 ± 1.92
zein/PCL-40	40	60	8:1	70.99 ± 1.72

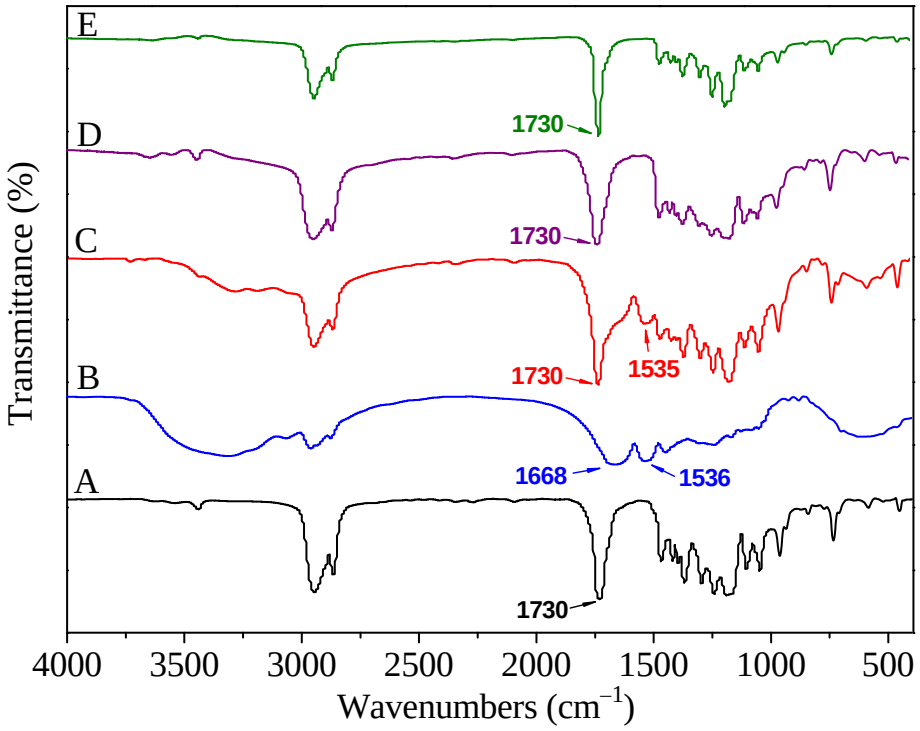

Figure 4.4 FTIR spectra: (A) PCL scaffold, (B) zein powder, (C) zein/PCL-40 scaffold, (D) zein/PCL-40 scaffold after immersion in PBS for 14 days and (E) zein/PCL-40 scaffold after immersion in PBS for 28 days.

4.3.4 Mechanical properties

Figure 4.5 shows the compressive stress–strain curves of the PCL and zein/PCL composite scaffolds. All of the curves show distinct characteristics of polymeric foam: a linear elastic region appeared at small strain, followed by a plateau region at larger strain and a densification region where the stress increased sharply at very large strain [201]. Compared to the PCL scaffold, the zein/PCL composite scaffolds exhibited lower σ_{10} value (the compressive stress at 10% strain). In addition, the σ_{10} value for the zein/PCL scaffolds decreased with the increasing amount of zein in the composite.

4.3.5 Hydrophilicity

Figure 4.6 shows the water contact angles of the different scaffolds. The presence of zein in the composite had an apparent effect on the water contact angles of the scaffolds. Compared with the PCL scaffold, the zein/PCL scaffolds had lower water contact angles. Moreover, the water contact angles of the zein/PCL scaffolds decreased with the increasing amount of zein in the composite.

4.3.6 *In vitro* degradation

In vitro degradation study was carried out to investigate the effect of zein content on the degradability of the zein/PCL scaffolds. Figure 4.7 illustrates the weight loss of the scaffolds after immersion in PBS for different time. A slight weight loss was observed for the PCL scaffold, which lost about 1.4% of its initial weight after immersion in PBS for 28 days. However, the zein/PCL biocomposite scaffolds presented noticeable

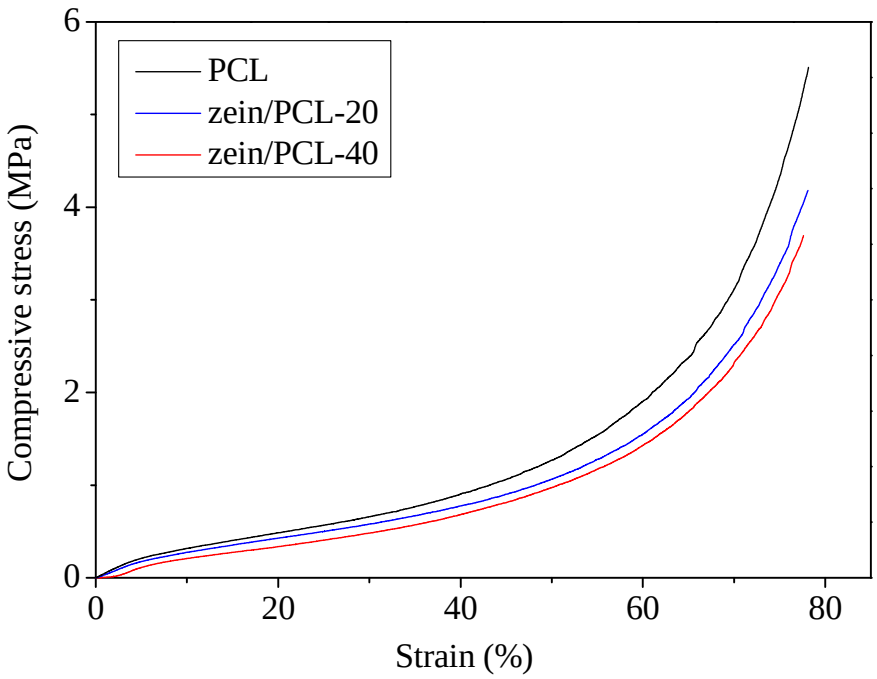

Figure 4.5 Compressive stress-strain curves of the different scaffolds.

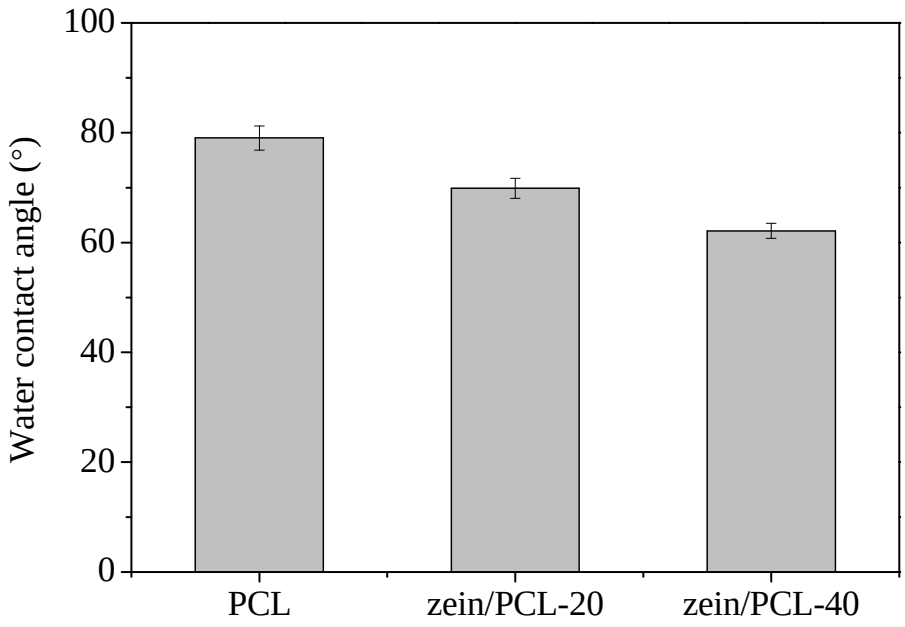

Figure 4.6 Water contact angles of the different scaffolds.

degradation during the 28-day immersion in PBS. Furthermore, the weight loss of the zein/PCL scaffolds increased with the increasing amount of zein in the composite. After immersion in PBS for 28 days, the weight loss for the zein/PCL-20 scaffold and the zein/PCL-40 scaffold were 15% and 32%, respectively. Considering that the original weight ratio of zein in the zein/PCL-40 scaffold was approximately 40%, it is estimated that a majority of the zein component degraded after 28-day immersion.

The FTIR spectra of the zein/PCL-40 scaffolds after immersion in PBS for 14 and 28 days are given in Figure 4.4 D and E. A decrease in the intensity of the peak at 1500–1550 cm^{-1} corresponding to amide II in zein was observed after 14-day immersion in PBS (Figure 4.4 D). This phenomenon can be attributed to the degradation of zein. As the immersion time prolonged, the characteristic peak of amide II at 1500–1550 cm^{-1} disappeared due to the continuous degradation of zein (Figure 4.4 E). The band at 1730 cm^{-1} corresponding to the C=O stretching of the ester bond in PCL remained unchanged after 28-day immersion, indicating that no obvious hydrolysis of the ester bonds occurred during that period. The weight loss results and the FTIR spectra suggest that a majority of the zein component degraded after 28-day immersion, while the hydrolysis of PCL was not obvious.

Figure 4.8 shows the pH variations of PBS during the 28-day immersion. No obvious pH variation was observed for the PCL scaffold during the whole immersion period. As for the zein/PCL composite scaffolds, only a slight decrease of pH value was

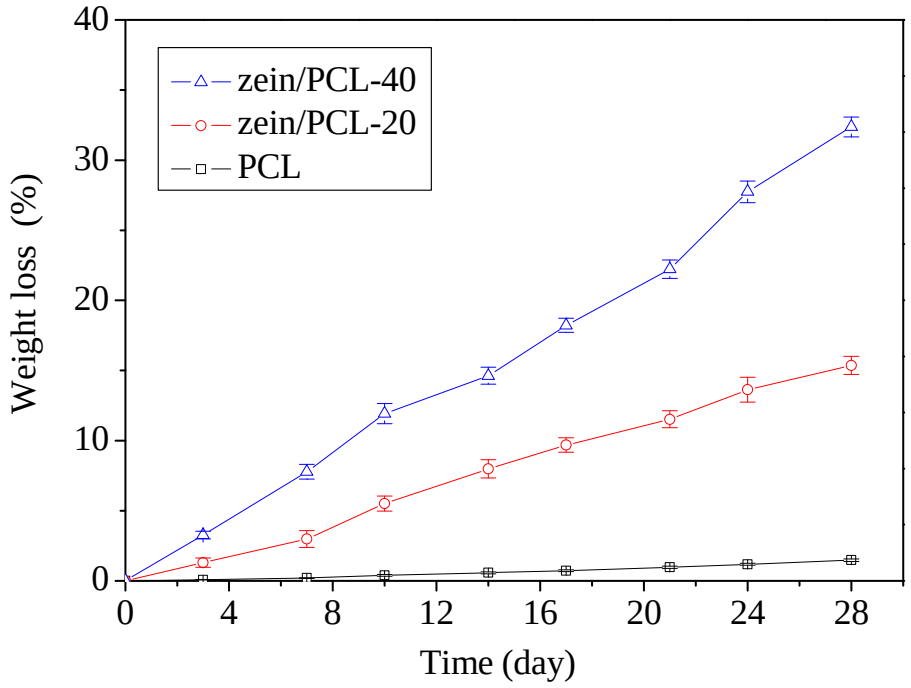

Figure 4.7 Weight loss of the different scaffolds during the immersion period.

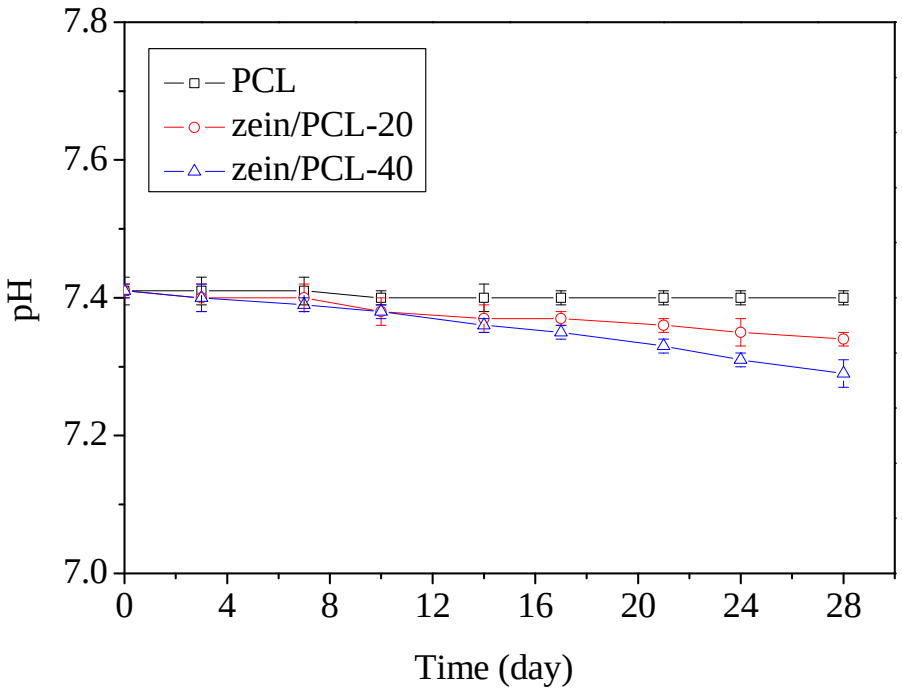

Figure 4.8 The pH variations of PBS during the immersion period.

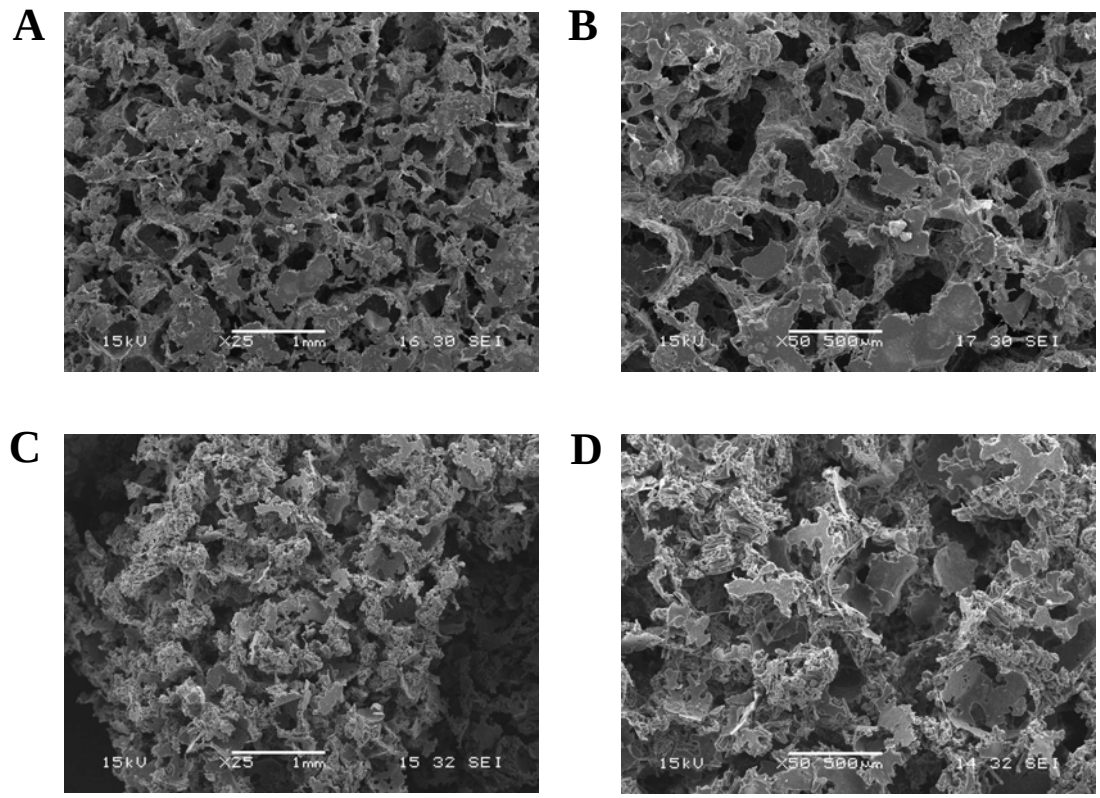

Figure 4.9 SEM images of the surface morphology of the zein/PCL-40 scaffolds: (A and B) before immersion and (C and D) after immersion in PBS for 28 days.

observed, which might be related to the degradation of zein.

Figure 4.9 shows the SEM images of the surface morphology of zein/PCL-40 scaffolds before and after immersion in PBS for 28 days. The *in vitro* degradation had a remarkable influence on the surface morphology of the scaffolds. A more irregular macroporous structure with larger voids was detected on the scaffold surface after 28-day immersion, which could be ascribed to the degradation of zein (Figure 4.9 C). Several small fissures and tiny pores appeared on the walls of the scaffold (Figure 4.9 D), which may possibly enhance the interconnectivity of the scaffold.

4.4 Discussion

In the present study, a blend of zein and PCL was used to fabricate porous scaffolds for bone tissue engineering. Among several processing techniques, the particulate leaching method was chosen since it could provide easy control of the pore structure [144]. Previous studies reported that the porous structure with pore size between 300 and 500 μm is suitable for cell penetration, tissue ingrowth and vascularization [13, 197, 202]. Thus, NaCl particles in the range of 300–500 μm were used as the porogen.

Both SEM and micro-CT were used to characterize the pore architecture of the scaffolds. SEM can qualitatively evaluate pore size and morphology. However, it is difficult to perform quantitative measurements from 2D SEM images [203]. Micro-CT can nondestructively quantify porosity and provide 3D visualization of the scaffold from any angle of view [203].

Due to the random porogen distribution in the bulk, the resulting scaffolds exhibited irregular pore structures as shown in Figure 4.2. Shi et al. [203] also reported the irregular pore architectures of the scaffolds fabricated by thermal-crosslinking–particulate-leaching technique. As observed from the SEM images (Figure 4.2 C and D), the zein/PCL-40 scaffold had macropores larger than 300 μm, which were formed due to the removal of NaCl particles. The formation of those macropores with sizes between 5 and 20 μm was a result of solvent extraction from polymer matrix. In addition, the micro-CT slice shown in (Figure 4.3 B) displays a well-interconnected pore structure. The co-existence of macropores with different sizes is not only favorable for the ingrowth of cells and new tissue but also beneficial to the exchange of nutrients and metabolic waste [79].

Mechanical property is an important factor in the design of bone tissue engineering scaffolds. Figure 4.5 shows the compressive stress–strain curves of the different scaffolds. All scaffolds behaved as polymeric foams with distinct linear elastic, collapse plateau and densification regions [201]. The σ_{10} value of the composite scaffolds decreased with the increasing content of zein. This might be attributed to a lower degree of crystallinity caused by the presence of zein.

Tuning the hydrophilicity of the biomaterial surface has strong influence on the adhesion and proliferation of cells [204]. The results showed that the surface of the zein/PCL composite scaffolds was more hydrophilic than that of the PCL scaffold, as

indicated by the decrease in the water contact angle. This phenomenon corresponds to the relatively more hydrophilic property of zein in comparison with the hydrophobic characteristic of PCL. Salerno et al. also found that the incorporation of zein in the composite improved the hydrophilicity of PCL [205].

The degradation property is crucial to the long-term success of a bone tissue engineering scaffold. In the present study, *in vitro* degradation behavior of the scaffolds in PBS was monitored in terms of changes in pH, weight loss and morphology. As shown in Figure 4.7, only a slight weight loss was observed for the PCL scaffold. The weight loss of the zein/PCL composite scaffolds was noticeable and increased with the increasing content of zein in the composite. Considering a negligible PCL weight loss during the 28-day immersion in PBS, the weight loss of the zein/PCL composite scaffold was ascribed to the degradation of zein.

This consideration was supported by the changes in FTIR spectra of the scaffolds during the immersion period. In Figure 4.4 D and E, a significant decrease in the intensity of characteristic bands of zein was observed while the C=O stretching of the ester bond in PCL remained unchanged. Compared to PCL, zein is characterized by improved solubility in aqueous environment [151, 153, 206]. The zein molecules on the surface or the superficial layer of the zein/PCL scaffolds might degrade first due to their exposure to the surrounding degradation medium. The degradation of those surface molecules then leave more space in the composite scaffolds, facilitating the

flow of degradation medium into the interior of scaffolds. The relatively faster degradation of zein leads to a more porous structure with enhanced interconnectivity, which is beneficial to cell colonization and new tissue ingrowth [206]. The slower degradation of PCL could help maintain the scaffolds' structure and strength, which is necessary for cell adhesion, proliferation and tissue infiltration [206].

The SEM images shown in Figure 4.9 provide evidence for the above consideration. After immersion in PBS for 28 days, an irregular macroporous structure with large voids and small fissures was observed. The gradual degradation of the zein/PCL composite scaffold is favorable to the objective of tissue engineering strategy, which is the substitution of the temporary matrix by the native tissue [128]. By adjusting the content of zein in the composite, the degradation rate of the zein/PCL composite scaffolds could be tailored to match with the rate of tissue regeneration.

Once implanted *in vivo*, the scaffolds will face a more complex environment. The results of the *in vitro* degradation tests could only provide a prediction of the *in vivo* degradation behavior of the scaffolds. Thus, a long-term *in vivo* implantation test is planned to investigate the biocompatibility and biodegradability of the zein/PCL biocomposite scaffolds.

4.5 Conclusion

The work presented in this chapter shows the fabrication and properties of the zein/PCL biocomposite scaffolds. The scaffolds fabricated by the particulate leaching

method have well-interconnected macroporous structure. The composite scaffolds exhibit enhanced hydrophilicity compared with the PCL scaffold. The results of the *in vitro* degradation study showed that the zein/PCL composite scaffolds degraded faster than the PCL scaffold during the 28-day immersion in PBS. Furthermore, the degradation rate of the scaffold could be tuned by adjusting the content of zein in the composite. These findings suggest that the zein/PCL biocomposite scaffolds may have potential application in bone tissue engineering.

Chapter 5

Fabrication and properties of porous scaffold of magnesium phosphate/polycaprolactone biocomposite for bone tissue engineering

F. Wu [a], C. Liu [b], B. O'Neill [a], J. Wei [b], Y. Ngothai [a]

[a] School of Chemical Engineering, The University of Adelaide, Adelaide, SA 5005, Australia
[b] The State Key Laboratory of Bioreactor Engineering, and Engineering Research Center for Biomedical Materials of Ministry of Education, East China University of Science and Technology, Shanghai 200237, China

This is a revised and corrected version of the paper which appears in:

Applied Surface Science, 2012, 258, 7589–7595.

STATEMENT OF AUTHORSHIP

Fabrication and properties of porous scaffold of magnesium phosphate/polycaprolactone biocomposite for bone tissue engineering

Applied Surface Science, 2012, 258, 7589–7595.

Fan Wu (Candidate)

Designed and performed experiments, interpreted and processed data, wrote manuscript

I hereby certify that the statement of contribution is accurate

Signed ……*Date*……

Changsheng Liu

Manuscript evaluation

I hereby certify that the statement of contribution is accurate and I give permission for the inclusion of the paper in the thesis

Signed ……*Date*……

Brian O'Neill

Manuscript evaluation

I hereby certify that the statement of contribution is accurate and I give permission for the inclusion of the paper in the thesis

Signed ……*Date*……

Jie Wei

Helped with the design of experiments and manuscript evaluation, acted as corresponding author

I hereby certify that the statement of contribution is accurate and I give permission for the inclusion of the paper in the thesis

Signed ……*Date*……

Yung Ngothai

Manuscript evaluation and acted as corresponding author

I hereby certify that the statement of contribution is accurate and I give permission for the inclusion of the paper in the thesis

Signed ……. *Date*.……..……..

Chapter 5 Preparation and characterization of porous scaffold of magnesium phosphate/polycaprolactone biocomposite for bone tissue engineering

5.1 Introduction

In bone tissue engineering strategy, scaffolds are of crucial importance since they act as temporary substrates for cell adhesion, proliferation and ultimately the regeneration of new tissue. From this perspective, scaffolds for bone regeneration should meet certain criteria: (1) the minimal requirement for pore size is considered to be 100 μm [13]. To enhance osteogenesis and the formation of capillaries, pore sizes > 300 μm are recommended [13]. (2) A highly porous structure is considered to favor osteogenesis [13]. (3) The scaffold should possess mechanical property similar to that of the bone repair site [13]. (4) The scaffold should have good biocompatibility. (5) The degradation rate of the scaffolds should match the bone regeneration rate.

PCL is a biodegradable aliphatic polyester. Owing to its good biocompatibility and easy-processing capability, PCL has been used for the fabrication of scaffolds for tissue engineering purposes [124]. Unfortunately, applications of PCL scaffolds might be limited due to its hydrophobicity and slow degradation rate. The hydrophobic property of PCL may adversely affect cell attachment and penetration into the porous structure. The degradation of PCL is considered through the hydrolytic cleavage of ester groups causing random chain scissions [124]. Previous

research demonstrated that some PCL-based polymers took about 3–4 years to degrade completely [125, 126].

With features of fast setting and high early strength, MPC has been widely used in civil engineering as rapid-repair materials. Recently, much attention has been paid to its clinic applications as bone substitution materials [157]. Liu [158] first reported the use of MPC as inorganic bone adhesive in screw fixation, artificial joints fixation and comminuted fracture fixation. Previous research has confirmed its good *in vivo* degradability and biocompatibility [159, 161, 207]. However, it is difficult to process MPC into porous scaffolds for tissue engineering applications due to its brittleness.

Since it is impossible to prepare scaffolds made of single material satisfying the numerous requirements, the fabrication of scaffolds using composite materials is promising. Researchers have combined PCL with bioactive glasses [143, 144] and bioceramics such as HA [137, 138, 168], TCP [139, 208] to produce composite scaffolds for bone regeneration. The presence of HA has been demonstrated to enhance the bioactivity [138]. The incorporation of bioglass has been shown to improve the hydrophilicity and bioactivity of the PCL scaffold [143].

In this study, we first synthesized magnesium phosphate (MP) powder through the hardening process of MPC. Then we used a blend of PCL and MP as the scaffolding material. The composite scaffolds were prepared using the particulate leaching method. The microstructure of the scaffolds was evaluated using micro-CT and SEM.

The mechanical properties were examined by compression tests. The hydrophilicity and degradability of the composite scaffolds were also investigated.

5.2 Materials and methods

5.2.1 Materials

PCL (M_n = 80,000, T_m = 60 °C and ρ = 1.145 g/cm^3) was purchased from Sigma–Aldrich. MP powder was synthesized through the hardening reaction of MPC. The cement powder was composed of MgO and $NH_4H_2PO_4$ in a molar ratio of 3.8:1. MgO was prepared by heating basic magnesium carbonate pentahydrate [$(MgCO_3)_4 \cdot Mg(OH)_2 \cdot 5H_2O$] in a furnace at 1500 °C for 6 h. The resultant powder was first cooled to room temperature, and then grounded in a planetary ball mill for 5 min, followed by sieving into 48–74 μm particles. The cement powder was then mixed with deionized water to form a homogeneous paste and stored in a 100% relative humidity environment at 37 °C for hardening. After hardening for 24 h, the cement sample was dried, ground and sieved into 48–74 μm powder. NaCl particles with size in the range of 250–450 μm were used as the porogen. All the chemicals except PCL were purchased from Sinopham Chemical Reagent Co., Ltd.

5.2.2 Preparation of composite scaffolds

The MP/PCL composite scaffolds were prepared by the particulate leaching method. PCL pellets were dissolved in dichloromethane and a certain amount of MP powder was added. The solution was sonicated for 10 min to disperse MP powder uniformly [162]. The ratio of the MP/PCL mixture to dichloromethane was fixed at 10%

(w/v). NaCl particles were then added into the MP/PCL mixture and stirred for 10 min. Subsequently, the mixture was transferred into the molds. The samples were air-dried by natural evaporation for 24 h and then vacuum-dried at 40 °C for 48 h to remove the solvent completely. The salt particles were leached out by immersing the samples in deionized water for 72 h at 37 °C. The water was refreshed three times a day to favor the complete dissolution of the salt. After leaching, the scaffolds were air-dried for 24 h and then vacuum-dried for 12 h. Two groups of composite scaffolds were prepared as described above by blending different amounts of MP powder (20 and 40 wt%) with PCL. Pure PCL scaffolds were prepared as the control. The compositions of the scaffolds prepared are listed in Table 5.1.

5.2.3 Characterization

5.2.3.1 Micro-CT analysis

The scaffolds (4 × 4 × 20 mm^3) were analyzed using a high-resolution micro-CT scanner (Skyscan 1072, Kontich, Belgium). The samples (n=3 for each group) were scanned at 11.01 μm resolution. The scan was carried out at a voltage of 50 kV and a current of 120 μA. No filter was applied. The obtained isotropic slice data were reconstructed into 2D images. These 2D images were compiled to build 3D models in CTan (Skyscan). The 3D models were visualized using CTvol (Skyscan). The 3D analysis was performed in CTan (Skyscan) for the calculation of porosity and pore size distribution.

5.2.3.2 Analysis by XRD and SEM

The scaffolds were characterized by XRD (D/MAX 2550, Rigaku) with Cu K_α radiation and Ni filter (λ =1.5406 A, 100 mA, 40 kV) in a continuous scan mode. The 2θ range was from 10° to 70° at a scanning speed of 10 °/min. The cross-sectional morphology of the scaffolds ($4 \times 4 \times 10$ mm^3) was examined by SEM (XL30 FEGSEM, Philips). The scaffolds were cut by a blade and coated with gold.

5.2.3.3 Mechanical properties

The compressive mechanical properties were measured according to the ASTM standard D695-02a with a universal testing machine (AG-2000A, Shimadzu Autograph, Shimadzu Co., Ltd.). Three cylindrical samples (diameter: 6 mm, height: 12 mm) of each composition were measured. The compression tests were carried out at a loading rate of 1 mm/min, until obtaining a maximum reduction in samples' height of 70%. The elastic modulus was calculated as the slope of the initial linear region of the stress-strain curve.

5.2.3.4 Hydrophilicity

The hydrophilicity of the scaffolds was evaluated by water contact angle measurements performed on a contact angle system (JC2000D3, Shanghai Zhongchen Digital Technology Apparatus Co., Ltd.). A water droplet (1 μL) was poured on the material surface and the water contact angle was measured after 30 s. Five measurements for each sample were performed and the results were expressed

as mean ± SD.

5.2.4 *In vitro* degradation study

For degradation experiments, samples (10 × 10 × 3 mm^3) were weighed (W_i), immersed in 0.01 M PBS (pH 7.4) and incubated at 37 °C with constant shaking at 100 rpm for 28 days. Three samples for each group were tested. The PBS solutions were changed twice a week. At preselected time point, the samples were removed from the solution and rinsed gently with deionized water. The samples were then dried at 37 °C until exhaustion and weighed (W_f). The weight loss was calculated according to the following equation [128]:

$$\text{weight loss (\%)} = \frac{(W_i - W_f)}{W_i} \times 100\% \quad (5.1)$$

The surface morphology of the scaffolds before and after degradation was characterized by SEM (JSM6360, JEOL). After immersion in PBS for several time periods, the scaffolds were analyzed using XRD (D/MAX 2550, Rigaku) with Cu K_α radiation and Ni filter (λ =1.5406 A, 100 mA, 40 kV) in a continuous scan mode. The 2θ range was from 10° to 70° at a scanning speed of 10 °/min.

5.3 Results

5.3.1 Micro-CT analysis

Micro-CT was used to characterize the pore structure of the scaffolds. As shown in Figure 5.1, the 3D reconstruction model of MP/PCL-40 scaffold showed a highly

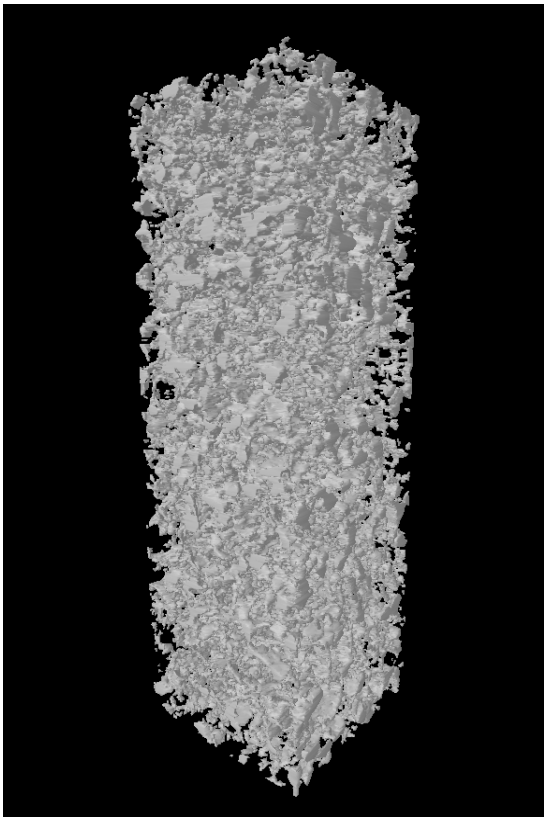

Figure 5.1 Micro-CT 3D reconstruction model of the MP/PCL-40 scaffold.

Table 5.1 Compositions and porosities of the MP/PCL composite scaffolds.

Scaffold	Matrix materials		NaCl/matrix (wt/wt)	Porosity (%)
	MP (wt%)	PCL (wt%)		
PCL	0	100	8:1	76.23 ± 1.39
MP/PCL-20	20	80	8:1	72.50 ± 2.08
MP/PCL-40	40	60	8:1	73.91 ± 3.67

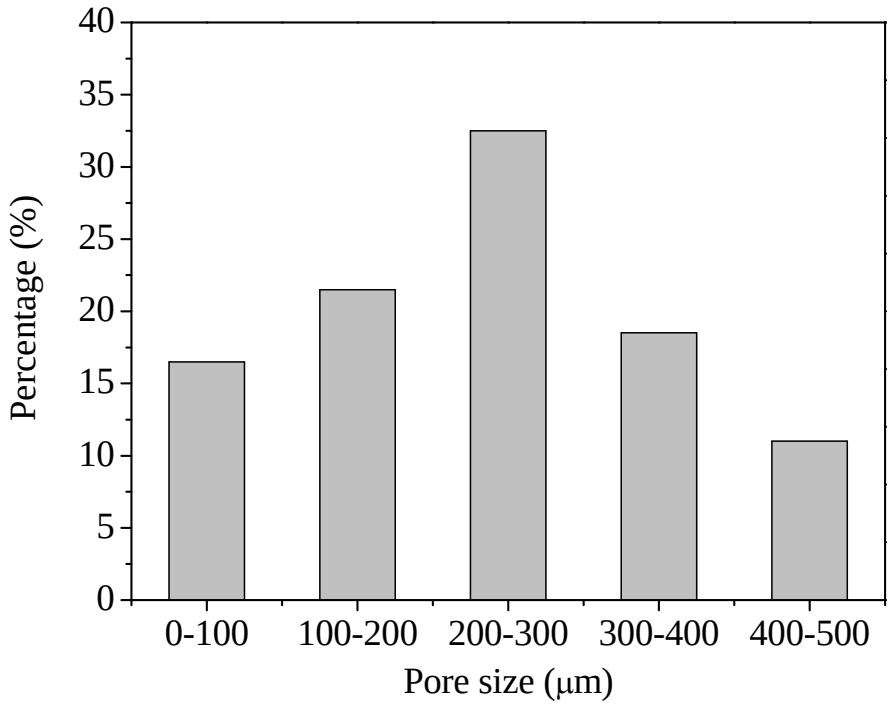

Figure 5.2 Pore size distribution of the MP/PCL-40 scaffold.

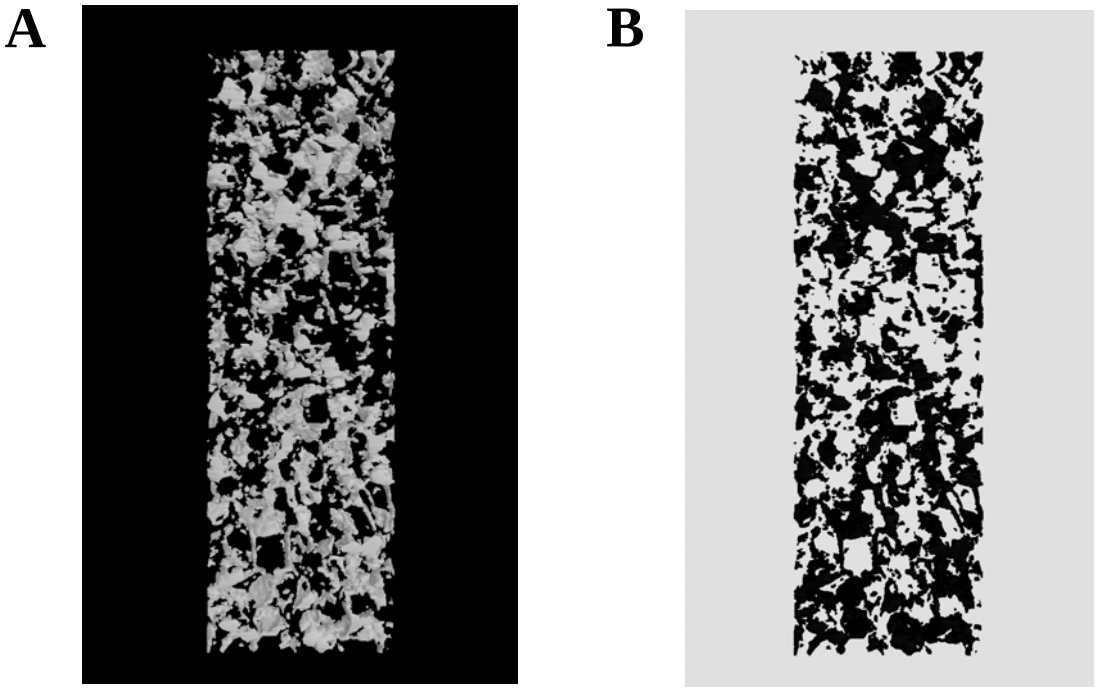

Figure 5.3 Micro-CT visualizations of a cross-section of MP/PCL-40 scaffold: (A) positive image (gray: scaffold; black: pore) and (B) negative image (black: scaffold; white: pore).

porous structure. From micro-CT data, structural parameters such as porosity and pore size distribution were calculated. Table 5.1 presents the porosities of the different scaffolds. The addition of 20 and 40 wt% MP particles into PCL matrix did not noticeably influence the porosity of PCL scaffolds. The porosity of the composite scaffolds could reach about 73%.

The MP/PCL-40 scaffold exhibits a wide pore size distribution as shown in Figure 5.2. Leaching of the porogen and extraction of the solvent led to the formation of pores with a range of sizes.

Figure 5.3 presents the micro-CT visualizations of a cross-section of MP/PCL-40 scaffold. In Figure 5.3 A, the scaffold appears in gray and the pores in black. The interconnectivity of the pores could be clearly observed from the negative image shown in Figure 5.3 B where black represents the scaffold and white represents the pores.

5.3.2 SEM analysis

SEM micrographs shown in Figure 5.4 present the cross-sectional morphology of the MP/PCL-40 scaffold. The composite scaffold shows macroporous structure with pore size varying from several microns to hundreds of microns.

5.3.3 XRD analysis

The XRD patterns of MP particles, PCL and MP/PCL-40 composite scaffold are

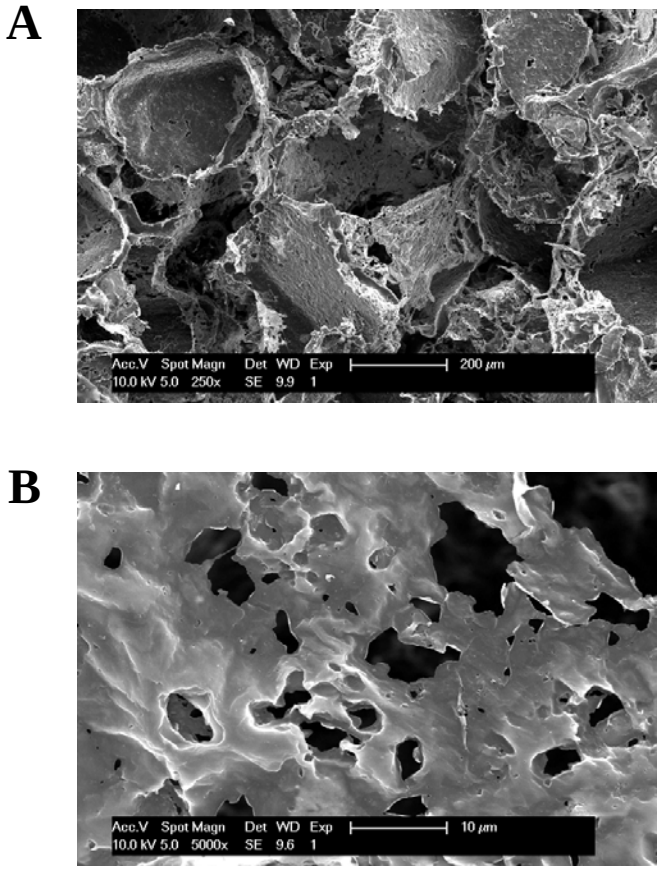

Figure 5.4 SEM images of the cross-sectional morphology of MP/PCL-40 scaffold: (A) macropores larger than 200 μm and (B) macropores less than 10 μm.

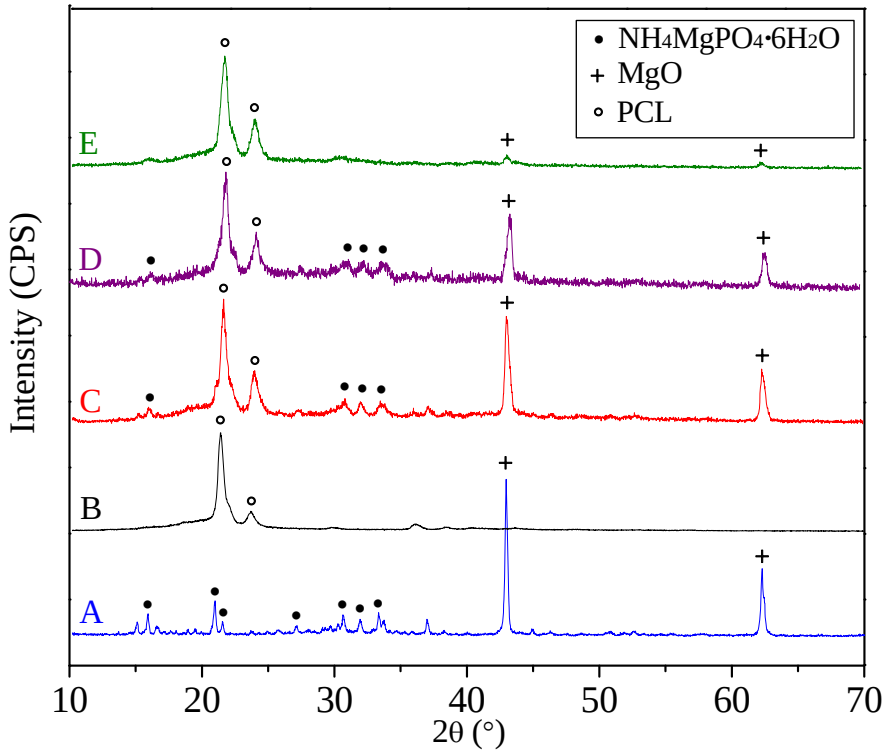

Figure 5.5 XRD patterns of (A) MP particles, (B) PCL, (C) MP/PCL-40 scaffold, (D) MP/PCL-40 scaffold after immersion in PBS for 14 days and (E) MP/PCL-40 scaffold after immersion in PBS for 28 days.

shown in Figure 5.5 A–C. The peaks of $NH_4MgPO_4 \cdot 6H_2O$ can be seen at 2θ = 15.7°, 20.8°, 21.4°, 27.0°, 30.6°, 31.8° and 33.2° in Figure 5.5 A. In addition, the peaks of unreacted MgO are observed at 2θ = 42.8° and 62.2°. Figure 5.5 A indicates that the chemical composition of the MP particles is a mixture of struvite and MgO. As shown in Figure 5.5 C, the composite scaffold exhibits two strong peaks at 2θ = 21.5° and 23.8° belonging to PCL, together with the peaks of struvite and MgO.

5.3.4 Mechanical properties

The compressive stress–strain curves of the PCL and MP/PCL composite scaffolds are shown in Figure 5.6. All curves exhibit distinct characteristics of porous polymer foam: a linear elastic region appeared at small strain, followed by a plateau region at larger strain and a solidifying region where the stress increased sharply at very large strain [201]. The PCL scaffolds had compressive modulus of 4.32 ± 0.13 MPa. The compressive moduli for MP/PCL-20 and MP/PCL-40 scaffolds were 3.62 ± 0.15 MPa and 2.37 ± 0.15 MPa, respectively.

5.3.5 Hydrophilicity

As shown in Figure 5.7, the water contact angle of the MP/PCL-40 scaffold was 68°, which was less than the corresponding 79° observed for the PCL scaffold. This implies that the surface of the MP/PCL composite scaffold was more hydrophilic than that of the PCL scaffold.

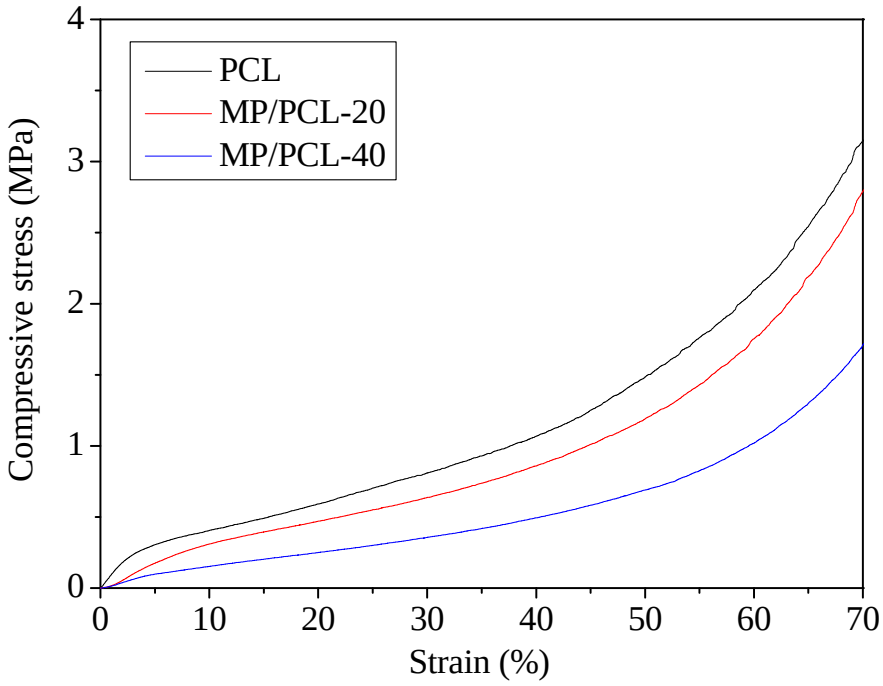

Figure 5.6 Compressive stress–strain curves of the different scaffolds.

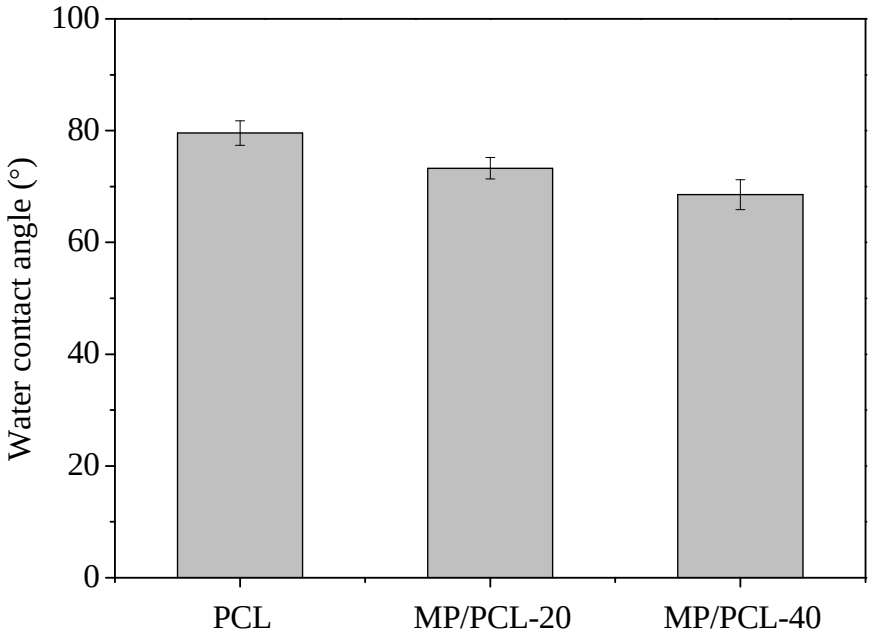

Figure 5.7 Water contact angles of the different scaffolds.

5.3.6 *In vitro* degradation

The weight loss data for the MP/PCL composite scaffolds and PCL scaffolds are summarized in Figure 5.8. The PCL scaffolds had a slight weight loss (less than 2%) during the incubation period. As for the composite scaffolds, the weight loss increased over the whole incubation period and proportionally to the MP content. At the end of the degradation period (28 days), the weight losses were around 17% for the MP/PCL-20 scaffolds and 32% for the MP/PCL-40 scaffolds, respectively.

The XRD patterns of the MP/PCL-40 scaffolds after immersion in PBS for 14 and 28 days are shown in Figure 5.5 D and E. The peak intensities of struvite and MgO distinctly decreased with the extension of incubation time.

Figure 5.9 shows the surface morphology of the MP/PCL-40 scaffolds before and after immersion in PBS for 28 days. After 28-day incubation in PBS, more macropores with sizes less than 100 μm appeared on the walls of the scaffolds (Figure 5.9 C). Under higher magnification (Figure 5.9 D), the presence of indentations and cracks was evident on the scaffold surface. The scaffold exhibited more surface roughness after immersion for 28 days.

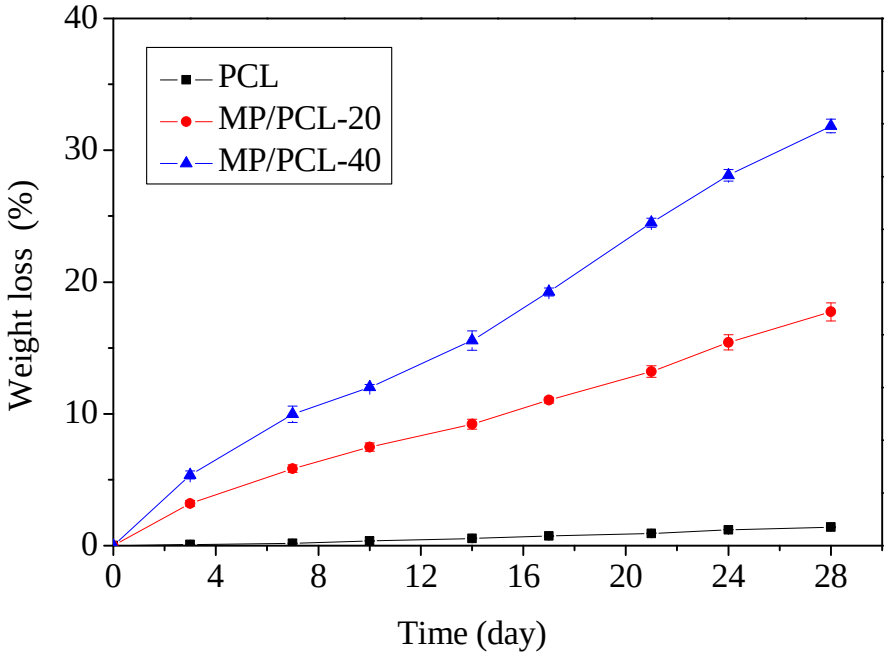

Figure 5.8 Weight losses of the different scaffolds during the immersion period.

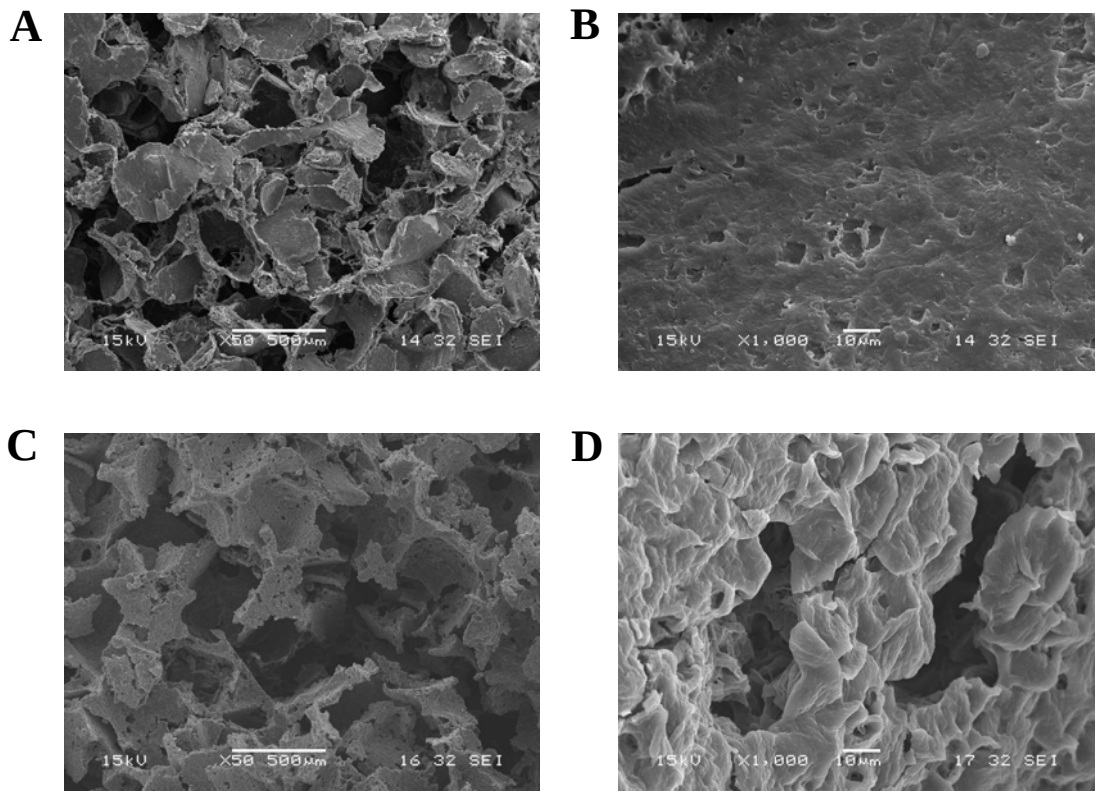

Figure 5.9 SEM images of the surface morphology of MP/PCL-40 scaffolds: (A and B) before immersion and (C and D) after immersion in PBS for 28 days.

5.4 Discussion

The architectural characteristics of a scaffold, including porosity, pore size and interconnectivity, play an important role in tissue regeneration [209]. In this study, both SEM and micro-CT were used to characterize the pore architecture of the scaffolds. The MP/PCL-40 composite scaffold exhibits a highly porous structure with porosity around 73%. The macropores with large sizes were formed due to the leaching of salt. As shown in Figure 5.4 A, the composite scaffold presents cubical macropores with pore morphology similar to the geometry of salt particles. Several macropores with sizes ranging from 1 to 10 μm are present on the walls of the scaffolds as shown in Figure 5.4 B. The formation of those macropores with smaller sizes was a result of solvent extraction. A proper combination of macropores with different sizes is favorable to cell adhesion and proliferation as well as the ingrowth of new tissue [79].

Pore interconnectivity plays an important role in promoting the ingrowth of cells and new tissue. Bernardo et al. [210] qualitatively assessed pore interconnectivity by observing the positive and negative slices of selected scaffold cross-section. From Figure 5.3, it can be seen that most of the macropores are well-interconnected. Good interconnectivity is believed to be beneficial to the flow transport of nutrients and wastes [203].

Hydrophilicity is an important characteristic that would affect the performance of a

biomaterial in application. Wei et al. [211] demonstrated that a more hydrophilic surface is favorable to cell attachment and spreading. Moreover, osteoblast prefers a more hydrophilic surface [212]. Water contact angle (WCA) has been used as an indicator of hydrophilicity in several studies [213-215].

Considering the hydrophilic nature of MP particles, we hypothesize that the incorporation of MP component may help reduce the hydrophobicity of PCL. This hypothesis was confirmed by the results of WCA measurement presented in Figure 5.7. Compared to PCL scaffold, a 13.8% decrease in WCA was observed for the MP/PCL-40 scaffold. This indicates that the incorporation of MP particles into the PCL matrix improved the hydrophilic property of polymer. In addition, depending on the amount of MP particles incorporated, the composite surface wettability can be adjusted to obtain different degrees of hydrophilicity.

Such an improvement of hydrophilicity indicated by a decrease in WCA has also been observed for other polymer/bioceramic composite scaffolds [199, 213, 214]. For instance, Yeo et al. [213] fabricated a composite scaffold consisting of PCL/β-TCP struts and collagen nanofibers. A decrease of 18.9% or 6.7% in WCA value was observed for composite scaffolds with or without collagen nanofibers [213]. Navarro et al. [214] developed a biodegradable scaffold made of PLA/calcium phosphate glass composite. The incorporation of 50% bioglass into the PLA matrix induced an 8% decrease in WCA [214].

In the design and manufacture of scaffolds for bone tissue engineering, appropriate degradability is an important factor that must be taken into account. As shown in Figure 5.8, only a slight weight loss was observed for the PCL scaffolds during the whole incubation period. Compared with the PCL scaffolds, the weight loss of the composite scaffolds was more obvious and gradually increased with the extension of incubation time. Taking the negligible weight loss of PCL into consideration, the weight loss of the composite scaffolds could be attributed to the degradation of struvite and the removal of MgO particles.

The degradation of struvite occurred through chemical dissolution. Both *in vitro* [216] and *in vivo* [217] studies have confirmed the good degradability of struvite. Gbureck and co-workers [217] evaluated the chemical dissolution of struvite-forming biocement *in vivo* in a heterotopic model without osteoclastic degradation. After 15 months' intramuscular implantation, the struvite phase completely dissolved as indicated by the disappearance of the main diffraction peaks of struvite in XRD pattern [217]. As indicated by XRD patterns in Figure 5.5, the peak intensity of struvite decreased with the extension of incubation time. A decrease in the peak intensity of MgO was also noticed in Figure 5.5. Considering the low solubility of MgO, a possible explanation for this result is the rinsing step during the degradation study, which likely caused the removal of MgO particles.

The removal of MP particles created several macropores with sizes smaller than 100

μm on the walls of the scaffolds, as can be seen from Figure 5.9. These macropores could assist in the diffusion of degradation medium into the interior of scaffolds, thus facilitating the hydrolytic degradation of PCL. Moreover, increased surface roughness of the composite scaffolds was observed after immersion for 28 days. The increased surface roughness may result from the surface erosion during the immersion period. Some researchers indicated that the surface erosion occurred via a random and bulk hydrolysis of the ester bonds in the PCL polymer chain [218]. Surface roughness of scaffolds has been shown to influence the adhesion and proliferation of osteoblast cells [219, 220].

In addition, the weight loss of the composite scaffolds increased with the MP content at each time point. The degradation rate of the composite scaffolds could be tailored to match with the rate of tissue regeneration by adjusting the MP content in the composite. The mechanical testing results show that the compressive modulus of the MP/PCL composite scaffold is lower than that of human trabecular bone (50 MPa) [221]. The composite scaffold is not suitable to be applied in high-load-bearing sites. With highly interconnected porous structure and fast degradation rate, the MP/PCL composite scaffold can be used in non-load-bearing applications or in combination with internal or external fixation devices, as suggested by Hutmacher et al. [10]. Guan and Davies [222] developed a composite scaffold for bone tissue engineering by combining PLGA with bioresorbable calcium phosphate cement particles. The scaffold was characterized by a highly interconnected macroporosity, with macropores of 0.8–1.8

mm and porosities ranging from 81% to 91% [222]. The compressive modulus of the composite scaffold was in the range of 2–7.5 MPa [222]. This composite scaffold can be applied as trabecular bone graft substitute [222].

5.5 Conclusion

The work presented in this chapter describes the preparation and characterization of the MP/PCL composite scaffolds. The composite scaffold exhibits an interconnected macroporous structure with porosity around 73%. The incorporation of MP particles led to an enhanced hydrophilicity of the composite scaffolds. The results of the *in vitro* degradation study indicate that the degradation rate of the composite scaffolds could be modulated by varying the amount of MP particles introduced into the polymer matrix. The results suggest that the MP/PCL composite scaffolds might be promising materials for bone tissue engineering applications. Future developments will be focused on the assessment of *in vivo* biocompatibility and degradability of the composite scaffolds.

Chapter 6 Conclusion

Overall, it has been demonstrated that the premixed and injectable PLA-modified cd-AB is a promising material for the reconstruction of bone defects. Both zein/PCL biocomposite scaffolds and MP/PCL composite scaffolds exhibited potential for applications in bone tissue engineering.

6.1 Premixed and injectable calcium deficient apatite biocement

To facilitate ease of handling by surgeons and to improve the properties of calcium phosphate cement, this study aimed to develop premixed and injectable bone cement as a potential bone graft substitute. In Chapter 3, a new premixed and injectable cd-AB was developed. The cement pastes could be prepared prior to surgery in a well-controlled environment thereby eliminating on-site mixing during surgery. The premixed cd-AB paste remained stable in the syringe and hardened only after being injected into the damaged site. When contacted with an aqueous environment, the premixed cd-AB paste exhibited excellent washout resistance. Due to the exchange of solvent with water, the premixed cd-AB required a longer setting time than that for the conventional cd-AB. The hydration products of premixed cd-AB were a mixture of nanocrystalline cd-HA and PLA. The degradation of premixed cd-AB was faster than conventional cd-AB in Tris-HCl solution. The premixed cd-AB supported the attachment and proliferation of MG-63 osteoblast-like cells, confirming good cytocompatibility. The premixed and injectable PLA-modified cd-AB may be useful

in dental, craniofacial and periodontal repairs.

6.2 Biocomposite scaffolds for bone tissue engineering

To overcome the limitations associated with the use of PCL scaffolds, zein (a natural corn protein) was incorporated into PCL matrix to develop zein/PCL biocomposite scaffolds for bone tissue engineering applications. The resulting composite scaffolds contained a well-interconnected macroporous structure and were fabricated via the solvent casting–particulate leaching method. Compared to the PCL scaffold, the composite scaffolds exhibited enhanced surface hydrophilicity. The results of the *in vitro* degradation study confirmed that the zein/PCL composite scaffolds degraded faster than the PCL scaffold during the 28-day immersion in PBS. Furthermore, the degradation rate of the scaffold could be tuned by adjusting the content of zein in the composite. These findings suggest that the zein/PCL biocomposite scaffolds may have potential application in bone tissue engineering. In Chapter 5, MP particles were introduced into PCL to fabricate MP/PCL composite scaffolds. The composite scaffold exhibited a strongly interconnected macroporous structure with porosity around 73%. The incorporation of MP particles led to an enhanced hydrophilicity of the composite scaffolds. The results of the *in vitro* degradation study indicate that the degradation rate of the composite scaffolds could be modulated by varying the amount of MP particles introduced into the polymer matrix. In conclusion, this study suggests that the MP/PCL composite scaffolds may provide promising materials for tissue engineering applications for bone regeneration.

6.3 Future work

There is still a need to evaluate and improve some properties for the materials developed in this study. Some ideas on future work are listed below.

6.3.1 Future work regarding premixed and injectable cd-AB

1. The long-term stability of premixed cd-AB should be investigated. The premixed cement pastes were prepared then stored in sealed syringes. The possibility to inject or handle the pastes after certain storage time needs to be studied. Critical factors influencing the pastes' stability include storage conditions (humidity and temperature) and the presence of water impurities in the liquid phase and/or the powder phase.

2. The rheological properties of premixed cd-AB need to be quantified to determine the key factors that influence the flow behavior of the cement paste.

3. To satisfy the requirement of clinical use, the setting time of premixed cd-AB must be shortened. More rapid setting could be achieved by the addition of a hardening accelerator and the optimization of particle sizes of TTCP and DCPA.

4. Likewise, the mechanical strength of premixed cd-AB should be improved to meet the requirement for potential applications in load-bearing areas. A texture measurement will be performed to explain the lower mechanical strength of premixed cd-AB in comparison with conventional cd-AB.

5. *In vivo* experiments need to be performed to determine the overall biocompatibility of premixed cd-AB. Meanwhile, the long-term *in vivo* degradability of the cement should be examined.

6. The cytotoxicity and biocompatibility of NMP will be assessed.

6.3.2 Future work regarding the zein/PCL scaffolds

1. The distribution of zein throughout the polymer matrix will be characterized to develop a greater understanding of its influence on the degradation behavior and mechanical properties of the scaffolds.

2. The mechanical properties of the zein/PCL composite scaffolds appeared to be insufficient for load-bearing applications. Therefore, there remains a clear need to improve their mechanical properties.

3. The effect of the NaCl concentration on the porosity of the scaffolds will be investigated. Samples prepared in the absence as well as in the presence of different amounts of NaCl particles will be characterized using micro-CT.

4. The hydrophilicity of the PCL/zein scaffolds should be further improved. Possible solution may involve a chemical surface modification of the scaffolds, e.g. surface treatment with sodium hydroxide solution.

5. This thesis presents the results from a short-term degradation study. A long-term *in*

vitro degradation test should be performed to understand the degradation mechanism and determine the kinetics of the degradation for the composite scaffolds. The influence of zein on the degradation of PCL should be further investigated.

6. The effects of zein within the PCL matrix on the biological function of bone-associated cells, such as cell adhesion, migration, differentiation and proliferation, need to be studied.

7. *In vivo* studies are needed to examine the biocompatibility and degradability of the zein/ PCL composite scaffolds.

8. Composites made of PCL and some other plant-derived proteins such as pea protein isolate and soy protein isolate will be used to fabricate tissue engineering scaffolds.

6.3.3 Future work regarding the PCL/MP scaffolds

1. The possibility of further improvement in the hydrophilicity of the MP/PCL scaffolds should be explored. A potential solution could be the modification of the distribution of MP particles. Hutmacher et al. [10] indicated that the ceramic particles should not only be embedded into the polymer matrix, but also exposed on the surface to improve osteoconductivity. The influence of MP particle size on the hydrophilicity of the composite scaffolds requires investigation.

2. The distribution of MP particles throughout the PCL matrix will be characterized to investigate its influence on the degradation behavior and mechanical properties of the scaffolds.

3. Micro-CT analysis will be performed to investigate whether the large macropores generated by the leaching of NaCl are homogeneously distributed in the scaffold. The effect of the sedimentation of NaCl particles during the solvent evaporation process on the distribution of macropores will be studied.

4. The influence of the incorporation of MP particles into the PCL scaffolds on the biological function of bone-associated cells needs to be studied. In particular, the synergistic effects of Mg^{2+} and PO_4^{3-} on the cellular responses require investigation.

5. *In vivo* studies will examine the biocompatibility and degradability of the MP/PCL composite scaffolds.

Chapter 7 References

[1] Fini M, Motta A, Torricelli P, Giavaresi G, Nicoli Aldini N, Tschon M, et al. The healing of confined critical size cancellous defects in the presence of silk fibroin hydrogel. Biomaterials 2005;26:3527-36.

[2] Greenwald AS, Boden SD, Goldberg VM, Khan Y, Laurencin CT, Rosier RN. Bone-graft substitutes: facts, fictions, and applications. J Bone Joint Surg 2001;83-A, Supplement 2, Part 2:98-103.

[3] Giannoudis PV, Dinopoulos H, Tsiridis E. Bone substitutes: an update. Injury 2005;36S:S20-S7.

[4] Young CS, Ladd PA, Browning CF, Thompson A, Bonomo J, Shockley K, et al. Release, biological potency, and biochemical integrity of recombinant human platelet-derived growth factor-BB (rhPDGF-BB) combined with Augment^{TM} bone graft or *GEM 21S* beta-tricalcium phosphate (β-TCP). J Control Release 2009;140:250-5.

[5] Laurencin CT, Khan Y, El-Amin SF. Bone graft substitutes. Expert Rev Med Devices 2006;3:49-57.

[6] Burguera EF, Xu HHK, Weir MD. Injectable and rapid-setting calcium phosphate bone cement with dicalcium phosphate dihydrate. J Biomed Mater Res B 2006;77B:126-34.

[7] LaPrade RF, Botker JC. Donor-site morbidity after osteochondral autograft transfer procedures. Arthroscopy 2004;20:e69-e73.

[8] Kainer MA, Linden JV, Whaley DN, Holmes HT, Jarvis WR, Jernigan DB, et al. Clostridium infections associated with musculoskeletal-tissue allografts. N Engl J Med 2004;350:2564-71.

[9] Langer R, Vacanti JP. Tissue engineering. Science 1993;260:920-6.

[10] Hutmacher DW, Schantz JT, Lam CXF, Tan KC, Lim TC. State of the art and future directions of scaffold-based bone engineering from a biomaterials perspective. J Tissue Eng Regen Med 2007;1:245-60.

[11] Rodan GA. Introduction to bone biology. Bone 1992;13:S3-S6.

[12] Sikavitsas VI, Temenoff JS, Mikos AG. Biomaterials and bone mechanotransduction. Biomaterials 2001;22:2581-93.

[13] Karageorgiou V, Kaplan D. Porosity of 3D biomateiral scaffolds and osteogenesis. Biomaterials 2005;26:5474-91.

[14] Liebschner MAK. Biomechanical considerations of animal models used in tissue engineering of bone. Biomaterials 2004;25:1697-714.

[15] Roodman GD. Advances in bone biology: the osteoclast. Endocr Rev 1996;17(4):308-32.

[16] Boyle WJ, Simonet WS, Lacey DL. Osteoclast differentiation and activation.

Nature 2003;423:337-42.

[17] Ducy P, Schinke T, Karsenty G. The osteoblast: a sophisticated fibroblast under central surveillance. Science 2000;289:1501-4.

[18] Teitelbaum SL. Bone resorption by osteoclasts. Science 2000;289:1504-8.

[19] Zhou H, Lawrence JG, Bhaduri SB. Fabrication aspects of PLA-CaP/ PLGA-CaP composites for orthopedic applications: A review. Acta Biomater 2012;8:1999-2016.

[20] Martins AM, Alves CM, Kasper FK, Mikos AG, Reis RL. Responsive and in situ-forming chitosan scaffolds for bone tissue engineering applications: an overview of the last decade. J Mater Chem 2010;20:1638-45.

[21] Bohner M. Resorbable biomaterials as bone graft substitutes. Materials Today 2010;13:24-30.

[22] Lange TA, Zerwekh JE, Peek RD, Mooney V, Harrison BH. Granular tricalcium phosphate in large cancellous defects. Ann Clin Lab Sci 1986;16:467-72.

[23] White E, Shors EC. Biomaterial aspects of interpore-200 porous hydroxyapatite. Dental Clin North Am 1986;30:49-67.

[24] Brown WE, Chow LC. Dental restorative cement pastes. United States1985.

[25] Brown WE, Chow LC. A new calcium phosphate, water-setting cement. In: PW B, editor. Cements Research Progress. Westerville, Ohio: American Ceramic Society;

1987.

[26] Bohner M. Calcium orthophosphates in medicine: from ceramics to calcium phosphate cements. Injury 2000;31(Suppl.4):D37-47.

[27] Dorozhkin SV. Calcium orthophosphate cements for biomedical application. J Mater Sci 2008;43:3028-57.

[28] Takechi M, Miyamoto Y, Ishikawa K, Nagayama M, Kon M, Asaoka K, et al. Effects of added antibiotics on the basic properties of anti-washout-type fast-setting calcium phosphate cement. J Biomed Mater Res 1998;39:308-16.

[29] Weiss P, Gauthier O, Bouler JM, Grimandi G, Daculsi G. Injectable bone substitute using a hydrophilic polymer. Bone 1999;25(2):67S-70S.

[30] Barralet JE, Tremayne M, Lilley KJ, Gbureck U. Modification of calcium phosphate cement with α-hydroxy acids and their salts. Chem Mater 2005;17:1313-9.

[31] Barralet JE, Hofmann M, Grover LM, Gbureck U. High-strength apatitic cement by modification with α-hydroxy acid salts. Advanced Materials 2003;15(24):2091-4.

[32] Khairoun I, Boltong MG, Driessens FCM, Planell JA. Some factors controlling the injectability of calcium phosphate bone cements. J Mater Sci Mater Med 1998;9:425-8.

[33] Alves HLR, Santos LA, Bergmann CP. Injectability evaluation of tricalcium phosphate bone cement. J Mater Sci Mater Med 2008;19:2241-6.

[34] Sarda S, Fernandez E, Llorens J, Martinez S, Nilsson M, Planell JA. Rheological properties of an apatitic bone cement during initial setting. J Mater Sci Mater Med 2001;12:905-9.

[35] Pina S, Olhero SM, Gheduzzi S, Miles AW, Ferreira JMF. Influence of setting liquid composition and liquid-to-powder ratio on properties of a Mg-substituted calcium phosphate cement. Acta Biomater 2009;5:1233-40.

[36] Barralet JE, Grover LM, Gbureck U. Ionic modification of calcium phosphate cement viscosity. Part II: Hypodermic injection and strength improvement of brushite cement. Biomaterials 2004;25:2197-203.

[37] Lemaitre J, Mirtchi A, Mortier A. Calcium phosphate cements for medical use: state of the art and perspectives of development. Silicates Industries 1987;9-10:141-6.

[38] Bohner M, Malsy AK, Camire CL, Gbureck U. Combining particle size distribution and isothermal calorimetry data to determine the reaction kinetics of α-tricalcium phosphate-water mixtures. Acta Biomater 2006;2:343-8.

[39] Gbureck U, Grolms O, Barralet JE, Grover LM, Thull R. Mechanical activation and cement formation of β-calcium phosphate. Biomaterials 2003;24:4123-31.

[40] Sugawara A, Fujikawa K, Takagi S, Chow LC. Histological analysis of calcium phosphate bone grafts for surgically created periodontal bone defects in dogs. Dent Mater J 2008;27:787-94.

[41] Apelt D, Theiss F, El-Warrak AO, Zlinszky K, Wolfisberger B, Bohner M, et al. In vivo behavior of three different injectable hydraulic calcium phosphate cements. Biomaterials 2004;25:1439-51.

[42] Ooms EM, Wolke JGC, van de Heuvel MT, Jeschke B, Jansen JA. Histological evaluation of the bone response to calcium phosphate cement implanted in cortical bone. Biomaterials 2003;24:989-1000.

[43] Ooms EM, Wolke JGC, van der Waerden JP, Jansen JA. Trabecular bone response to injectable calcium phosphate (Ca-P) cement. J Biomed Mater Res 2002;61:9-18.

[44] Lu JX, Descamps M, Dejou J, Koubi G, Hardouin P, Lemaitre J, et al. The biodegradation mechanism of calcium phosphate biomaterials in bone. J Biomed Mater Res 2002;63:408-12.

[45] Kuemmerle JM, Oberle A, Oechslin C, Bohner M, Frei C, Boecken I, et al. Assessment of the suitability of a new brushite calcium phosphate cement for cranioplasty - an experimental study in sheep. J Craniomaxillofac Surg 2005;33:37-44.

[46] Gisep A, Wieling R, Bohner M, Matter S, Schneider E, Rahn B. Resorption patterns of calcium-phosphate cements in bone. J Biomed Mater Res A 2003;66A:532-40.

[47] Burguera EF, Xu HHK, Takagi S, Chow LC. High strength hydroxyapatite

cement based on dicalcium phosphate dihydrate for bone repair. J Biomed Mater Res A 2004;71A:272-82.

[48] Julien M, Khairoun I, LeGeros RZ, Delplace S, Pilet P, Weiss P, et al. Physico-chemical-mechanical and in vitro biological properties of calcium phosphate cements with doped amorphous calcium phosphates. Biomaterials 2007;28:956-65.

[49] Liu CS, Shao HF, Chen FY, Zheng HY. Rheological properties of concentrated aqueous injectable calcium phosphate cement slurry. Biomaterials 2006;27:5003-13.

[50] Ginebra MP, Espanol M, Montufar EB, Perez RA, Mestres G. New processing approaches in calcium phosphate cements and their applications in regenerative medicine. Acta Biomater 2010;6:2863-73.

[51] Cherng AM, Chow LC, Takagi S. In vitro evaluation of a calcium phosphate cement root canal filler/sealer. J Endodontics 2001;27:613-5.

[52] Sugawara A, Fujikawa K, Kusama K, Nishiyama M, Murai S, Takagi S, et al. Histopathologic reaction of a calcium phosphate cement for alveolar ridge augmentation. J Biomed Mater Res 2002;61:47-52.

[53] Lewis G. Injectable bone cements for use in vertebroplasty and kyphoplasty: state of the art review. J Biomed Mater Res B 2006;76B:456-68.

[54] Burguera EF, Xu HHK, Sun LM. Injectable calcium phosphate cement: effects of powder-to-liquid ratio and needle size. J Biomed Mater Res B 2008;84B:493-502.

[55] Ishikawa K, Matsuya S, Nakagawa M, Udoh K. Basic properties of apatite cement containing spherical tetracalcium phosphate made with plasma melting method. J Mater Sci Mater Med 2004;15:13-7.

[56] Bohner M, Baroud G. Injectability of calcium phosphate pastes. Biomaterials 2005;26:1553-63.

[57] Habib M, Baroud G, Gitzhofer F, Bohner M. Mechanisms underlying the limited injectability of hydraulic calcium phosphate paste. Acta Biomater 2008;4:1465-71.

[58] Gbureck U, Barralet JE, Spatz K, Grover LM, Thull R. Ionic modification of calcium phosphate cement viscosity. Part I: Hypodermic injection and strength improvement of apatite cement. Biomaterials 2004;25:2187-95.

[59] Baroud G, Bohner M, Heini P, Steffen T. Injection biomechanics of bone cements used in vertebroplasty. Bio-Medical Materials and Engineering 2004;14:487-504.

[60] Chow LC. Next generation calcium phosphate-based biomaterials. Dent Mater J 2009;28(1):1-10.

[61] Ishikawa K. Effects of spherical tetracalcium phosphate on injectability and basic properties of apatitic cement. Key Eng Mater 2003;240-242:369-72.

[62] Ginebra MP, Rilliard A, Fernandez E, Elvira C, Roman JS, Planell JA. Mechanical and rheological improvement of a calcium phosphate cement by the addition of a polymeric drug. J Biomed Mater Res 2001;57:113-8.

[63] Baroud G, Cayer E, Bohner M. Rheological characterization of concentrated aqueous β-tricalcium phosphate suspensions: The effect of liquid-to-powder ratio, milling time, and additives. Acta Biomater 2005;1:357-63.

[64] Leroux L, Hatim Z, Freche M, Lacout JL. Effects of various adjuvants (lactic acid, glycerol, and chitosan) on the injectability of a calcium phosphate cement. Bone 1999;25(2):31S-4S.

[65] Habib M, Baroud G, Galea L, Bohner M. Evaluation of the ultrasonication process for injectability of hydraulic calcium phosphate pastes. Acta Biomater 2012;8:1164-8.

[66] Carey LE, Xu HHK, Simon Jr CG, Takagi S, Chow LC. Premixed rapid-setting calcium phosphate composites for bone repair. Biomaterials 2005;26:5002-14.

[67] Xu HHK, Carey LE, Simon Jr CG, Takagi S, Chow LC. Premixed calcium phosphate cements: synthesis, physical properties, and cell cytotoxicity. Dent Mater 2007;23:433-41.

[68] Xu HHK, Carey LE, Simon Jr CG. Premixed macroporous calcium phosphate cement scaffold. J Mater Sci:Mater Med 2007;18:1345-53.

[69] Fleming GJP, Marquis PM, Shortall ACC. The influence of clinically induced variability on the distribution of compressive fracture strengths of a hand-mixed zinc phosphate dental cement. Dent Mater 1999;15:87-97.

[70] Peersman G, Laskin R, Davis J, Peterson MGE, Richart T. Prolonged operative

time correlates with increased infection rate after total knee arthroplasty. HSS Journal 2006;2:70-2.

[71] Takagi S, Chow LC, Hirayama S, Sugawara A. Premixed calcium-phosphate cement pastes. J Biomed Mater Res B 2003;67B:689-96.

[72] Grover LM, Hofmann MP, Gbureck U, Kumarasami B, Barralet JE. Frozen delivery of brushite calcium phosphate cements. Acta Biomater 2008;4:1916-23.

[73] Sugawara A, Chow LC, Takagi S, Chohayeb H. In vitro evaluation of the sealing ability of a CPC when used as a root canal sealer-filler. J Endodont 1990;16:162-5.

[74] Sugawara A, Kusama K, Nishimura S, Nishiyama M, Moro I, Kudo I, et al. Histopathological reaction of a calcium phosphate cement root canal filler. J Hard Tissue Biol 1995;4:1-7.

[75] Han B, Ma PW, Zhang LL, Yin YJ, Yao KD, Zhang FJ, et al. β-TCP/MCPM-based premixed calcium phosphate cements. Acta Biomater 2009;5:3165-77.

[76] Aberg J, Brisby H, Henriksson HB, Lindahl A, Thomsen P, Engqvist H. Premixed acidic calcium phosphate cement: characterization of strength and microstructure. J Biomed Mater Res B 2010;93B:436-41.

[77] Rezwan K, Chen QZ, Blaker JJ, Boccaccini AR. Biodegradable and bioactive porous polymer/inorganic composite scaffolds for bone tissue engineering. Biomaterials 2006;27:3413-31.

[78] Chen GP, Ushida T, Tateishi T. Hybrid biomaterials for tissue engineering: a preparative method for PLA or PLGA-collagen hybrid sponges. Adv Mater 2000;12:455-7.

[79] Hutmacher DW. Scaffolds in tissue engineering bone and cartilage. Biomaterials 2000;21:2529-43.

[80] Woodard JR, Hilldore AJ, Lan SK, Park CJ, Morgan AW, Eurell JAC, et al. The mechanical properties and osteoconductivity of hydroxyapatite bone scaffolds with multi-scale porosity. Biomaterials 2007;28:45-54.

[81] LeGeros RZ. Properties of osteoconductive biomaterials: calcium phosphates. Clin Orthop Relat Res 2002; 395:81-98.

[82] Boyde A, Corsi A, Quarto R, Cancedda R, Bianco P. Osteoconduction in large macroporous hydroxyapatite ceramic implants: evidence for a complementary integration and disintegration mechanism. Bone 1999;24:579-89.

[83] Tamai N, Myoui A, Tomita T, Nakase T, Tanaka J, Ochi T, et al. Novel hydroxyapatite ceramics with an interconnective porous structure exhibit superior osteoconduction in vivo. J Biomed Mater Res 2002;59:110-7.

[84] Oonishi H. Orthopaedic applications of hydroxyapatite. Biomaterials 1991;12:171-8.

[85] Tuli P, Farbod F, Beal B, Jackson IT. The use of hydroxyapatite granules for the correction of skeletal facial deformities. Eur J Plast Surg 2012;35:203-8.

[86] Wei GB, Ma PX. Structure and properties of nano-hydroxyapatite / polymer composite scaffolds for bone tissue engineering. Biomaterials 2004;25:4749-57.

[87] Ohsawa K, Neo M, Matsuoka H, Akiyama H, Ito H, Kohno H, et al. The expression of bone matrix protein mRNAs around β-TCP particles implanted into bone. J Biomed Mater Res 2000;52:460-6.

[88] Kondo N, Ogose A, Tokunaga K, Ito T, Arai K, Kudo N, et al. Bone formation and resorption of highly purified β-tricalcium phosphate in the rat femoral condyle. Biomaterials 2005;26:5600-8.

[89] Horch HH, Sader R, Pautke C, Neff A, Deppe H, Kolk A. Synthetic, pure-phase β-tricalcium phosphate ceramic granules (Cerasorb®) for bone regeneration in the reconstructive surgery of the jaws. Int J Oral Maxillofac Surg 2006;35:708-13.

[90] Knabe C, Koch C, Rack A, Stiller M. Effect of β-tricalcium phosphate particles with varying porosity on osteogenesis after sinus floor augmentation in humans. Biomaterials 2008;29:2249-58.

[91] Dong J, Uemura T, Shirasaki Y, Tateishi T. Promotion of bone formation using highly pure porous β-TCP combined with bone marrow-derived osteoprogenitor cells. Biomaterials 2002;23:4493-502.

[92] Suarez-Gonzalez D, Lee JS, Lan Levengood SK, Vanderby Jr R, Murphy WL. Mineral coatings modulate β-TCP stability and enable growth factor binding and release. Acta Biomater 2012;8:1117-24.

[93] Hench LL. Bioceramics: from concept to clinic. J Am Ceram Soc 1991;74:1487-510.

[94] Kokubo T. Bioactive glass ceramics: properties and applications. Biomaterials 1991;12:155-63.

[95] Hench LL, Splinter RJ, Allen WC, Greenlee Jr TK. Bond mechanisms at the interface of ceramic prosthetic materials. J Biomed Mater Res 1971;5:117-41.

[96] Wilson J, Pigott GH, Schoen FJ, Hench LL. Toxicology and biocompatibility of bioglasses. J Biomed Mater Res 1981;15:805-17.

[97] Wilson J, Low SB. Bioactive ceramics for peridontal treatment: comparative studies in the Patus monkey. J Appl Biomater 1992;3:123-9.

[98] Shirtliff VJ, Hench LL. Bioactive materials for tissue engineering, regeneration and repair. J Mater Sci 2003;38:4697-707.

[99] Mano JF, Sousa RA, Boesel LF, Neves NM, Reis RL. Bioinert, biodegradable and injectable polymeric matrix composites for hard tissue replacement: state of the art and recent developments. Compos Sci Technol 2004;64:789-817.

[100] Ciardelli G, Chiono V, Vozzi G, Pracella M, Ahluwalia A, Barbani N, et al. Blends of poly(ε-caprolactone) and polysaccharides in tissue engineering applications. Biomacromolecules 2005;6:1961-76.

[101] Gomes ME, Ribeiro AS, Malafaya PB, Reis RL, Cunha AM. A new approach

based on injection moulding to produce biodegradable starch-based polymeric scaffolds: morphology, mechanical and degradation behaviour. Biomaterials 2001;22:883-9.

[102] Salgado AJ, Coutinho OP, Reis RL, Davies JE. In vivo response to starch-based scaffolds designed for bone tissue engineering applications. J Biomed Mater Res A 2007;80A:983-9.

[103] Pereira CS, Vasquez B, Cunha AM, Reis RL, San Roman J. New starch-based thermoplastic hydrogels for use as bone cements or drug-delivery carriers. J Mater Sci Mater Med 1998;9:825-33.

[104] Espigares I, Elvira C, Mano JF, Vasquez B, San Roman J, Reis RL. New biodegradable and bioactive acrylic bone cements based on starch blends and ceramic fillers. Biomaterials 2002;23:1883-95.

[105] Malafaya PB, Elvira C, Gallardo A, San Roman J, Reis RL. Porous starch-based drug delivery systems processed by a microwave treatment. J Biomat Sci Polym Ed 2001;12:1227-41.

[106] Elvira C, Mano JF, San Roman J, Reis RL. Starch-based biodegradable hydrogels with potential biomedical applications as drug delivery systems. Biomaterials 2002;23:1955-66.

[107] Sousa RA, Mano JF, Reis RL, Cunha AM, Bevis MJ. Mechanical performance of starch based bioactive composite biomaterials molded with preferred orientation.

Polym Eng Sci 2002;42:1032-45.

[108] Sarasam A, Madihally SV. Characterization of chitosan-polycaprolactone blends for tissue engineering applications. Biomaterials 2005;26:5500-8.

[109] Ong SY, Wu J, Moochhala SM, Tan MH, Lu J. Development of a chitosan-based wound dressing with improved hemostatic and antimicrobial properties. Biomaterials 2008;29:4323-32.

[110] van der Lubben IM, Verhoef JC, Borchard G, Junginger HE. Chitosan and its derivatives in mucosal drug and vaccine delivery. Eur J Pharm Sci 2001;14:201-7.

[111] de Campos AM, Diebold Y, Carvalho ELS, Sanchez A, Alonso MJ. Chitosan nanoparticles as new ocular drug delivery systems: in vitro stability, in vivo fate, and cellular toxicity. Pharmaceut Res 2004;21:803-10.

[112] Madihally SV, Matthew HWT. Porous chitosan scaffolds for tissue engineering. Biomaterials 1999;20:1133-42.

[113] Sell SA, McClure MJ, Garg K, Wolfe PS, Bowlin GL. Electrospinning of collagen/biopolymers for regenerative medicine and cardiovascular tissue engineering. Adv Drug Deliv Rev 2009;61:1007-19.

[114] Cen L, Liu W, Cui L, Zhang WJ, Cao YL. Collagen tissue engineering: development of novel biomaterials and applicaitons. Pediatric Res 2008;63:492-6.

[115] Kolacna L, Bakesova J, Varga F, Kostakova E, Planka L, Necas A, et al.

Biochemical and biophysical aspects of collagen nanostructurein the extracellular matrix. Physiol Res 2007;56(Suppl 1):S51-S60.

[116] Drury JL, Mooney DJ. Hydrogels for tissue engineering: scaffold design variables and applications. Biomaterials 2003;24:4337-51.

[117] Lam CXF, Hutmacker DW, Schantz J, Woodruff MA, Teoh SH. Evaluation of polycaprolactone scaffold degradation for 6 months in vitro and in vivo. J Biomed Mater Res A 2009;90A:906-19.

[118] Wu LB, Ding JD. In vitro degradation of three-dimensional porous poly(D,L-lactide-*co*-glycolide) scaffolds for tissue engineering. Biomaterials 2004;25:5821-30.

[119] Middleton JC, Tipton AJ. Synthetic biodegradable polymers as orthopedic devices. Biomaterials 2000;21:2335-46.

[120] Shalaby SW, Johnson RA. Synthetic absorbable polyesters. In: Shalaby SW, editor. Biomedical polymers: designed-to-degrade systems. New York: Hanser; 1994. p. 1-34.

[121] You Y, Min BM, Lee SJ, Lee TS, Park WH. *In vitro* degradation behavior of electrospun polyglycolide, polylactide, and poly(lactide-*co*-glycolide). J Appl Polym Sci 2005;95:193-200.

[122] Miller RA, Brady JM, Cutright DE. Degradation rates of oral resorbable implants (polylactates and polyglycolates): rate modification with changes in

PLA/PGA copolymer ratios. J Biomed Mater Res 1977;11:711-9.

[123] Yang SF, Leong KF, Du ZH, Chua CK. The design of scaffolds for use in tissue engineering. Part I. Traditional factors. Tissue Eng 2001;7(6):679-89.

[124] Pena J, Corrales T, Izquierdo-Barba I, Doadrio AL, Vallet-Regi M. Long term degradation of poly(ε-caprolactone) films in biologically related fluids. Polym Degrad Stabil 2006;91:1424-32.

[125] Sun HF, Mei L, Song CX, Cui XM, Wang PY. The in vivo degradation, absorption and excretion of PCL-based implant. Biomaterials 2006;27:1735-40.

[126] Pitt CG, Chasalow FI, Hibionada YM, Klimas DM, Schindler A. Aliphatic polyesters. I. The degradation of poly(ε-caprolactone) in vivo. J Appl Polym Sci 1981;26:3779-87.

[127] Seyednejad H, Gawlitta D, Kuiper RV, de Bruin A, van Nostrum CF, Vermonden T, et al. In vivo biocompatibility and biodegradation of 3D-printed porous scaffolds based on a hydroxyl-functionalized poly(ε-caprolactone). Biomaterials 2012;33:4309-18.

[128] Gomes ME, Azevedo HS, Moreira AR, Ella V, Kellomaki M, Reis RL. Starch-poly(ε-caprolactone) and starch-poly(lactic acid) fibre-mesh scaffolds for bone tissue engineering applications: structure, mechanical properties and degradation behavior. J Tissue Eng Regen Med 2008;2:243-52.

[129] Duarte ARC, Mano JF, Reis RL. Enzymatic degradation of 3D scaffolds of

starch-poly-(ε-caprolactone) prepared by supercritical fluid technology. Polym Degrad Stabil 2010;95:2110-7.

[130] Sarasam AR, Samli AI, Hess L, Ihnat MA, Madihally SV. Blending chitosan with polycaprolactone: porous scaffolds and toxicity. Macromol Biosci 2007;7:1160-7.

[131] Wan Y, Wu H, Cao XY, Dalai S. Compressive mechanical properties and biodegradability of porous poly(caprolactone)/chitosan scaffolds. Polym Degrad Stabil 2008;93:1736-41.

[132] Malheiro VN, Caridade SG, Alves NM, Mano JF. New poly(ε-caprolactone)/chitosan blend fibers for tissue engineering applications. Acta Biomater 2010;6:418-28.

[133] Neves SC, Moreira Teixeira LS, Moroni L, Reis RL, van Blitterswijk CA, Alves NM, et al. Chitosan/poly(ε-caprolactone) blend scaffolds for cartilage repair. Biomateirals 2011;32:1068-79.

[134] Lee SJ, Liu J, Oh SH, Soker S, Atala A, Yoo JJ. Development of a composite vascular scaffolding system that withstands physiological vascular conditions. Biomateirals 2008;29:2891-8.

[135] Venugopal J, Zhang YZ, Ramakrishna S. Fabrication of modified and functionalized polycaprolactone nanofibre scaffolds for vascular tissue engineering. Nanotechnology 2005;16:2138-42.

[136] Blaker JJ, Maquet V, Jerome R, Boccaccini AR, Nazhat SN. Mechanical properties of highly porous PDLLA/Bioglass® composite foams as scaffolds for bone tissue engineering. Acta Biomater 2005;1:643-52.

[137] Heo SJ, Kim SE, Wei J, Hyun YT, Yun HS, Kim DH, et al. Fabrication and characterization of novel nano- and micro-HA/PCL composite scaffolds using a modified rapid prototyping process. J Biomed Mater Res A 2009;89A:108-16.

[138] Lebourg M, Anton JS, Ribelles JLG. Hybrid structure in PCL-HAp scaffold resulting from biomimetic apatite growth. J Mater Sci: Mater Med 2010;21:33-44.

[139] Lei Y, Rai B, Ho KH, Teoh SH. In vitro degradation of novel bioactive polycaprolactone-20% tricalcium phosphate composite scaffolds for bone engineering. Mater Sci Eng C 2007;27:293-8.

[140] Yeo A, Rai B, Sju E, Cheong JJ, Teoh SH. The degradation profile of novel, bioresorbable PCL-TCP scaffolds: an in vitro and in vivo study. J Biomed Mater Res A 2008;84A:208-18.

[141] Lam CXF, Teoh SH, Hutmacher DW. Comparison of the degradation of polycaprolactone and polycaprolactone-(β-tricalcium phosphate) scaffolds in alkaline medium. Polym Int 2007;56:718-28.

[142] Fabbri P, Cannillo V, Sola A, Dorigato A, Chiellini F. Highly porous polycaprolactone-45S5 Bioglass ® scaffolds for bone tissue engineering. Compos Sci Technol 2010;70:1869-78.

[143] Li X, Shi JL, Dong XP, Zhang LX, Zeng HY. A mesoporous bioactive glass / polycaprolactone composite scaffold and its bioactivity behavior. J Biomed Mater Res A 2008;84A:84-91.

[144] Cannillo V, Chiellini F, Fabbri P, Sola A. Production of Bioglass®45S5-polycaprolactone composite scaffolds via salt-leaching. Compos Struct 2010;92:1823-32.

[145] Corradini E, Mattoso LHC, Guedes CGF, Rosa DS. Mechanical, thermal and morphological properties of poly(ε-caprolactone)/zein blends. Polym Advan Technol 2004;15:340-5.

[146] Shukla R, Cheryan M. Zein: the industrial protein from corn. Ind Crop Prod 2001;13:171-92.

[147] Liu XM, Sun QS, Wang HJ, Zhang L, Wang JY. Microspheres of corn protein, zein, for an ivermecin drug delivery system. Biomaterials 2005;26:109-15.

[148] Hurtado-Lopez P, Murdan S. Formulation and characterisation of zein microspheres as delivery vehicles. J Drug Delivery Sci Technol 2005;15(4):267-72.

[149] Wang HJ, Lin ZX, Liu XM, Sheng SY, Wang JY. Heparin-loaded zein microsphere film and hemocompatibility. J Control Release 2005;105(1-2):120-31.

[150] Dong J, Sun QS, Wang JY. Basic study of corn protein, zein, as a biomaterial in tissue engineering, surface morphology and biocompatibility. Biomaterials 2004;25(19):4691-7.

[151] Gong SJ, Wang HJ, Sun QS, Xue ST, Wang JY. Mechanical properties and in vitro biocompatibility of porous zein scaffolds. Biomaterials 2006;27:3793-9.

[152] Wang HJ, Gong SJ, Lin ZX, Fu JX, Xue ST, Huang JC, et al. *In vivo* biocompatibility and mechanical properties of porous zein scaffolds. Biomaterials 2007;28:3952-64.

[153] Qu ZH, Wang HJ, Tang TT, Zhang XL, Wang JY, Dai KR. Evaluation of the zein/inorganics composite on biocompatibility and osteoblastic differentiation. Acta Biomater 2008;4:1360-8.

[154] Yang QB, Wu XL. Factors influencing properties of phosphate cement-based binder for rapid repair of concrete. Cement Concrete Res 1999;29:389-96.

[155] Abdelrazig BEI, Sharp JH, EI-Jazairi B. The microstructure and mechanical properties of mortars made from magnesia-phosphate cement. Cem Concr Res 1989;19:247-58.

[156] Hall DA, Stevens R. Effect of water content on the structure and mechanical properties of magnesia-phosphate cement mortar. J Am Ceram Soc 1998;81:1550-6.

[157] Wu F, Wei J, Guo H, Chen FP, Hong H, Liu CS. Self-setting bioactive calcium-magnesium phosphate cement with high strength and degradability for bone regeneration. Acta Biomater 2008;4:1873-84.

[158] Liu CS. Inorganic bone adhesion agent and its use in human hard tissue repair. United States: East China University of Science and Technology; 2006.

[159] Wu ZZ, Zhang J, Chen TY, Li LJ, Liu CS, Guo H, et al. Experimental study on magnesium phosphate cement in fracture treatment. Chinese Journal of Reparative and Reconstructive Surgery 2006;20(9):912-5.

[160] Wu ZZ, Zhang J, Chen TY, Liu CS, Chen ZW. Experimental study of a new type of cement on tibia plateau fractures treatment. Clinical Medical Journal of China 2005;12(2):261-4.

[161] Yu YL, Wang J, Liu CS, Zhang BW, Chen HH, Guo H, et al. Evaluation of inherent toxicology and biocompatibility of magnesium phosphate bone cement. Colloid Surface B 2010;76:496-504.

[162] Maquet V, Boccaccini AR, Pravata L, Notingher I, Jerome R. Porous poly(α-hydroxyacid)/Bioglass® composite scaffolds for bone tissue engineering. I: preparation and in vitro characterisation. Biomaterials 2004;25:4185-94.

[163] Lu HH, El-Amin SF, Scott KD, Laurencin CT. Three-dimensional, bioactive, biodegradable, polymer-bioactive glass composite scaffolds with improved mechanical properties support collagen synthesis and mineralization of human osteoblast-like cells in vitro. J Biomed Mater Res A 2003;64A:465-74.

[164] Bretcanu O, Misra SK, Mohammad Yunos D, Boccaccini AR, Roy I, Kowalczyk T, et al. Electrospun nanofibrous biodegradable polyester coatings on Bioglass®-based glass-ceramics for tissue engineering. Mater Chem Phys 2009;118:420-6.

[165] Baino F, Verne E, C Vitale-Brovarone. Feasibility, tailoring and properties of polyurethane/bioactive glass composite scaffolds for tissue engineering. J Mater Sci Mater Med 2009;20:2189-95.

[166] Taboas JM, Maddox RD, Krebsbach PH, Hollister SJ. Indirect solid free form fabrication of local and global porous, biomimetic and composite 3D polymer-ceramic scaffolds. Biomaterials 2003;24:181-94.

[167] Shor L, Gueceri S, Wen X, Gandhi M, Sun W. Fabrication of three-dimensional polycaprolactone/hydroxyapatite tissue scaffolds and osteoblast-scaffold interactions in vitro. Biomaterials 2007;28(35):5291-7.

[168] Eosoly S, Brabazon D, Lohfeld S, Looney L. Selective laser sintering of hydroxyapatite/poly(ε-caprolactone) scaffolds. Acta Biomater 2010;6(7):2511-7.

[169] Blaker JJ, Bismarck A, Boccaccini AR, Young AM, Nazhat SN. Premature degradation of poly(α-hydroxyesters) during thermal processing of Bioglass®-containing composites. Acta Biomater 2010;6:756-62.

[170] Kokubo T, Takadama H. How useful is SBF in predicting in vivo bone bioactivity? Biomaterials 2006;27:2907-15.

[171] Guarino V, Causa F, Netti PA, Ciapetti G, Pagani S, Martini D, et al. The role of hydroxyapatite as solid signal on performance of PCL porous scaffolds for bone tissue regeneration. J Biomed Mater Res B 2008;86B:548-57.

[172] Driessens FCM, Boltong MG, de Maeyer EAP, Wenz R, Nies B, Planell JA.

The Ca/P range of nanoapatitic calcium phosphate cements. Biomaterials 2002;23:4011-7.

[173] Fernandez E, Gil FJ, Ginebra MP, Driessens FCM, Planell JA. Calcium phosphate bone cements for clinical applications. Part I: solution chemistry. J Mater Sci: Mater Med 1999;10:169-76.

[174] Liu CS, Shen W, Chen JG. Solution property of calcium phosphate cement hardening body. Mater Chem Phys 1999;58:78-82.

[175] Tofighi A, Schaffer K, Palazzolo R. Calcium phosphate cement (CPC): a critical development path. Key Eng Mater 2008;361-363:303-6.

[176] Felix Lanao RP, Leeuwenburgh SCG, Wolke JGC, Jansen JA. Bone response to fast-degrading, injectable calcium phosphate cements containing PLGA microparticles. Biomaterials 2011;32:8839-47.

[177] Driessens FCM. Formation and stability of calcium phosphate in relation to the phase composition of the mineral in calcified tissues. In: de Groot K, editor. Bioceramics of calcium phosphates. Boca Raton, Florida: CRC Press; 1983. p. 1-32.

[178] Brown PW, Fulmer M. Kinetics of hydroxyapatite formation at low temperature. J Am Ceram Soc 1991;75:934-40.

[179] Royals MA, Fujita SM, Yewey GL, Rodriguez J, Schultheiss PC, Dunn RL. Biocompatibility of a biodegradable in situ forming implant system in rhesus monkeys. J Biomed Mater Res 1999;45:231-9.

[180] Strickley RG. Solubilizing excipients in oral and injectable formulations. Pharmaceut Res 2004;21:201-30.

[181] Kempe S, Metz H, Mader K. Do in situ forming PLG/NMP implants behave similar *in vitro* and *in vivo*? A non-invasive and quantitative EPR investigation on the mechanisms of the implant formation process. J Control Release 2008;130:220-5.

[182] Zhou SB, Zheng XT, Yu XJ, Wang JX, Weng J, Li XH, et al. Hydrogen bonding interaction of poly(D,L-lactide)/hydroxyapatite nanocomposites. Chem Mater 2007;19:247-53.

[183] Pina S, Torres PMC, Ferreira JMF. Injectability of brushite-forming Mg-substituted and Sr-substituted α-TCP bone cements. J Mater Sci: Mater Med 2010;21:431-8.

[184] Pina S, Torres PM, Goetz-Neunhoeffer F, Neubauer J, Ferreira JMF. Newly developed Sr-substituted α-TCP bone cements. Acta Biomater 2010;6:928-35.

[185] Ishikawa T, Wakamura M, Kondo S. Surface characterization of calcium hydroxylapatite by Fourier transform infrared spectroscopy. Langmuir 1989;5:140-4.

[186] van den Vreken NMF, Pieters IY, Declercq HA, Cornelissen MJ, Verbeeck RMH. Characterization of calcium phosphate cements modified by addition of amorphous calcium phosphate. Acta Biomater 2010;6:617-25.

[187] Chern Lin JH, Kuo KH, Ding SJ, Ju CP. Surface reaction of stoichiometric and calcium-deficient hydroxyapatite in simulated body fluid. J Mater Sci: Mater Med

2001;12:731-41.

[188] Navarro M, Ginebra MP, Clement J, Martinez S, Avila G, Planell JA. Physicochemical degradation of Titania-stabilized soluble phosphate glasses for medical applications. J Am Ceram Soc 2003;86(8):1345-52.

[189] Chow LC, Markovic M, Frukhtbeyn SA, Takagi S. Hydrolysis of tetracalcium phosphate under a near-constant composition condition ---effects of pH and particle size. Biomaterials 2005;26:393-401.

[190] Cherng A, Takagi S, Chow LC. Effects of hydroxypropyl methylcellulose and other gelling agents on the handling properties of calcium phosphate cement. J Biomed Mater Res 1997;35(3):273-7.

[191] Le Renard P, Jordan O, Faes A, Petri-Fink A, Hofmann H, Ruefenacht D, et al. The in vivo performance of magnetic particle-loaded injectable, in situ gelling, carriers for the delivery of local hyperthermia. Biomaterials 2010;31:691-705.

[192] Schiller C, Epple M. Carbonated calcium phosphates are suitable pH-stabilising fillers for biodegradable polyesters. Biomaterials 2003;24:2037-43.

[193] Li S, Garreau H, Vert M. Structure-property relationships in the case of the degradation of massive poly(α-hydroxy acids) in aqueous media. Part 1: poly(DL-lactic acid). J Mater Sci Mater Med 1990;1:123-30.

[194] Wang HB, Lee JK, Moursi A, Lannutti JJ. Ca/P ratio effects on the degradation of hydroxyapatite *in vitro*. J Biomed Mater Res A 2003;67A:599-608.

[195] Navarro M, Ginebra MP, Planell JA, Barrias CC, Barbosa MA. In vitro degradation behavior of a novel bioresorbable composite material based on PLA and a soluble CaP glass. Acta Biomater 2005;1:411-9.

[196] Guo H, Su JC, Wei J, Kong H, Liu CS. Biocompatibility and osteogenicity of degradable Ca-deficient hydroxyapatite scaffolds from calcium phosphate cement for bone tissue engineering. Acta Biomater 2009;5:268-78.

[197] Cheung HY, Lau KT, Lu TP, Hui D. A critical review on polymer-based bio-engineered materials for scaffold development. Compos Part B-Eng 2007;38:291-300.

[198] Sabir MI, Xu XX, Li L. A review on biodegradable polymeric materials for bone tissue engineering applications. J Mater Sci 2009;44:5713-24.

[199] Wei J, Chen FP, Shin JW, Hong H, Dai CL, Su JC, et al. Preparation and characterization of bioactive mesoporous wollastonite - Polycaprolactone composite scaffold. Biomaterials 2009;30:1080-8.

[200] Forato LA, Bicudo TDC, Colnago LA. Conformation of α zeins in solid state by fourier transform IR. Biopolymers 2003;72(6):421-6.

[201] Gibson LJ, Ashby MF. Cellular Solids: Structure and Properties. Cambridge, UK: Cambridge University Press; 1997.

[202] Lien SM, Ko LY, Huang TJ. Effect of pore size on ECM secretion and cell growth in geltain scaffold for articular cartilage tissue engineering. Acta Biomater

2009;5:670-9.

[203] Shi XF, Sitharaman B, Pham QP, Liang F, Wu K, Billups WE, et al. Fabrication of porous ultra-short single-walled carbon nanotube nanocomposite scaffolds for bone tissue engineering. Biomaterials 2007;28:4078-90.

[204] Liu CM, Chen Y, Wang XM, Huang J, Chang PR, Anderson DP. Improvement in physical properties and cytocompatibility of zein by incorporation of pea protein isolate. J Mater Sci 2010;45:6775-85.

[205] Salerno A, Oliviero M, Di Maio E, Netti PA, Rofani C, Colosimo A, et al. Design of novel three-phase PCL/TZ-HA biomaterials for use in bone regeneration applications. J Mater Sci-Mater M 2010;21:2569-81.

[206] Salerno A, Zeppetelli S, Di Maio E, Iannace S, Netti PA. Novel 3D porous multi-phase composite scaffolds based on PCL, thermoplastic zein and HA prepared via supercritical CO_2 foaming for bone regeneration. Compos Sci Technol 2010;70:1838-46.

[207] Wu ZZ, Meng DH, Zhang J. Experimental study of magnesium phosphate cement on dog tibia plateau fracture treatment. Clinical Medical Journal of China 2009;16(1):133-5.

[208] Yeo A, Sju E, Rai B, Teoh SH. Customizing the degradation and load-bearing profile of 3D polycaprolactone-tricalcium phosphate scaffolds under enzymatic and hydrolytic conditions. J Biomed Mater Res B 2008;87B:562-9.

[209] Hollister SJ. Porous scaffold design for tissue engineering. Nat Mater 2005;4:518-24.

[210] Bernardo E, Colombo P, Cacciotti I, Bianco A, Bedini R, Pecci R, et al. Porous wollastonite-hydroxyapatite bioceramics from a preceramic polymer and micro- or nano-sized fillers. J Eur Ceram Soc 2012;32:399-408.

[211] Wei JH, Yoshinari M, Takemoto S, Hattori M, Kawada E, Liu BL, et al. Adhesion of mouse fibroblasts on hexamethyldisiloxane surfaces with wide range of wettability. J Biomed Mater Res B 2007;81B:66-75.

[212] Zhou YF, Hutmacher DW, Varawan SL, Lim TM. In vitro bone engineering based on polycaprolactone and polycaprolactone-tricalcium phosphate composites. Polym Int 2007;56(3):333-42.

[213] Yeo MG, Lee H, Kim GH. Three-dimensional hierarchical composite scaffolds consisting of polycaprolactone, β-tricalcium phosphate, and collagen nanofibers: fabrication, physical properties, and in vitro cell activity for bone tissue regeneration. Biomacromolecules 2011;12:502-10.

[214] Navarro M, Aparicio C, Charles-Harris M, Ginebra MP, Engel E, Planell JA. Development of a biodegradable composite scaffold for bone tissue engineering: physicochemical, topographical, mechanical, degradation, and biological properties. Adv Polym Sci 2006;200:209-31.

[215] Jeon HJ, Jin G, Kim GH. The effect of microsized roughness in

nano/microsized hierarchical surfaces replicated from a lotus leaf on the activities of osteoblast-like cells(MG63). J Mater Chem 2012;22:7584-91.

[216] Grobardt C, Ewald A, Grover LM, Barralet JE, Gbureck U. Passive and active in vitro resorption of calcium and magnesium phosphate cements by osteoclastic cells. Tissue Eng: Part A 2010;16(12):3687-95.

[217] Klammert U, Ignatius A, Wolfram U, Reuther T, Gbureck U. In vivo degradation of low temperature calcium and magnesium phosphate ceramics in a heterotopic model. Acta Biomater 2011;7:3469-75.

[218] Burkersroda FV, Schedl L, Gopferich A. Why degradable polymers undergo surface erosion or bulk erosion. Biomaterials 2002;23:4221-31.

[219] Kay S, Thapa A, Haberstroh KM, Webster TJ. Nanostructured polymer / nanophase ceramic composites enhance osteoblast and chondrocyte adhesion. Tissue Eng 2002;8:753-61.

[220] Liu HN, Slamovich EB, Webster TJ. Increased osteoblast functions among nanophase titania / poly(lactide-co-glycolide) composites of the highest nanometer surface roughness. J Biomed Mater Res A 2006;78A:798-807.

[221] Goldstein SA. The mechanical properties of trabecular bone: dependence on anatomic location and function. J Biomech 1987;20:1055-61.

[222] Guan LM, Davies JE. Preparation and characterization of a highly macroporous biodegradable composite tissue engineering scaffold. J Biomed Mater

Res A 2004;71A:480-7.

Appendix 1 Equations

Appendix 1.1 Assessment of the weight loss of cement

$$\text{weight loss (\%)} = \frac{(W_0 - W_t)}{W_0} \times 100\%$$

Where:

W_0 weight of cement before degradation

W_t weight of cement after degradation for certain time

Appendix 1.2 Assessment of the weight loss of scaffold

$$\text{weight loss (\%)} = \frac{(W_i - W_f)}{W_i} \times 100\%$$

Where:

W_i weight of scaffold before degradation

W_f weight of scaffold after degradation for certain time

Appendix 2 Raw data

Appendix 2.1 Weight of the premixed cd-AB and conventional cd-AB samples during degradation

Group	Name	Day 0	Day 3	Day 7	Day 10	Day 13	Day 17	Day 22	Day 25	Day 28
		weight (g)	weight (g)	weight (g)	weight (g)	weight (g)	weight (g)	weight (g)	weight (g)	weight (g)
cd-AB + H_2O	1	0.1793	0.1764	0.1759	0.1751	0.1741	0.1731	0.1722	0.1709	0.1684
cd-AB + H_2O	2	0.1659	0.1633	0.1626	0.1617	0.1612	0.1608	0.1597	0.158	0.157
cd-AB + H_2O	3	0.1538	0.1513	0.1509	0.1505	0.1495	0.1486	0.147	0.1462	0.1454
cd-AB + 10% PLA-NMP	4	0.1729	0.1678	0.1657	0.1636	0.1616	0.1593	0.1575	0.1556	0.1535
cd-AB + 10% PLA-NMP	5	0.1557	0.1511	0.1494	0.1485	0.1476	0.1455	0.1433	0.1421	0.1403
cd-AB + 10% PLA-NMP	6	0.1428	0.1395	0.138	0.1367	0.1358	0.1347	0.1333	0.1322	0.1309
cd-AB + 15% PLA-NMP	7	0.1824	0.1766	0.1734	0.1704	0.168	0.1654	0.1632	0.1608	0.1586
cd-AB + 15% PLA-NMP	8	0.1651	0.1601	0.1579	0.1549	0.1526	0.1499	0.1481	0.1457	0.1439
cd-AB + 15% PLA-NMP	9	0.1502	0.1458	0.1444	0.1424	0.1404	0.1383	0.1366	0.1343	0.1322
cd-AB + 20% PLA-NMP	10	0.1697	0.1642	0.1605	0.1577	0.1545	0.1516	0.1486	0.146	0.1412
cd-AB + 20% PLA-NMP	11	0.1571	0.1522	0.1491	0.1482	0.1454	0.1436	0.1412	0.1396	0.1353
cd-AB + 20% PLA-NMP	12	0.1437	0.139	0.1358	0.1339	0.1319	0.1294	0.1267	0.1237	0.1203

Appendix 2.2 Weight loss ratios of the premixed cd-AB and conventional cd-AB samples during degradation

Group	Name	Day 0	Day 3	Day 7	Day 10	Day 13	Day 17	Day 22	Day 25	Day 28
		weight loss (%)	weight loss (%)	weight loss (%)	weight loss (%)	weight loss (%)	weight loss (%)	weight loss (%)	weight loss (%)	weight loss (%)
cd-AB + H_2O	1	0	1.6174	1.8963	2.3424	2.9002	3.4579	3.9598	4.6849	6.0792
cd-AB + H_2O	2	0	1.5672	1.9892	2.5316	2.833	3.0741	3.7372	4.7619	5.3647
cd-AB + H_2O	3	0	1.6255	1.8856	2.1456	2.7958	3.381	4.4213	4.9415	5.4616
cd-AB + 10% PLA-NMP	4	0	2.9497	4.1643	5.3788	6.5356	7.8658	8.9069	10.0058	11.2204
cd-AB + 10% PLA-NMP	5	0	2.9544	4.0462	4.6243	5.2023	6.5511	7.964	8.7347	9.8908
cd-AB + 10% PLA-NMP	6	0	2.3109	3.3613	4.2717	4.902	5.6723	6.6527	7.423	8.3333
cd-AB + 15% PLA-NMP	7	0	3.1798	4.9342	6.5789	7.8947	9.3202	10.5263	11.8421	13.0482
cd-AB + 15% PLA-NMP	8	0	3.0285	4.361	6.1781	7.5712	9.2065	10.2968	11.7505	12.8407
cd-AB + 15% PLA-NMP	9	0	2.9294	3.8615	5.1931	6.5246	7.9228	9.0546	10.5859	11.984
cd-AB + 20% PLA-NMP	10	0	3.241	5.4213	7.0713	8.957	10.6659	12.4337	13.9658	16.7943
cd-AB + 20% PLA-NMP	11	0	3.119	5.0923	5.6652	7.4475	8.5933	10.1209	11.1394	13.8765
cd-AB + 20% PLA-NMP	12	0	3.2707	5.4976	6.8198	8.2116	9.9513	11.8302	13.9179	16.2839

Appendix 2.3 Weight of the PCL scaffolds and zein/PCL composite scaffolds during degradation

Group	Name	Day 0	Day 3	Day 7	Day 10	Day 14	Day 17	Day 21	Day 24	Day 28
		weight (g)	weight (g)	weight (g)	weight (g)	weight (g)	weight (g)	weight (g)	weight (g)	weight (g)
PCL	1	0.1594	0.1593	0.1591	0.1587	0.1584	0.1582	0.1577	0.1574	0.1570
PCL	2	0.1701	0.1700	0.1697	0.1694	0.1691	0.1688	0.1685	0.1682	0.1678
PCL	3	0.1221	0.1220	0.1219	0.1217	0.1215	0.1213	0.1210	0.1207	0.1202
zein/PCL-20	4	0.0798	0.0785	0.0769	0.0751	0.0732	0.0719	0.0711	0.0689	0.0678
zein/PCL-20	5	0.0857	0.0846	0.0833	0.0815	0.0795	0.0779	0.0758	0.0748	0.0729
zein/PCL-20	6	0.0925	0.0916	0.0902	0.0872	0.0847	0.0832	0.0813	0.0791	0.0776
zein/PCL-40	7	0.0668	0.0647	0.0612	0.0593	0.0573	0.0543	0.0521	0.0485	0.0453
zein/PCL-40	8	0.0751	0.0728	0.0695	0.0656	0.0636	0.0618	0.0588	0.0536	0.0502
zein/PCL-40	9	0.0614	0.0592	0.0568	0.0541	0.0526	0.0502	0.0473	0.0447	0.0419

Appendix 2.4 Weight loss ratios of the PCL scaffolds and zein/PCL composite scaffolds during degradation

Group	Name	Day 0	Day 3	Day 7	Day 10	Day 14	Day 17	Day 21	Day 24	Day 28
		weight loss (%)	weight loss (%)	weight loss (%)	weight loss (%)	weight loss (%)	weight loss (%)	weight loss (%)	weight loss (%)	weight loss (%)
PCL	1	0	0.0627	0.1882	0.4391	0.6274	0.7528	1.0665	1.2547	1.5056
PCL	2	0	0.0588	0.2352	0.4115	0.5879	0.7643	0.9406	1.1170	1.3521
PCL	3	0	0.0819	0.1638	0.3276	0.4914	0.6552	0.9009	1.1466	1.5561
zein/PCL-20	4	0	1.6291	3.6341	5.8897	8.2707	9.8997	10.9023	13.6591	15.0376
zein/PCL-20	5	0	1.2835	2.8005	4.9008	7.2345	9.1015	11.5519	12.7188	14.9358
zein/PCL-20	6	0	0.9730	2.4865	5.7297	8.4324	10.0541	12.1081	14.4865	16.1081
zein/PCL-40	7	0	3.1437	8.3832	11.2275	14.2216	18.7126	22.0060	27.3952	32.1856
zein/PCL-40	8	0	3.0626	7.4567	12.6498	15.3129	17.7097	21.7044	28.6285	33.1558
zein/PCL-40	9	0	3.5831	7.4919	11.8893	14.3322	18.2410	22.9642	27.1987	31.7590

Appendix 2.5 Weight of the PCL scaffolds and MP/PCL composite scaffolds during degradation

Group	Name	Day 0	Day 3	Day 7	Day 10	Day 14	Day 17	Day 21	Day 24	Day 28
		weight (g)	weight (g)	weight (g)	weight (g)	weight (g)	weight (g)	weight (g)	weight (g)	weight (g)
PCL	1	0.1565	0.1564	0.1562	0.1559	0.1556	0.1553	0.1550	0.1546	0.1543
PCL	2	0.1771	0.1769	0.1768	0.1765	0.1762	0.1758	0.1755	0.1750	0.1747
PCL	3	0.1397	0.1396	0.1395	0.1392	0.1389	0.1387	0.1384	0.1380	0.1377
MP/PCL-20	4	0.1410	0.1366	0.1332	0.1306	0.1275	0.1258	0.1230	0.1198	0.1158
MP/PCL-20	5	0.1188	0.1152	0.1118	0.1095	0.1078	0.1056	0.1026	0.0997	0.0986
MP/PCL-20	6	0.1248	0.1205	0.1172	0.1158	0.1138	0.1108	0.1083	0.1059	0.1019
MP/PCL-40	7	0.1507	0.1421	0.1349	0.1326	0.1278	0.1212	0.1136	0.1078	0.1036
MP/PCL-40	8	0.1390	0.1319	0.1249	0.1220	0.1162	0.1123	0.1055	0.0998	0.0942
MP/PCL-40	9	0.1651	0.1564	0.1498	0.1456	0.1402	0.1338	0.1242	0.1195	0.1122

Appendix 2.6 Weight loss ratios of the PCL scaffolds and MP/PCL composite scaffolds during degradation

Group	Name	Day 0	Day 3	Day 7	Day 10	Day 14	Day 17	Day 21	Day 24	Day 28
		weight loss (%)	weight loss (%)	weight loss (%)	weight loss (%)	weight loss (%)	weight loss (%)	weight loss (%)	weight loss (%)	weight loss (%)
PCL	1	0	0.0639	0.1917	0.3834	0.5751	0.7668	0.9585	1.2141	1.4058
PCL	2	0	0.1129	0.1694	0.3388	0.5082	0.7340	0.9034	1.1858	1.3552
PCL	3	0	0.0716	0.1432	0.3579	0.5727	0.7158	0.9306	1.2169	1.4316
MP/PCL-20	4	0	3.1206	5.5319	7.3759	9.5745	10.7801	12.7660	15.0355	17.8723
MP/PCL-20	5	0	3.0303	5.8923	7.8283	9.2593	11.1111	13.6364	16.0774	17.0034
MP/PCL-20	6	0	3.4455	6.0897	7.2115	8.8141	11.2179	13.2212	15.1442	18.3494
MP/PCL-40	7	0	5.7067	10.4844	12.0106	15.1958	19.5753	24.6184	28.4672	31.2541
MP/PCL-40	8	0	5.1079	10.1439	12.2302	16.4029	19.2086	24.1007	28.2014	32.2302
MP/PCL-40	9	0	5.2695	9.2671	11.8110	15.0818	18.9582	24.7729	27.6196	32.0412

Appendix 2.7 Porosities of the PCL scaffolds and zein/PCL composite scaffolds obtained from micro-CT analysis

Group	Name	Porosity (%)
PCL	1	76.69
PCL	2	74.23
PCL	3	78.04
zein/PCL-20	4	71.84
zein/PCL-20	5	74.73
zein/PCL-20	6	75.46
zein/PCL-40	7	69.61
zein/PCL-40	8	70.41
zein/PCL-40	9	72.92

Appendix 2.8 Porosities of the PCL scaffolds and MP/PCL composite scaffolds obtained from micro-CT analysis

Group	Name	Porosity (%)
PCL	1	77.83
PCL	2	75.43
PCL	3	75.41
MP/PCL-20	4	72.21
MP/PCL-20	5	70.57
MP/PCL-20	6	74.71
MP/PCL-40	7	77.51
MP/PCL-40	8	70.18
MP/PCL-40	9	74.03